



Universiteit
Leiden
The Netherlands

Potentiation of Gram-positive specific antibiotics against Gram-negative bacteria through outer membrane disruption
Wesseling, C.M.J.

Citation

Wesseling, C. M. J. (2022, July 5). *Potentiation of Gram-positive specific antibiotics against Gram-negative bacteria through outer membrane disruption*. Retrieved from <https://hdl.handle.net/1887/3421483>

Version: Publisher's Version

License: [Licence agreement concerning inclusion of doctoral thesis in the Institutional Repository of the University of Leiden](#)

Downloaded from: <https://hdl.handle.net/1887/3421483>

Note: To cite this publication please use the final published version (if applicable).



Chapter 2

Structure-activity studies with bis-amidines that potentiate Gram-positive specific antibiotics against Gram-negative pathogens

Charlotte M.J. Wesseling, Cornelis J. Slingerland, Shanice Veraar, Samantha Lok, and Nathaniel I. Martin

Parts of this chapter have been published: *ACS Infect. Dis.* **2021**.

Abstract

Pentamidine, an FDA approved antiparasitic drug, was recently identified as an outer membrane disrupting synergist that potentiates erythromycin, rifampicin, and novobiocin against Gram-negative bacteria. The same study also described a preliminary structure-activity relationship study using commercially available pentamidine analogues. We here report the design, synthesis, and evaluation of a broader panel of bis-amidines inspired by pentamidine. The present study both validates the previously observed synergistic activity reported for pentamidine, while further assessing the capacity for structurally similar bis-amidines to also potentiate Gram-positive specific antibiotics against Gram-negative pathogens. Among the bis-amidines prepared, a number were found to exhibit synergistic activity greater than pentamidine. These synergists were shown to effectively potentiate the activity of Gram-positive specific antibiotics against multiple Gram-negative pathogens such as *A. baumannii*, *K. pneumoniae*, *P. aeruginosa* and *E. coli*, including polymyxin- and carbapenem-resistant strains.

1. Introduction

The growing threat of antimicrobial resistance (AMR) has led to projections that by 2050 the world may be confronted with as many as 10 million annual AMR-associated deaths.¹ Society is already dealing with the rising tide posed by this global health challenge: each year, 700,000 people die due to infections with drug-resistant pathogens.² At present, the most critical threats are presented by Gram-negative pathogens, including *Acinetobacter baumannii* (carbapenem-resistant), *Pseudomonas aeruginosa* (carbapenem-resistant), and the *Enterobacteriaceae* (carbapenem-resistant and ESBL-producing strains), such as *Escherichia coli* and *Klebsiella pneumoniae*, according to the World Health Organization (WHO).³

In treating infections due to Gram-negative bacteria there is an increased interest in strategies aimed at disrupting the outer membrane (OM) so as to potentiate a number of clinically used antibiotics that on their own are only effective against Gram-positive bacteria.⁴⁻⁶ In an elegant approach recently reported by Brown and coworkers, a panel of 1440 previously approved drugs was screened to identify compounds capable of disrupting the OM of Gram-negative bacteria.⁷ The assay used in the screen was based on findings that at low temperatures, OM synthesis is altered in *E. coli* making it more susceptible to vancomycin.^{8,9} This led to the hypothesis that compounds that antagonize vancomycin in *E. coli* grown at 15°C would likely also impact the OM integrity.^{7,10} Among the hits identified using this innovative screen, the small molecule bis-amidine pentamidine (**1**) (Figure 1) exhibited the most effective capacity to antagonize the activity of vancomycin.⁷

Pentamidine is used clinically to treat *Pneumocystis jiroveci* pneumonia, trypanosomiasis, and leishmaniasis.¹¹⁻¹³ Apart from its antiprotozoal activity, pentamidine is also known to have moderate antibacterial activity against Gram-positive species.^{14,15} Furthermore, pentamidine has also been shown to have anti-cancer activity by restoring the tumor-suppressing activity of p53, is capable to bind A/T-rich regions of double-stranded DNA, and can non-specifically bind and disrupt tRNA secondary structures.¹⁶⁻¹⁹ Unsurprisingly, this broadly active compound has a high incidence of side effects such as nephrotoxicity, hypotension, hypoglycaemia, or local reactions to the injection.¹¹⁻¹³ The Brown group's discovery that pentamidine potentiates the anti-Gram-negative activity of rifampicin, erythromycin, and novobiocin further highlights the multifaceted nature of the compound.⁷

It is well established that the disruption of the Gram-negative OM, for example, with the well-studied polymyxin B nonapeptide (PMBN), can potentiate the activity of hydrophobic, Gram-positive specific antibiotics.^{7,20} In keeping with these findings, it is also known that polymyxin-resistance also reduces the synergistic potential of PMBN.^{7,20} In this regard, it is notable that the synergistic activity of pentamidine in combination with novobiocin, when evaluated against wild-type and polymyxin-resistant strains of *A. baumannii*, was observed both *in vitro* and *in vivo*.⁷

In addition to pentamidine, Brown and coworkers also examined the synergistic activity of other commercially available bis-amidines by performing checkerboard assays, from which the fractional inhibitory concentration index (FICI) was derived, serving as a measure of synergistic activity.^{7,21} These studies highlighted the necessity of two amidine groups for effective potentiation of Gram-positive antibiotics against an *E. coli* indicator

strain.⁷ In addition, the linker used to connect the benzamidine moieties was also found to play a key role in determining the activity of the compounds evaluated.⁷ Based on these studies, two analogues were identified as having enhanced synergistic activities relative to pentamidine (compounds **2** and **3**, Figure 1). The conclusions drawn from these studies suggest that increased linker length and hydrophobicity, along with decreased linker flexibility, contributes to an increase in synergistic activity for these bis-amidines.⁷

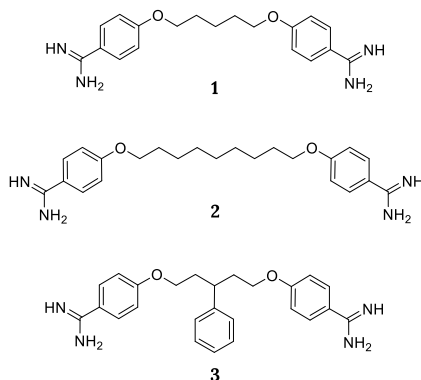


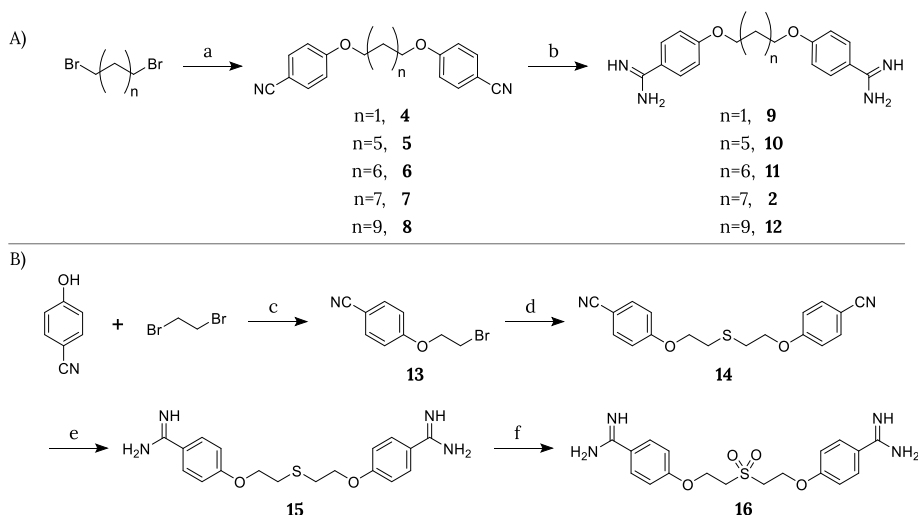
Figure 1. Structures of pentamidine (**1**) and analogues **2** and **3** previously found to exhibit synergy with Gram-positive antibiotics against Gram-negative species.⁷

Inspired by these findings, we here describe structure-activity relationship (SAR) studies designed to provide a broad understanding of the structural features required for potent and selective synergy by bis-amidines. While the previous study of Brown and coworkers evaluated the synergistic potential of commercially available bis-amidines, we here report the design, synthesis, and evaluation of a number of novel bis-amidines. In addition to screening for synergistic activity, the new compounds here studied were also assessed for their capacity to selectively target the Gram-negative OM membrane rather than act as non-specific membrane disruptors. Our findings serve to both validate published accounts, while also revealing new, more potent, and selective bis-amidine based synergists.

2. Results and Discussion

2.1. Synthesis and initial screening

Linear linkers. To further explore the correlation between linker length and synergistic activity, a set of linear pentamidine analogues was selected. In addition to the previously reported nonamidine (**2**) and propamidine (**9**), we also synthesized heptamidine (**10**), octamidine (**11**), and undecamidine (**12**) analogues (Scheme 1A). Pentamidine (**1**) was also synthesized by the same route to allow for comparison with the commercial material (Supporting information, Scheme S1), which subsequently revealed no difference in the synergistic activity of the in-house prepared and commercial materials (data not shown).



Scheme 1. Synthesis of pentamidine analogues containing different linear spacers between the benzamidine groups. Reagents and conditions: (a) 4-Cyanophenol, NaH, DMF, 80°C, 1h (59%-quant.); (b) i) LHMDs, THF, 48h, rt, ii) HCl (dioxane), 0°C to rt, overnight (49%-quant.); (c) K_2CO_3 , DMF, 100°C, 5h (43%); (d) $\text{Na}_2\text{S}\cdot 9\text{H}_2\text{O}$, DMSO, 115°C, 1h (93%); (e) i) LHMDs, THF, rt, 48h; ii) HCl (dioxane), rt, overnight (64%); (f) m -CPBA, DCM, 0°C, 2h (32%).

As shown in Scheme 1A, the dibenzonitrile intermediates were prepared from the commercially available α,ω -dibromo-alkanes via a Williamson ether synthesis according to literature protocols.²² Crystallization from ethanol resulted in the pure intermediates **4-8** in good to excellent yields. The transformation of the nitrile groups into the corresponding amidine is classically performed via the Pinner reaction followed by treatment with ammonia.²³⁻²⁷ However, recent publications have described the same transformation by the more convenient use of a lithium bis(trimethylsilyl)amide (LHMDs) solution followed by an acidic quench.²⁸⁻³¹ In the synthesis of pentamidine we therefore evaluated the treatment of the corresponding bis-nitrile precursor with LHMDs (1 M in tetrahydrofuran (THF)) followed by a quench with saturated ethanolic HCl, 4 M HCl in dioxane, or 1 M HCl (aq) (See Supporting information, Scheme S1 and S2). These trial experiments revealed that quenching with 4 M HCl in dioxane resulted in the highest yield, and these conditions were therefore also applied in the preparation of the bis-amidines **2**, **9-12**, which were subsequently isolated in good yields after high-

performance liquid chromatography (HPLC) purification. In addition to probing linker length, we also explored the impact of heteroatom substitution in the linker. Notably, thioether analogue **15** has been previously prepared and tested for antimicrobial activity.^{15,32} Thioether **15** was therefore synthesized as indicated in Scheme 1B, also providing ready access to the more hydrophilic sulfone analogue **16** obtained by *m*-CPBA treatment of **15**.

The inherent antibacterial activities of pentamidine (**1**) and the bis-amidines **2**, **3**, **9-12**, **15**, and **16** were first assessed against an indicator strain *E. coli* BW25113. This revealed a trend wherein compounds containing linkers of eight or more carbons exhibited moderate antibacterial activity with minimum inhibitory concentration (MIC) values of 50 µg/mL (See Table 1). Neither the thioether linked species **15** or sulfone linked **16** showed any inherent activity up to the maximum concentration tested (200 µg/mL). Next, the synergistic activity of the compounds was assessed in combination with both erythromycin and rifampicin using the same indicator *E. coli* strain. Checkerboard assays were performed in which a dilution series of the synergist was evaluated in combination with the antibiotic of interest, also serially diluted. The resulting “checkerboard” or 2-dimensional MIC readout, makes it possible to identify the lowest concentration of both components that results in the most potent synergistic effect. The highest concentrations tested among the synergists correspond to their inherent MIC values (or up to 200 µg/mL in case where no antibacterial activity was observed). For erythromycin the highest concentration tested was 200 µg/mL and for rifampicin it was 12 µg/mL.

In general, a trend was observed wherein bis-amidines with longer linker lengths showed a great capacity to potentiate the activity of erythromycin (Table 1). Compared with pentamidine (FICI 0.500), nonamidine (**2**), and heptamidine (**10**) were found to be the most effective synergists with FICI values of 0.094 and 0.125, respectively, while the shorter propamidine (**9**) exhibited activity on par with pentamidine (Figure 2). The synergistic activities observed when the same panel of bis-amidines was evaluated with rifampicin corroborates the findings with erythromycin (Table 1 and Supporting information Figure S2). These findings highlight the importance of linker length and hydrophobicity for synergistic activity. All analogues containing linkers greater than five carbon atoms demonstrated more potent synergy than the observed for pentamidine. By comparison, propamidine (**9**), containing a three carbon spacer and thioether **15** (isosteric to pentamidine) exhibited synergistic activities comparable to pentamidine. It is also interesting to note that the introduction of the more polar sulfone-linker as in **16** led a complete loss of synergistic activity (Table 1, Supporting information, Figure S1, S2, and Table S1, S2).

Examination of the effect of these bis-amidines on red blood cells revealed another feature that correlates with linker length. Specifically, the enhanced antimicrobial activity and synergistic potential in combination with erythromycin observed for analogues containing longer linkers is accompanied by an increase in hemolytic activity (Table 1 and Supporting information Figures S17 and S18 and Table S17). While propamidine (**9**) and pentamidine (**1**) have little inherent antibacterial activity (MIC of 200 µg/mL or higher) and are moderate synergists with erythromycin (FICI of 0.500), they are also non-hemolytic (erythrocytes treated with compounds at 200 µg/mL for 20 h. at 37°C, non-hemolytic defined as <10%³³). By comparison, the slightly longer heptamidine (**10**) has an inherent antimicrobial activity (MIC 200 µg/mL) along with enhanced synergistic activity with erythromycin (FICI ≤0.125) but also a slight increase in

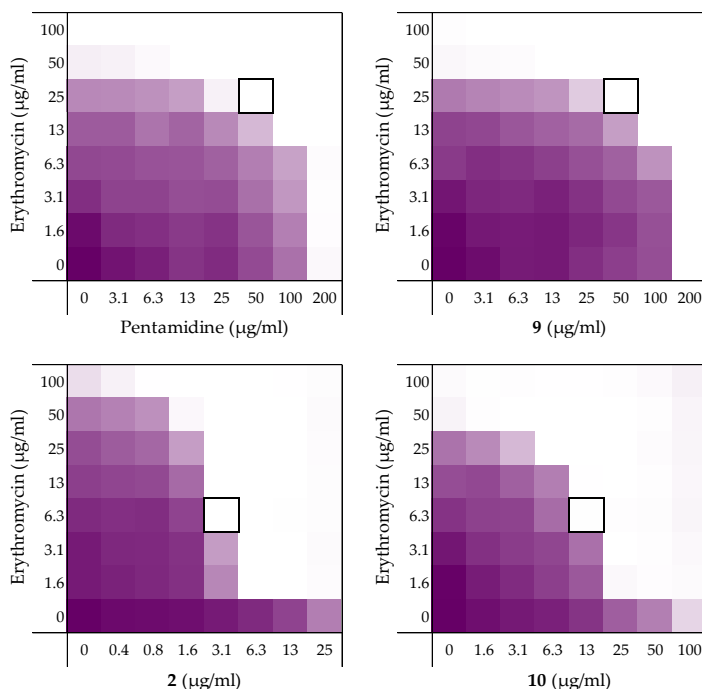


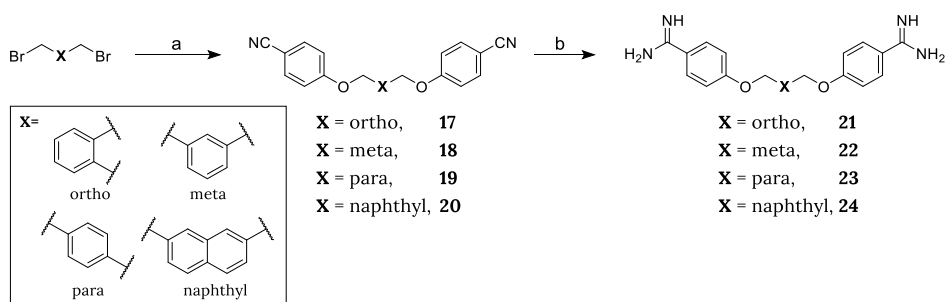
Figure 2. Representative checkerboard assays for pentamidine (**1**), propamidine (**9**), nonamidine (**2**) and heptamidine (**10**) in combination with erythromycin versus *E. coli* BW25113. In each case, the bounded box in the checkerboard assays indicates the combination of compound and antibiotic resulting in the lowest FICI (See Table 1). OD₆₀₀ values were measured using a plate reader and transformed to a gradient: purple represents growth, white represents no growth. An overview of all checkerboard assays with erythromycin can be found in the Supporting information, Figure S1.

hemolytic activity to 9.2%. However, the longer octamidine (**11**), nonamidine (**2**), and undecamidine (**12**) exhibit very significant levels of hemolysis (16–87%), suggesting that both the inherent antimicrobial activity (MIC 50 µg/mL) and potent synergistic activity in combination with erythromycin (FICI ≤0.094–0.156) of these analogues are driven by a general membrane disruption mechanism and not a selective disruption of the Gram-negative OM. Based on these findings, it appears that the “tipping point” associated with the desirable synergistic effects versus the unwanted hemolytic activity appears to be for C₇ spaced bis-amidine analogue heptamidine (**10**). These findings served to inform the design of the next series of analogues.

2.2. Linkers with reduced flexibility

Building on our initial findings with the linear bis-amidines, we next examined the effect of reducing the rotational flexibility of the linker. In the Brown group’s earlier study, it was noted that phenyl substituted bis-amidine **3** (Figure 1) was an extremely effective synergist, an effect that was attributed in part to its decreased molecular flexibility.⁷ To this end, we prepared a series of bis-amidines (Scheme 2, compounds **21–24**) that incorporate linkers comprising different planar, aromatic motifs as a means of even further restricting flexibility. For purposes of comparison, we also prepared compound **3**

(Supporting information Scheme S3) and confirmed its synergistic activity (Table 1, Supporting information Figure S1 and S2). Notable, however, was the finding that compound **3** also exhibits significant hemolytic activity (above 10%³³) (See Table 1 and Supporting information, Figure S18 and Table S17) suggesting that impressive synergistic activity associated with the compound is not selective for the Gram-negative OM and is due instead to general membrane disruption. The synthetic route used to access bis-amidines **21–24** is shown in Scheme 2 and was based largely on the published preparation of these and similar compounds previously evaluated as anti-parasitic agents.^{22,34–39} The *meta*-oriented linker in compound **22** most closely mimics the 5-carbon spacer found in pentamidine, while analogues **21** and **23** differ slightly due to the *ortho*- and *para*-orientations of the benzene core. In the case of compound **24**, a 2,7-disubstituted naphthalene motif was envisioned to mimic of the 7-carbon spacer found in heptamidine (**10**). The synthesis of compounds **21–24** started from the corresponding commercially available dibromo-xylenes or 2,7-bis(bromomethyl)naphthalene, which were transformed into the corresponding bis-nitriles **17–20** by treatment with 4-cyanophenol and NaH in dimethylformamide (DMF) at 80°C. In this case, recrystallization of the intermediates **17**, **19**, and **20** from ethanol was not successful. However, based on an acceptable purity (as assessed by NMR), the crude bis-nitriles **19** and **20** could be used directly without a need for further purification, while bis-nitrile **17** was purified using column chromatography. Transformation into the corresponding bis-amidines was in turn performed by treatment with LHMDS³⁴ followed by acidic quench with 4 M HCl in dioxane to provide compounds **21–24** in acceptable yields after HPLC purification.



Scheme 2. Synthesis of bis-amidines containing rigid aromatic spacers. Reagents and conditions: (a) 4-Cyanophenol, NaH, DMF, 80°C, 1h (79%-quant.); (b) i) LHMDS, THF, 48h; ii) HCl (dioxane, 0°C to rt, overnight (19–83%).

Evaluation of the inherent antimicrobial activity of compounds **21–24** as well as their ability to synergize with erythromycin revealed **22** and **24** to be the most effective of these four of compounds (FICI of ≤ 0.094 with erythromycin) (Figure 3 and Table 1). *o*-Xylene analogue **21** also exhibited enhanced synergistic activity relative to pentamidine (≤ 0.125 vs. 0.500) while *p*-xylene analogue **23** showed less activity (FICI ≤ 0.313). Interestingly, while none of compounds **21–24** showed any inherent antibacterial activity up to 200 $\mu\text{g/mL}$, the 2,7-naphthalene linked analogue **24** was found to exhibit significant hemolytic activity (75%) (See Table 1). These findings are in line with previous studies in which compound **24** was evaluated as an anti-protozoal where it was also found to exhibit

significant toxicity against a rat L6 muscle cell line.³⁸ By comparison, compounds **21** and **22** were found to be non-hemolytic and demonstrate potent synergy when combined with erythromycin with FICI values of ≤ 0.125 and ≤ 0.094 , respectively (Table 1). Similarly, **21** and **22** were also found to significantly potentiate the activity of rifampicin against the same *E. coli* indicator strain with FICI values of ≤ 0.094 and ≤ 0.188 , respectively (Table 1). These findings support the hypothesis that reduced linker flexibility is beneficial for synergistic activity and also reveal the importance of the orientation of the benzamidines on the aromatic nucleus. This is most clearly demonstrated by the potent synergy exhibited by the *ortho*- and *meta*-xylene analogues **21** and **22** (FICI ≤ 0.094 – 0.188) in contrast to the much less active *para*-xylene linked **23** (FICI ≤ 0.313 – 0.375).

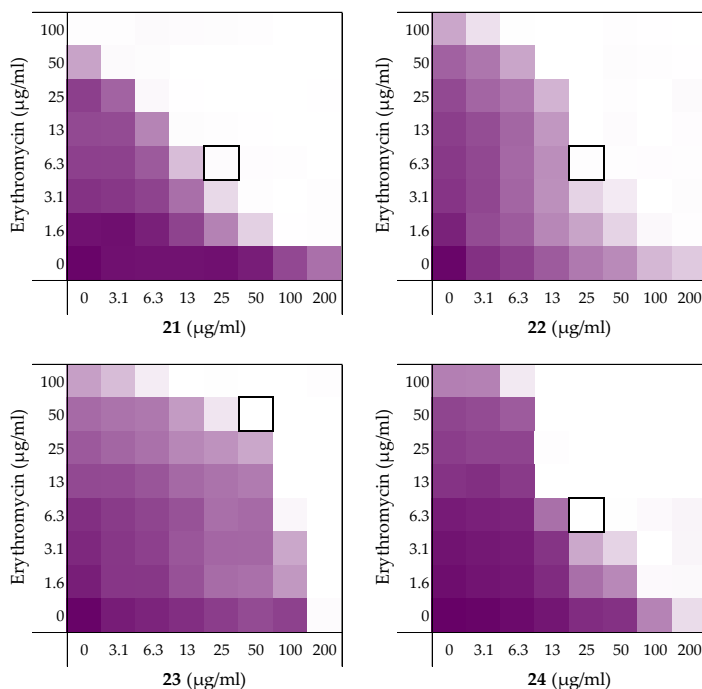
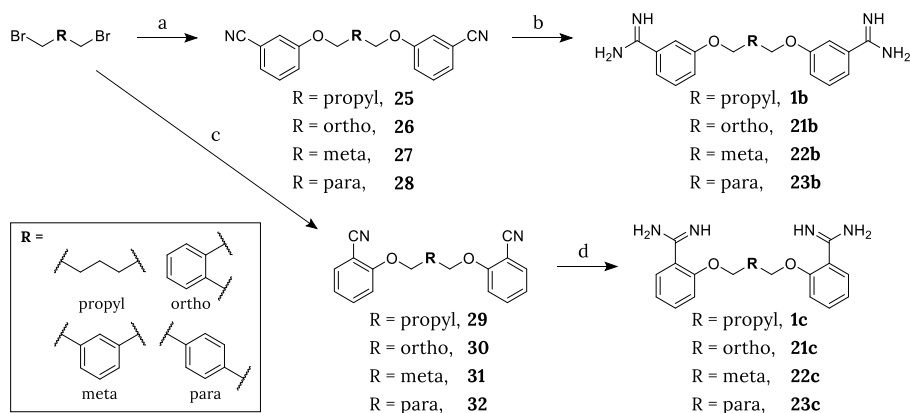


Figure 3. Checkerboard assays for compounds **21**–**24** in combination with erythromycin versus *E. coli* BW25113. In each case, the bounded box in the checkerboard assays indicates the combination of compound and antibiotic resulting in the lowest FICI (see Table 1). OD₆₀₀ values were measured using a plate reader and transformed to a gradient: purple represents growth, white represents no growth. An overview of all checkerboard assays with erythromycin can be found in the Supporting information, Figure S1.

2.3. Altering the position of the amidine moiety

The rigidity of the xylene-based linkers described above not only affects the spacing but also the positioning of the amidine groups. In the case of pentamidine (**1**) and compounds **21**–**23**, the amidine moieties are positioned *para* relative to the linker. We, therefore, next prepared a series of analogues wherein the positioning of the amidine groups was shifted to either the *meta*- or *ortho*-positions (Scheme 3). While the *meta*-amidine analogues **1b**,

21b-23b are known in the literature,^{24,35,38-41} *ortho*-amidine analogues **1c**, **21c-23c** have not been previously described. The synthesis of the *meta*-amidine analogues was performed following the same protocol employed for the preparation of the corresponding *para*-amidines but using 3-cyanophenol in place of 4-cyanophenol (Scheme 3). For the preparation of the *ortho*-amidine analogues, the intermediate bis-nitriles were prepared in an analogous fashion, however, conversion to the product bis-amidines required a different set of conditions. Unlike the route used in the preparation of the *para*- and *meta*-bis-amidines, treatment of the *ortho*-bis-nitrile intermediates **29-32** with LHMDS failed to yield the expected amidine product. For this reason, an alternative, previously reported three-step procedure for the conversion of nitriles to amidines, was instead employed.⁴² In doing so, the nitrile is first converted to the corresponding N-hydroxyamidine by treatment with hydroxylamine hydrochloride. The N-hydroxy group is then acetylated with Ac₂O followed by reduction to the amidine product using zinc powder (Scheme 3). After HPLC purification, the *ortho*-bis-amidines (**1c**, **21c-23c**) were obtained in yields suitable for subsequent evaluation.



Scheme 3. Synthesis of bis-amidine analogues **1b**, **21b-23b** and **1c**, **21c-23c**. Reagents and conditions: (a) 3-Cyanophenol, NaH, DMF, 80°C, 1h (63%-quant); (b) i) LHMDS, THF, 48h, ii) HCl (dioxane), 0°C to rt, overnight (72%-quant); (c) 2-Cyanophenol, NaH, DMF, 80°C, 1h (83-99%); (d) (i) NH₂OH·HCl, DIPEA, EtOH, 85°C, 6h; (ii) Ac₂O, AcOH, rt, 4h; (iii) Zn powder, AcOH, 35°C, 6h (12-48%).

As for pentamidine (**1**) and the other *para*-bis-amidines **21-23**, no inherent antimicrobial activity or hemolysis was observed for the *meta*-substituted analogues **1b**, **21b-23b** or the *ortho*-substitute analogues **1c**, **21c-23c** (Table 1). Assessment of synergy with erythromycin showed that the *meta*-bis-amidines maintain a reasonable degree of synergistic activity (Figure 4) while the *ortho*-bis-amidines show no such ability (Table 1). In general, the *meta*-orientated bis-amidines are less effective synergists than the corresponding *para*-orientated compounds, a trend also observed in synergy studies with rifampicin (Table 1). An exception to this was observed for compounds **23** and **23b** both containing the *p*-xylene linker. In this case, the placement of the amidine groups at the *meta*-position relative to the linker results in a slight decrease in FICI from 0.313 for compound **23** to 0.250 for **23b** when tested in combination with erythromycin. An even more pronounced potentiation effect was seen when these compounds were evaluated with rifampicin. In this case, compound **23** was found to have an FICI value of 0.375 while

for **23b**, the FICI value calculated was 0.156, making it one of the most potent, non-hemolytic, rifampicin synergists identified (Table 1). Collectively, these findings indicate that both the geometry of the linker and the positioning of the amidines in the benzamidine moieties are interrelated structural features that play a key role in dictating optimal synergistic activity.

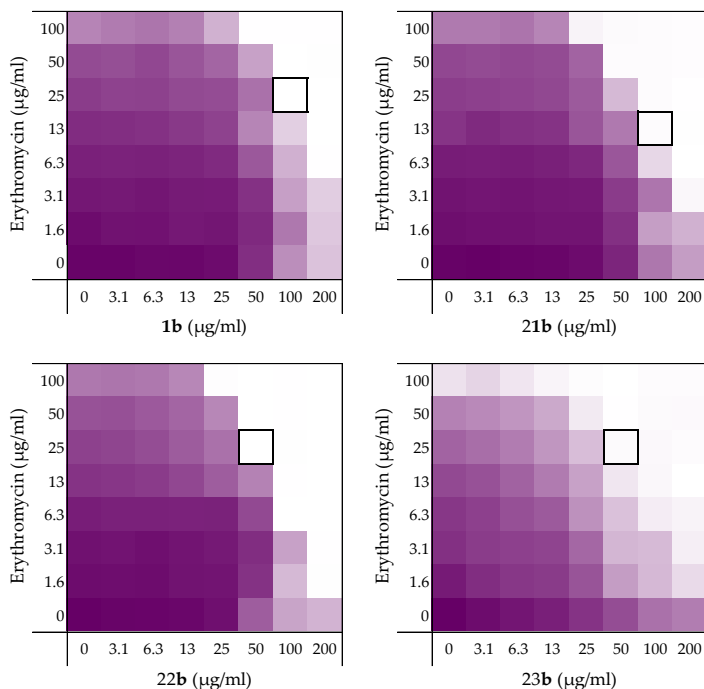


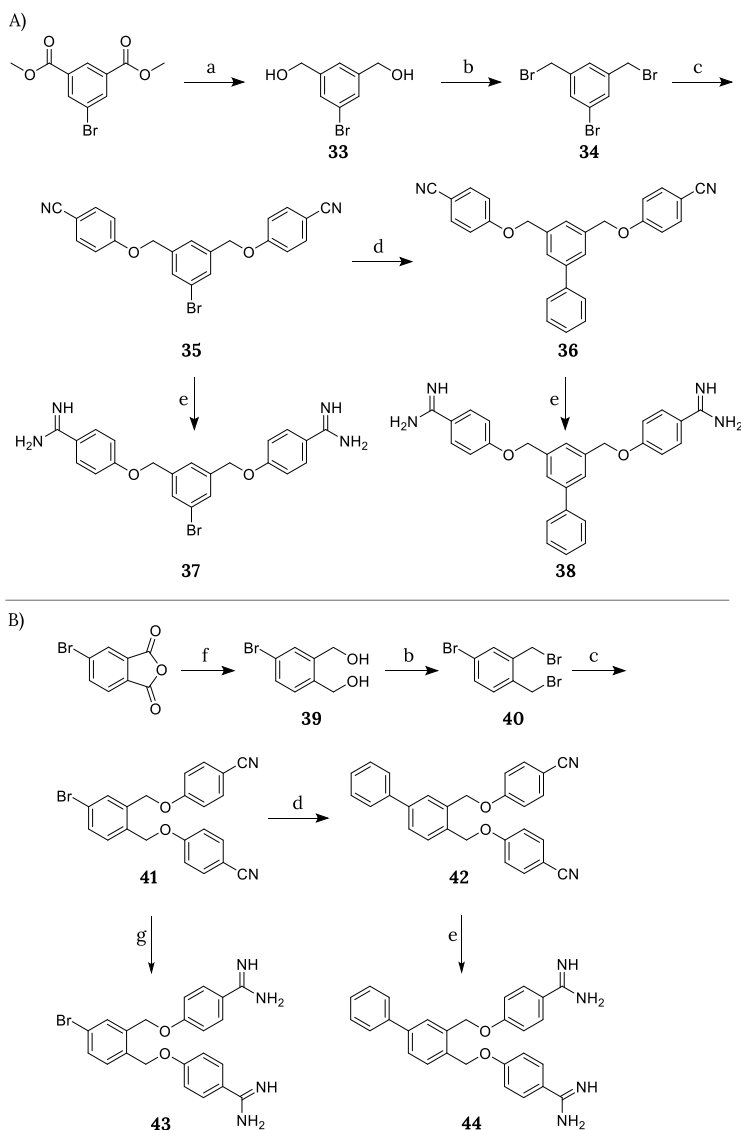
Figure 4. Checkerboard assays for compounds **1b**, **21b**–**23b** in combination with erythromycin versus *E. coli* BW25113. In each case, the bounded box in the checkerboard assays indicates the combination of compound and antibiotic resulting in the lowest FICI (see Table 1). OD₆₀₀ values were measured using a plate reader and transformed to a gradient: purple represents growth, white represents no growth. An overview of all checkerboard assays with erythromycin can be found in the Supporting information, Figure S1.

2.4. Increasing linker hydrophobicity

As described above, bis-amidines with more hydrophobic linkers typically show enhanced synergistic activity but often at the cost of increased hemolysis. In this light, compounds **21** and **22** were deemed to be particularly interesting given that they exhibit potent synergistic activity with both erythromycin and rifampicin while displaying no appreciable hemolytic activity. To examine the possibility of further enhancing these compounds we next prepared analogues wherein an additional phenyl group, as for compound **3**, was added as a substituent to the aromatic linkers in both **21** and **22** to give analogues **38** and **44** (Scheme 4). The synthetic route used also provided ready access to brominated intermediates **35** and **41**. Given the hydrophobic character of halogen atoms,⁴³ we opted to also convert these intermediates to the corresponding bis-amidines **37** and **43**. The synthesis of *meta*-linked analogues **37** and **38** started with the reduction

of dimethyl 5-bromoisophthalate to give diol **33**.⁴⁴ An Appel reaction was then applied to transform the diol into tribromide **34**,⁴⁵ followed by reaction with 4-cyanophenol to yield bis-nitrile **35**.²² A portion of **35** was subsequently used in a Suzuki coupling employing phenylboronic acid resulting in intermediate **36**.⁴⁶⁻⁴⁸ Both **35** and **36** were then converted to the corresponding bis-amidines by treatment with LHMDS followed by HCl quench and HPLC purification to give **37** and **38**. The preparation of **43** and **44** followed a similar synthetic strategy but started with the reduction of 4-bromophthalic anhydride using lithium aluminum hydride and ZnCl₂.⁴⁹ The resulting diol **39** was cleanly converted to tribromide **40**, which was subsequently transformed into the brominated bis-nitrile intermediate **41**. A portion of **41** was then transformed into intermediate **42** using the same Suzuki conditions applied in the previous preparation of **36**.⁴⁶⁻⁴⁸ Notably, while bis-nitrile **42** was readily transformed into the desired bis-amidine **44** using the LHMDS protocol, when the same conditions were applied to **41** an unexpected dehalogenation occurred. As an alternative, the same three-step process, described above for the preparation of **21b-23b**, was successfully applied to convert the bis-nitrile to the desired bis-amidine **43**.⁴²

Compounds **37**, **38**, **43**, and **44** were found to show no significant inherent antimicrobial activity when tested against *E. coli* BW25113 (Table 1). As expected, the introduction of the hydrophobic side-chains improved the synergistic activity with FICI values ranging from 0.047 to 0.094 (Figure 5 and Table 1). Unfortunately, however, and not entirely unexpectedly, the increased hydrophobicity of these analogues was also found to result in a severe increase in hemolytic activity (Table 1) indicating that the enhanced synergistic activity observed is likely due to non-specific membrane disruption.



Scheme 4. Synthesis of A) *meta*-linked or B) *ortho*-linked bis-amidines containing bromo (**37**, **43**) or phenyl substitution (**38**, **44**) on the central aromatic core. Reagents and conditions: a) i) DIBALH, DCM, 0°C, 1h; ii) Rochelle salt (quench), rt, overnight (96%); (b) PPh₃, CBr₄, DCM, rt, 2h (55–74%); (c) 4-Cyanophenol, NaH, DMF, 80°C, 1h (87–99%); (d) Phenylboronic acid, Pd(dppf)Cl₂·DCM, THF/Na₂CO₃ (aq) (1:1), 65°C, 8–18h (8–80%); (e) i) LHMDS, THF, rt, 48h; ii) HCl (dioxane), 0°C – rt, overnight (17–75%); f) i) LAH, ZnCl₂, THF, rt, 6h; ii) Rochelle salt (quench), rt, overnight (95%); (g) i) NH₂OH·HCl, DIPEA, EtOH, 85°C, 6h; ii) Ac₂O, AcOH, rt, 4h; iii) Zn powder, AcOH, 35°C, 6h (7%).

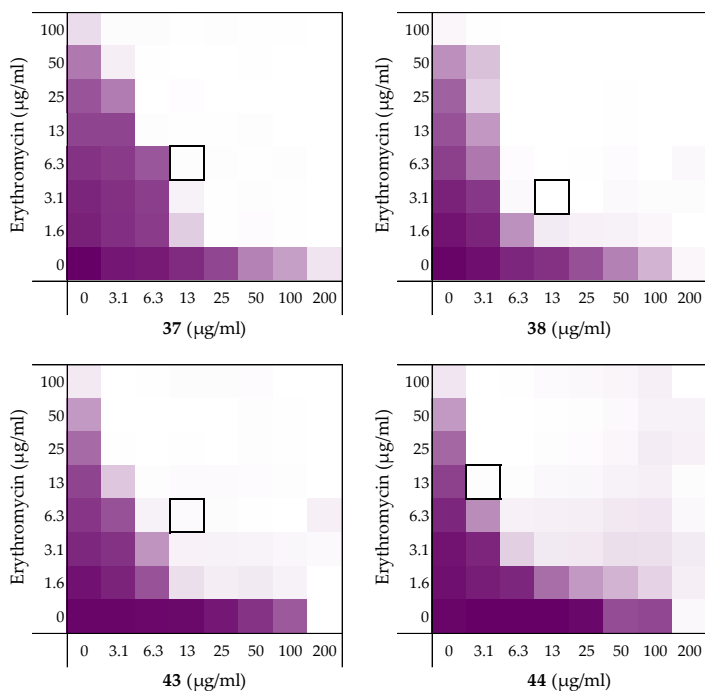
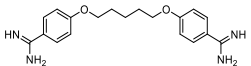
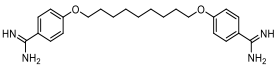
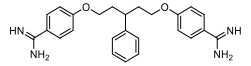
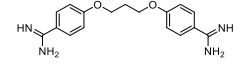
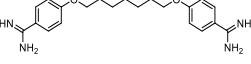
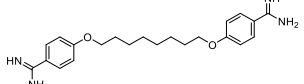
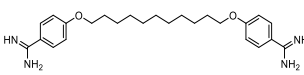
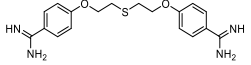
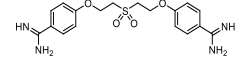
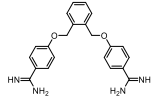
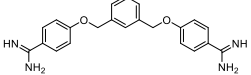
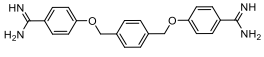
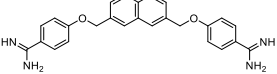
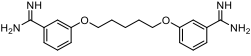
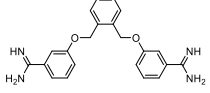


Figure 5. Checkerboard assays for compounds **37**, **38**, **43**, and **44** in combination with erythromycin versus *E. coli* BW25113. In each case, the bounded box in the checkerboard assays indicates the combination of compound and antibiotic resulting in the lowest FICI (see Table 1). OD₆₀₀ values were measured using a plate reader and transformed to a gradient: purple represents growth, white represents no growth. An overview of all checkerboard assays with erythromycin can be found in the Supporting information, Figure S1.

Table 1. Overview of synergy with erythromycin against *E. coli* BW25113 and hemolysis data.

	Structures	MIC ($\mu\text{g/mL}$)	erythromycin		rifampicin		HA (%) ^b
			MIC ($\mu\text{g/mL}$)	FICI ^a	MIC ($\mu\text{g/mL}$)	FICI	
1		200	100	0.500	12	0.375	0.4
2		50	>100	≤ 0.094	6	≤ 0.094	82
3		>200	>100	≤ 0.063	6	≤ 0.063	13
9		≥ 200	100	0.500	12	≤ 0.500	0.6
10		>100	100	≤ 0.125	12	0.078	9.2
11		50	>100	≤ 0.156	12	≤ 0.125	16
12		50	>100	≤ 0.133	12	≤ 0.078	87
15		>200	100	≤ 0.375	6	≤ 0.500	0.0
16		>200	50	>0.5	6	>0.5	0.1
21		>200	100	≤ 0.125	12	≤ 0.094	0.5
22		>200	>100	≤ 0.094	12	≤ 0.188	1.1
23		≥ 200	>100	≤ 0.313	6	0.375	0.4
24		≥ 200	>100	≤ 0.094	12	0.031	75
1b		>200	>100	≤ 0.375	12	≤ 0.375	0.1
21b		>200	>100	≤ 0.313	6	≤ 0.313	0.4

22b		>200	>100	≤0.250	6	≤0.250	1.6
23b		>200	>100	≤0.250	>12	≤0.156	3.7
1c		>200	>100	>0.5	12	>0.5	0.7
21c		>200	>100	>0.5	12	>0.5	0.4
22c		>200	>100	>0.5	12	>0.5	0.0
23c		>200	>100	>0.5	12	>0.5	0.0
37		>100	>100	≤0.063	>12	≤0.125	57
38		≥100	>100	≤0.047	>12	≤0.039	58
43		≥100	>100	≤0.094	12	0.094	57
44		≥200	>100	≤0.078	12	≤0.047	82
PMBN		>200	200	≤0.125	3	≤0.039	-

^aSynergy defined as FICI ≤0.5.²¹ See Supporting Information Tables S1 and S2 for full data used in calculating the FICIs with erythromycin and rifampicin respectively; ^bHemolytic activity of all compounds after 20 hours of incubation at 200 µg/mL. Values <10% were defined as non-hemolytic.³³

2.5. Exploring the synergistic range

Erythromycin, rifampicin, novobiocin, and vancomycin are typically used to treat Gram-positive infections.^{50–55} However, when combined with OM disrupting agents, these antibiotics can also display efficacy against Gram-negative bacteria.^{6,20} The Brown group's recent study with pentamidine showed that erythromycin, rifampicin, and novobiocin were most effectively potentiated by this bis-amidine.⁷ With this in mind, we next investigated the broader synergy of the most promising compounds identified in our present study, namely, compounds **21**, **22**, and **23b**. As noted above, these three compounds were all found to be more active than pentamidine in potentiating the activity of erythromycin and rifampicin against an indicator *E. coli* stain while showing no hemolytic activity. To this end, compounds **21**, **22**, and **23b** were evaluated against an expanded panel of organisms, including several *E. coli* strains (including carbapenem- and polymyxin-resistant strains) and ATCC strains of *A. baumannii*, *K. pneumoniae*, and *P. aeruginosa*. In addition, the well-studied OM disruptor PMBN and pentamidine itself were taken along as benchmarks in the expanded assessment of compounds **21**, **22**, and **23b**.

2.5.1. Synergy with novobiocin and vancomycin

Building from the synergy studies with erythromycin and rifampicin described above, compounds **21**, **22**, and **23b** were next tested for the ability to potentiate novobiocin and vancomycin, along with pentamidine (**1**) and PMBN (Figure 6, Supporting information Figures S3 and S4). In agreement with previous studies, novobiocin and vancomycin showed no antimicrobial activity against the indicator *E. coli* BW25113 strain at the highest concentration tested of 200 µg/mL.^{7,56} Checkerboard assays with compounds **21**, **22**, and **23b** in combination with novobiocin revealed the compounds to be superior synergists compared to pentamidine (Table 2, Figure 6), a finding in line with the results obtained when the same bis-amidines were evaluated with erythromycin and rifampicin. In general, PMBN was found to be a more potent synergist than the bis-amidines with the exception of compound **22** in combination with erythromycin which resulted in very effective growth prevention of the *E. coli* indicator strain. When tested in combination with vancomycin, none of the bis-amidines showed any synergistic activity, while PMBN maintained a potent effect (Table 2). These findings are in line with previously reported observations in which pentamidine was found not to synergize with vancomycin.⁷

Table 2. FICI values of pentamidine (**1**), **21**, **22**, **23b**, and PMBN against *E. coli* BW25113 in combination with Gram-positive-specific antibiotics rifampicin, novobiocin, and vancomycin.^a

	Erythromycin	Rifampicin	Novobiocin	Vancomycin
Pentamidine (1)	0.500	0.375	≤0.281	>0.5 ^b
21	≤0.125	≤0.094	≤0.125	>0.5 ^b
22	≤0.094	≤0.188	≤0.078	>0.5 ^b
23b	≤0.250	≤0.156	≤0.188	>0.5 ^b
PMBN	≤0.125	≤0.039	≤0.047	≤0.156

^aMIC and minimal synergistic concentrations (MSC) data can be found in the Supporting information, Table S1–S4. ^bSynergy defined as an FICI ≤0.5.²¹

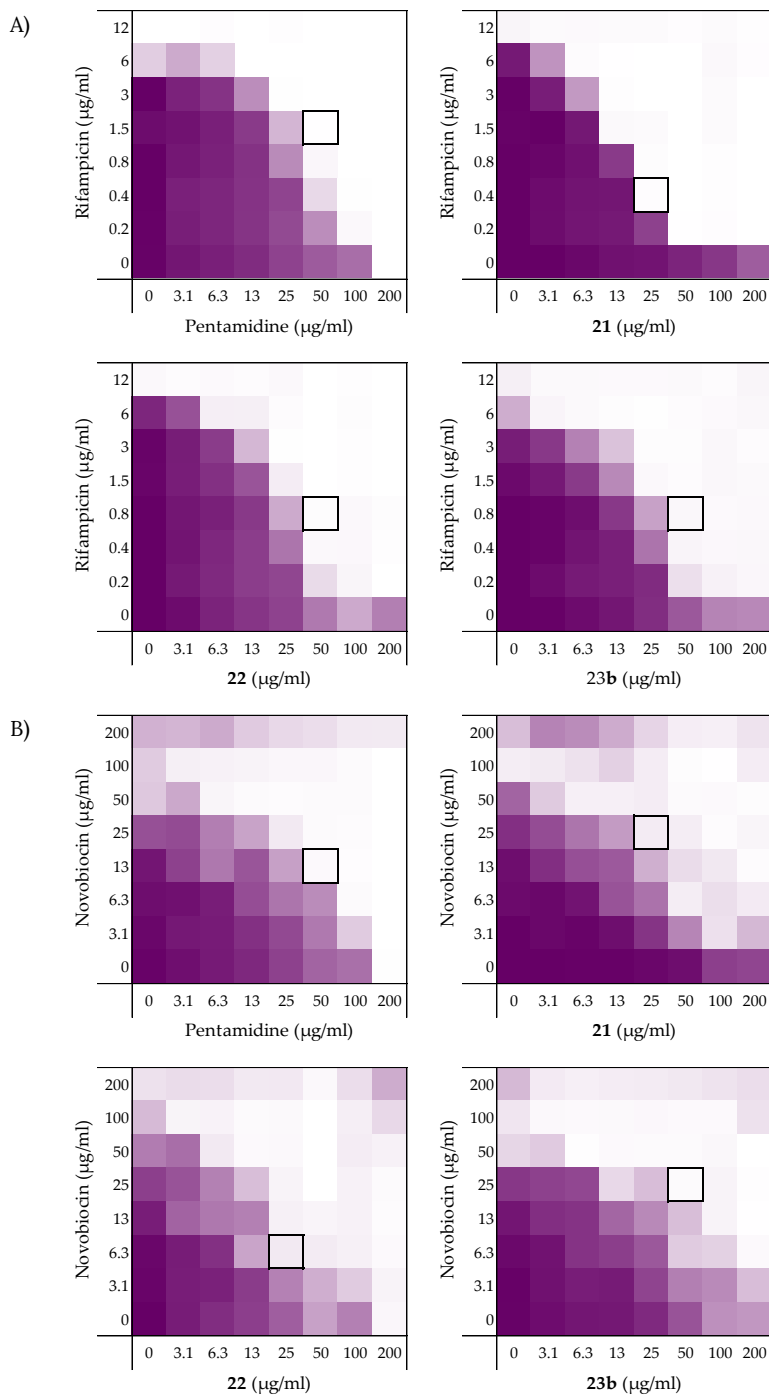


Figure 6. Checkerboard assays of compounds pentamidine (**1**), **21**, **22**, and **23b** in combination with A) rifampicin and B) novobiocin against *E. coli* BW25113. In each case, the bounded box in the checkerboard assays indicates the combination of compound and antibiotic resulting in the lowest

FICI (see Table 2). OD₆₀₀ values were measured using a plate reader and transformed to a gradient: purple represents growth, white represents no growth. The poor aqueous solubility of novobiocin results in the background signal observed in the OD₆₀₀ read-out at when tested at concentrations ≥ 100 $\mu\text{g/mL}$. An overview of all checkerboard assays with rifampicin, novobiocin and vancomycin can be found in the Supporting information, Figure S2-S4.

2.5.2. Synergy against other *E. coli* strains.

The next phase of our investigation involved assessing the synergistic activity of the most promising compounds identified against an expanded panel of *E. coli* strains. For these screens, we opted to focus on rifampicin as the companion antibiotic given that it is bactericidal while erythromycin is considered to be bacteriostatic.^{11,57} In our initial screens, a more clear-cut distinction of growth versus no growth was indeed observed for rifampicin, possibly due to its bactericidal nature (see Figures 3 and 6A). Furthermore, given that the MIC of rifampicin is significantly lower against the Gram-negative strains used versus the MICs of erythromycin or novobiocin, potential solubility issues at the highest antibiotic concentrations tested were not a problem.

In selecting an expanded panel of *E. coli* strains, we sought to examine a variety of features ranging from the OM composition to resistance profile. In the case of *E. coli*, the structure of the lipopolysaccharide (LPS) layer is known to affect their susceptibility to antibiotics⁵⁸ and we therefore reasoned that it could also play a role in the synergistic activity of compounds targeting the OM. This was seen as particularly relevant for the pentamidine analogues investigated here, given that previous studies have suggested that pentamidine interacts with lipid A.⁷ With this in mind, *E. coli* ATCC25922 (smooth LPS) and *E. coli* W3110 (rough LPS) were selected, along with the indicator lab strain *E. coli* BW25113 also known to possess a rough LPS layer.⁵⁹⁻⁶¹ Additionally, a clinical isolate *E. coli* 552060.1 was included, which, like most clinical isolates, has a smooth LPS layer.^{58,62} The inherent antimicrobial activity of rifampicin, pentamidine (**1**), compounds **21**, **22**, **23b**, and PMBN was first established against these *E. coli* strains (Supporting information Figures S5-S7 and Tables S5-S7). In keeping with our initial checkerboard assays with rifampicin and the *E. coli* BW25113 strain (Table 1), compound **21** in nearly all cases showed the lowest FICI values among the bis-amidines evaluated against the expanded *E. coli* panel (Figure 7A and Table 3). In general, the bis-amidines tested all showed effective synergy with little difference observed for the rough or smooth LPS strains.

The expanded screening was continued with *E. coli* bearing *mcr*-1, *mcr*-2, and *mcr*-3 genotypes known to confer polymyxin resistance. For this purpose, a lab strain *E. coli* BW25113 *mcr*-1, transformed with the pGDP2 plasmid, was also included to directly assess the effect of the phosphoethanolamine transferase responsible for lipid A modification.⁶³⁻⁶⁵ The bis-amidines displayed synergy with rifampicin against all *mcr*-positive strains evaluated (Figure 7B, Table 3, Supporting information Figures S8-S12, and Tables S8-S12). Again, in nearly all cases, compound **21** gave the lowest FICI values among the bis-amidines evaluated, with synergy comparable to that of PMBN, which was found to be generally less effective against *mcr*-positive strains than non-*mcr* strains (Table 3).

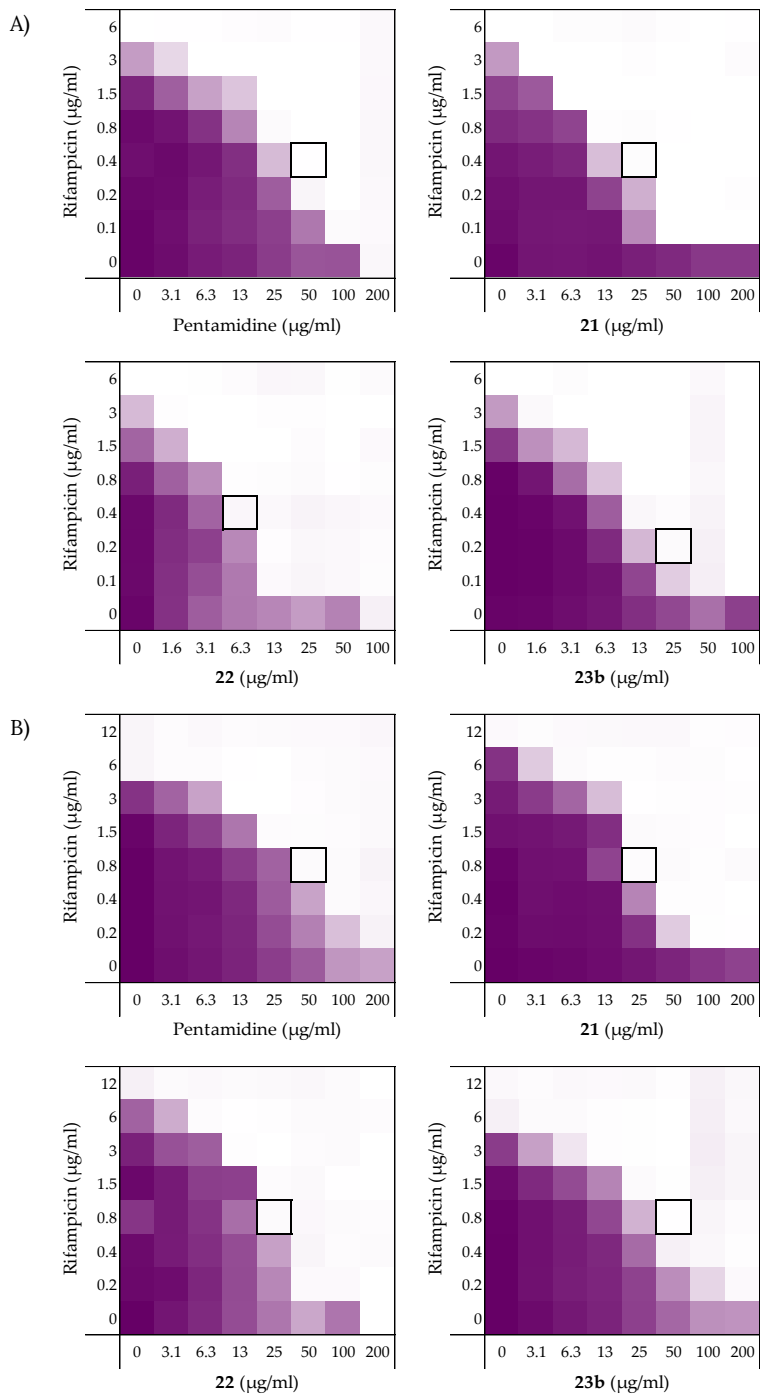
In addition, carbapenem-resistant *E. coli* RC0089, a clinical isolate producing New Delhi β -lactamase 1 (NDM-1), was also evaluated to assess whether this resistance mechanism affected the synergistic activity of the bis-amidines here studied. Notably, the MIC of rifampicin was significantly elevated against this strain (MIC of >192 $\mu\text{g/mL}$,

see Supporting information Figure S13 and Table S13). While the bis-amidines were again found to synergize with rifampicin, the FICI values calculated were elevated, with the exception of compound **22** (Figure 7C and Table 3). Interestingly, this strain also resulted in an increased FICI for PMBN.

Table 3. FICI values of pentamidine (**1**), **21**, **22**, **23b**, and PMBN in combination with rifampicin against different *E. coli* strains including polymyxin- and carbapenem-resistant strains.^a

Strain	Pentamidine (1)	21	22	23b	PMBN
Wild-type					
BW25113	0.375	≤0.094	≤0.188	≤0.156	≤0.039
ATCC25922	0.313	≤0.125	0.094	0.156	≤0.047
W3110	≤0.188	≤0.188	0.313	≤0.188	≤0.031
552060.1	0.375	≤0.094	0.250	≤0.188	≤0.047
Polymyxin-resistant					
BW25113 mcr-1	≤0.250	≤0.094	≤0.156	≤0.188	≤0.156
mcr-1	≤0.188	≤0.188	≤0.188	≤0.188	≤0.094
EQASmcr-1	≤0.250	≤0.125	0.188	≤0.188	≤0.125
EQASmcr-2	0.375	≤0.125	0.313	≤0.125	≤0.156
EQASmcr-3	≤0.188	≤0.125	≤0.188	≤0.188	≤0.094
Carbapenem-resistant					
RC0089	≤0.375	≤0.250	≤0.156	≤0.375	≤0.188

^aMIC and minimal synergistic concentrations (MSC) data can be found in the Supporting information, Table S2, S5-S13.



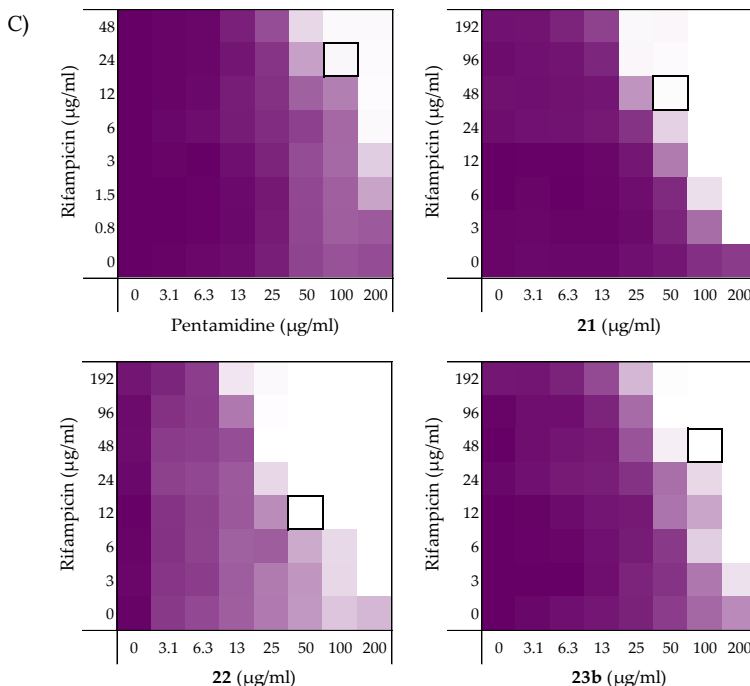


Figure 7. Checkerboard assays of compounds pentamidine (**1**), **21**, **22**, and **23b** in combination with rifampicin versus A) *E. coli* ATCC25922; B) *E. coli* EQASmcr-1; C) *E. coli* RC0089. In each case, the bounded box in the checkerboard assays indicates the combination of compound and antibiotic resulting in the lowest FICI (see Table 3). OD₆₀₀ values were measured using a plate reader and transformed to a gradient: purple represents growth, white represents no growth. An overview of all checkerboard assays with rifampicin with the *E. coli* strains can be found in the Supporting information, Figure S5–S13.

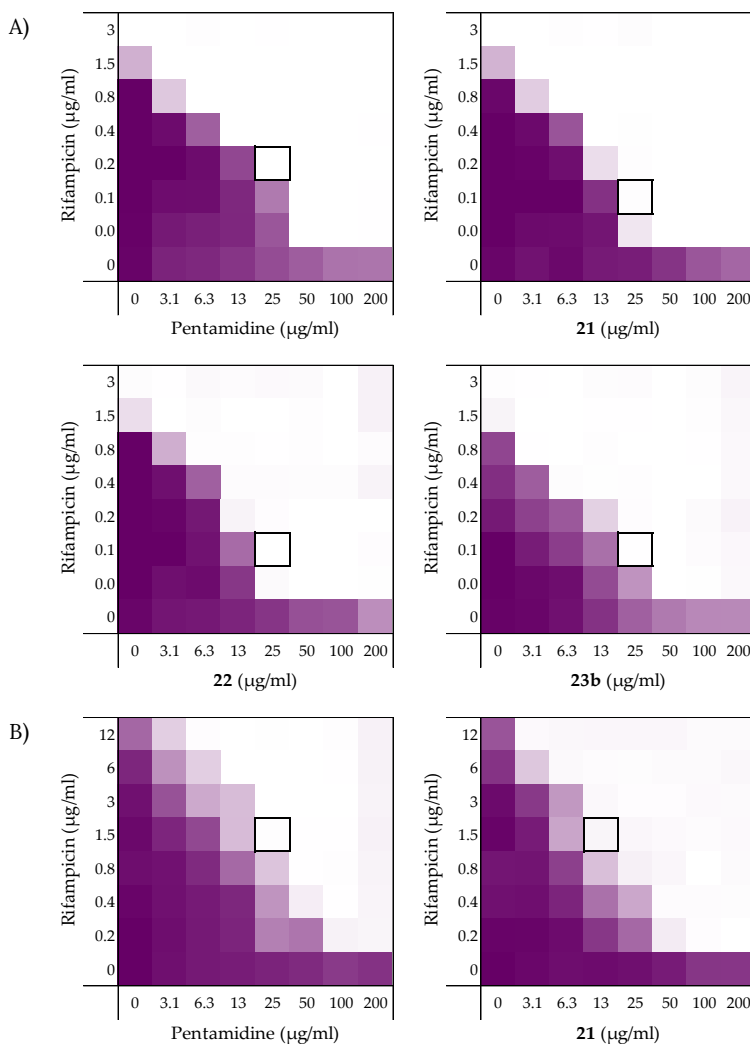
2.5.3. Synergy against *A. baumannii*, *K. pneumoniae*, and *P. aeruginosa*

In addition to studying the synergistic activity of the selected bis-amidines against the *E. coli* strains described above, we also investigated their capacity to potentiate the activity of rifampicin against the selected strains of *A. baumannii*, *K. pneumoniae*, and *P. aeruginosa* (Figure 8, Table 4). As for the *E. coli* strains, the inherent antimicrobial activities of rifampicin, pentamidine (**1**), compounds **21**, **22**, **23b**, and PMBN were first established against each strain (Supporting information Table S14–S16). Full checkerboard assays with the *A. baumannii* and *K. pneumoniae* strains tested showed the bis-amidines and PMBN to be effective synergists. In general, compounds **21**, **22**, and **23b** were found to be more potent than pentamidine (**1**), while PMBN was found to be an even more effective synergist. Among the bis-amidines tested, compound **22** displayed the most effective potentiation of rifampicin. Interestingly, when tested against *P. aeruginosa*, the FICIs determined for pentamidine and compounds **21**, **22**, and **23b** were significantly elevated while PMBN maintained potent synergistic activity.

Table 4. FICI values of pentamidine (**1**), **21**, **22**, **23b**, and PMBN in combination with rifampicin against different Gram-negative pathogens.^a

Strain	Pentamidine (1)	21	22	23b	PMBN
<i>A. baumannii</i> ATCC17978	≤0.125	≤0.094	≤0.094	≤0.094	≤0.023
<i>K. pneumoniae</i> ATCC13883	≤0.125	≤0.094	≤0.078	≤0.125	≤0.070
<i>P. aeruginosa</i> ATCC27853	≤0.500	≤0.313	≤0.250	≤0.375	0.031

^aMIC and minimal synergistic concentrations (MSC) data can be found in the Supporting information, Tables S14–S16.



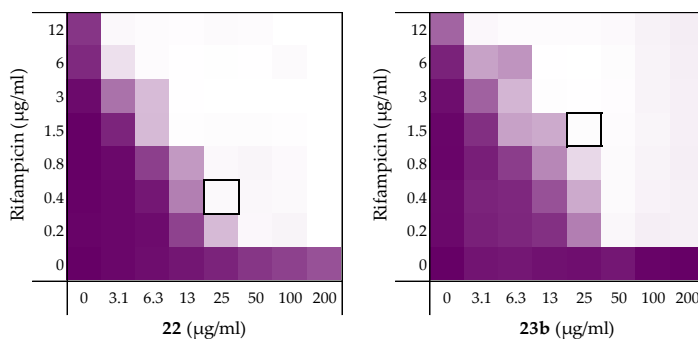


Figure 8. Checkerboard assays of pentamidine (**1**), **21**, **22**, and **23b** in combination with rifampicin and versus A) *A. baumannii* ATCC17978 and B) *K. pneumoniae* ATCC13883. In each case, the bounded box in the checkerboard assays indicates the combination of compound and antibiotic resulting in the lowest FICI (see Table 4). OD₆₀₀ values were measured using a plate reader and transformed to a gradient: purple represents growth, white represents no growth. An overview of all checkerboard assays with rifampicin with the *E. coli* strains can be found in the Supporting information, Figures S14–S16.

2.6. Mechanistic studies

To characterize the mechanism of action of the bis-amidines here studied, we next investigated the capacity of the most active compounds to disrupt the Gram-negative OM. This line of investigation was based in part on the previously noted interaction of pentamidine with lipid A and also on the knowledge that the potentiation of antibiotics like erythromycin, rifampicin, and novobiocin generally relies on OM disruption.^{7,20,66} To this end, we employed an established assay relying on the fluorescent properties of N-phenyl-naphthalen-1-amine (NPN) allowing for the real time monitoring and quantification of OM disruption.⁶⁷ In the presence of intact bacterial cells, NPN exhibits relatively low levels of fluorescence. However, in the event that the OM is disrupted, NPN can gain entry to the phospholipid layer resulting in a detectable increase in fluorescence that can, in turn, be measured.⁶⁷ For this assay, we selected compounds **21** and **22** based on their consistently potent activity in the various synergy assays described above. The bacterial strain used was *E. coli* BW25113 and pentamidine (**1**) and PMBN were taken along as benchmarks. As illustrated in Figure 9, a clear, dose-dependent increase in the fluorescent signal is observed for both **21** and **22**, indicating effective OM disruption. In general, both compounds appear to outperform pentamidine in their ability to disrupt the OM with compound **22** also exhibiting a stronger effect than PMBN (see Supporting information, Figure S19 for NPN fluorescence at higher concentrations of bis-amidines and PMBN).

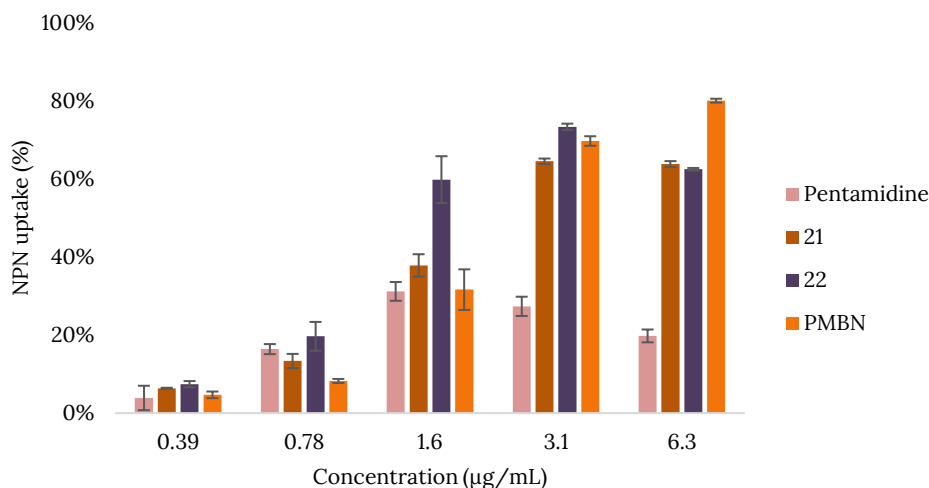


Figure 9. Outer membrane permeabilization assay of pentamidine (**1**), compounds **21**, **22**, and PMBN with *E. coli* BW25113 using N-phenyl-1-naphthylamine (NPN) as fluorescent probe. The read-out was performed after 60 minutes of incubation using a plate reader with λ_{ex} 355 nm and λ_{em} 420 nm. The NPN uptake values shown are relative to the uptake signal obtained upon treating the cells with 100 µg/mL colistin as previously reported.⁶⁸ All values corrected for background signal of the negative control. Error bars represent the standard deviation based on n=3 technical replicates.

3. Conclusion

We here describe structure-activity relationship studies aimed at delivering new insights into the capacity for small-molecule bis-amidines to potentiate the activity of Gram-positive specific antibiotics against Gram-negative bacteria. Inspired by the finding that the anti-parasitic drug pentamidine disrupts the Gram-negative OM to synergize with antibiotics like erythromycin, rifampicin, and novobiocin, we prepared a number of structurally similar bis-amidines and characterized their synergistic potential with the same antibiotics. Our studies confirm that the length, rigidity, and hydrophobicity of the linker unit present in these bis-amidines play an important role in determining their ability to potentiate Gram-positive specific antibiotics.⁷ Also of note, however, is the finding that the potent synergy exhibited by bis-amidines containing long, hydrophobic linkers is likely driven by nonspecific membrane disruption as indicated by the strong hemolytic activity associated with these analogues. Further assessment of the linker motif also revealed that, in general, a single aromatic ring provides a desirable balance of enhanced synergistic activity relative to pentamidine, without introducing hemolytic activity. Further examination of the relative positioning of the benzamidine groups on the aromatic linker and as well as the *ortho*-, *meta*-, and *para*-, geometry of the amidine moieties themselves, identified compounds **21**, **22**, and **23b** as most promising. These compounds were found to consistently outperform pentamidine in their ability to potentiate the activity of erythromycin, rifampicin, and novobiocin against a number of *E. coli* strains including polymyxin-resistant and carbapenem-resistant variants. Additional screening showed that among the bis-amidines here studied, compounds **21**, **22**, and **23b** maintain their superior synergistic activity against other Gram-negative pathogens including *A. baumannii*, *K. pneumoniae*, and *P. aeruginosa*. Mechanistic studies also confirm that these bis-amidines effectively induce Gram-negative OM disruption. Taken together, the findings here reported provide a broader understanding of the potential for bis-amidines to be used as synergists in expanding the activity of Gram-positive specific antibiotics against Gram-negative bacteria.

4. Materials and methods

General procedures. All reagents employed were of American Chemical Society (ACS) grade or finer and were used without further purification unless otherwise stated. For compound characterization, ¹H NMR spectra were recorded at 400 MHz with chemical shifts reported in parts per million (ppm) downfield relative to CHCl₃ (7.26) or DMSO (δ 2.50). ¹H NMR data are reported in the following order: multiplicity (s, singlet; d, doublet; t, triplet; q, quartet and m, multiplet), coupling constant (J) in hertz (Hz) and the number of protons. Where appropriate, the multiplicity is preceded by br, indicating that the signal was broad. ¹³C NMR spectra were recorded at 101 MHz with chemical shifts reported relative to CDCl₃ (δ 77.16) or DMSO (δ 39.52). HRMS analysis was performed on a Shimadzu Nexera X2 UHPLC system with a Waters Acquity HSS C18 column (2.1 × 100 mm, 1.8 μm) at 30 °C and equipped with a diode array detector. The following solvent system, at a flow rate of 0.5 mL/min, was used: solvent A, 0.1 % formic acid in water; solvent B, 0.1 % formic acid in acetonitrile. Gradient elution was as follows: 95:5 (A/B) for 1 min, 95:5 to 15:85 (A/B) over 6 min, 15:85 to 0:100 (A/B) over 1 min, 0:100 (A/B) for 3 min, then reversion back to 95:5 (A/B) for 3 min. This system was connected to a Shimadzu 9030 QTOF mass spectrometer (ESI ionisation) calibrated internally with Agilent's API-TOF reference mass solution kit (5.0 mM purine, 100.0 mM ammonium trifluoroacetate and 2.5 mM hexakis(1H,1H,3H-tetrafluoropropoxy)phosphazine) diluted to achieve a mass count of 10000. Compounds **13**, **14**, **33**, and **34** were synthesized as previously described and had NMR spectra and mass spectra consistent with the assigned structures.^{32,69} Compounds **1**, **2**, **4-6**, **8-11**, **15**, **18**, **19**, **21-23**, **1b**, **21b-23b**, **39**, **40**, **45**, **47**, and **48** were synthesized using optimized protocols as described below and gave NMR spectra and mass spectra consistent for the same compounds previously described in literature.^{22,29,32,34,38,39,70-74} Purity of the final compounds **1-3**, **9-12**, **15**, **16**, **21-24**, **1b**, **21b-23b**, **1c**, **21c-23c**, **37**, **38**, **43**, and **44** was confirmed to be ≥ 95% by analytical RP-HPLC using a Shimadzu Prominence-i LC-2030 system with a Dr. Maisch Reprosil Gold 120 C18 column (4.6 × 250 mm, 5 μm) at 30 °C and equipped with a UV detector monitoring at 214 nm. The following solvent system, at a flow rate of 1 mL/min, was used: solvent A, 0.1 % TFA in water/acetonitrile, 95/5; solvent B, 0.1 % TFA in water/acetonitrile, 5/95. Gradient elution was as follows: 95:5 (A/B) for 2 min, 95:5 to 0:100 (A/B) over 30 min, 0:100 (A/B) for 1 min, then reversion back to 95:5 (A/B) over 1 min, 95:5 (A/B) for 3 min. The compounds were purified via preparative HPLC using a BESTA-Technik system with a Dr. Maisch Reprosil Gold 120 C18 column (25 × 250 mm, 10 μm) and equipped with a ECOM Flash UV detector monitoring at 214 nm. The following solvent system, at a flow rate of 12 mL/min, was used: solvent A, 0.1 % TFA in water/acetonitrile 95/5; solvent B, 0.1 % TFA in water/acetonitrile 5/95. Unless stated otherwise in the protocol, the gradient elution was as follows: 100:0 (A/B) to 0:100 (A/B) over 25 min, 0:100 (A/B) for 3 min, then reversion back to 100:0 (A/B) over 1 min, 100:0 (A/B) for 1 min.

4.1. Synthesis

4,4'-(pentane-1,5-diylbis(oxy))dibenzimidamide/pentamidine (1) This protocol was based on the synthesis of structurally similar amidine containing compounds previously described in literature.²⁸⁻³¹ 4,4'-(pentane-1,5-diylbis(oxy))dibenzonitrile (94 mg, 0.3 mmol) was dissolved in dry THF (2 mL) under argon atmosphere and LHMDs (1.2 mL, 1 M THF solution, 4.0 eq.) was added. The reaction was stirred at room temperature for 48 hours or longer until complete conversion to the bis-amidine (monitored by LCMS). The solution was cooled to 0 °C and quenched with HCl (4.5 mL, 4 M dioxane solution, 60 eq.). The mixture was stirred at room temperature overnight, then diluted with diethyl ether and filtered. The precipitate was purified by preparative HPLC with the gradient 0-100% in 30 minutes to give pentamidine (**1**) (120 mg, quant.). ¹H NMR (400 MHz, DMSO-d₆) δ 9.14 (s, 4H), 9.06 (s, 4H), 7.81 (d, J = 8.9 Hz, 4H), 7.15 (d, J = 8.9 Hz, 4H), 4.12 (t, J = 6.4 Hz, 4H), 1.88 – 1.75 (m, 4H), 1.65 – 1.52 (m, 2H). ¹³C NMR (101 MHz, DMSO) δ 164.70, 163.06, 130.19, 119.50, 114.79, 68.05, 28.21, 22.09. HRMS (ESI): calculated for C₁₉H₂₄N₄O₂ [M+H]⁺ 341.1977, found 341.1977.

4,4'-((nonane-1,9-diylbis(oxy))dibenzimidamide/nonamidine (2) Following the procedure as described for compound **1**, using compound **7** (100 mg, 0.28 mmol), LHMDS (1.5 mL, 1 M THF solution, 5.4 eq.) and HCl (5 mL, 4 M dioxane solution, 71 eq.), afforded the crude product. Purification by preparative HPLC with the gradient 20–100% in 30 minutes afforded compound **2** (86 mg, 84%). ¹H NMR (400 MHz, DMSO-*d*₆) δ 9.14 (d, *J* = 6.2 Hz, 8H), 7.81 (d, *J* = 8.9 Hz, 4H), 7.13 (d, *J* = 9.0 Hz, 4H), 4.07 (t, *J* = 6.5 Hz, 4H), 1.78 – 1.67 (m, 4H), 1.48 – 1.27 (m, 10H). ¹³C NMR (101 MHz, DMSO) δ 164.82, 163.12, 130.21, 119.50, 114.82, 68.16, 29.01, 28.77, 28.52, 25.47. HRMS (ESI): calculated for C₂₃H₃₂N₄O₂ [M+H]⁺ 397.2604, found 397.2597.

4,4'-((3-phenylpentane-1,5-diyl)bis(oxy))dibenzimidamide (3) 4,4'-((3-phenylpentane-1,5-diyl)bis(oxy))dibenzonitrile (109 mg, 0.28 mmol) was dissolved in the LHMDS solution (1.1 mL, 1 M THF solution, 4.0 eq.) under argon atmosphere. The reaction was stirred at room temperature for 48 hours or longer until complete conversion to the bis-amidine (monitored by LCMS). The solution was cooled to 0 °C and quenched with HCl (4.5 mL, 4 M dioxane solution, 60 eq.). The mixture was stirred at room temperature overnight, then diluted with diethyl ether and filtered. The precipitate was purified by preparative HPLC with the gradient 20–100% in 30 minutes to give compound **3** (27.4 mg, 23%). ¹H NMR (400 MHz, DMSO-*d*₆) δ 9.11 (d, *J* = 12.6 Hz, 8H), 7.77 (d, *J* = 8.9 Hz, 4H), 7.34 – 7.16 (m, 5H), 7.05 (d, *J* = 9.0 Hz, 4H), 4.00 – 3.90 (m, 2H), 3.83 (dd, *J* = 15.0, 8.9 Hz, 2H), 3.14 – 3.04 (m, 1H), 2.29 – 2.16 (m, 2H), 2.13 – 2.00 (m, 2H). ¹³C NMR (101 MHz, DMSO) δ 164.81, 162.92, 143.38, 130.21, 128.62, 127.69, 126.58, 119.64, 66.21, 38.31, 35.10. HRMS (ESI): calculated for C₂₅H₂₈N₄O₂ [M+H]⁺ 417.2291, found 417.2287.

4,4'-((propane-1,3-diylbis(oxy))dibenzonitrile (4) These conditions were based on literature protocols.²² 4-cyanophenol (0.29 g, 2.4 mmol, 2.4 eq.) was suspended in dry DMF (3 mL) under argon atmosphere. The suspension was cooled to 0 °C using an ice bath and NaH (96 mg, 60% dispersion in mineral oil, 2.4 eq.) was slowly added. The reaction was stirred until a clear solution appeared, the ice bath was removed and 1,3-dibromopropane (202 mg, 1 mmol) was added. The reaction mixture was heated to 80 °C for 1 hour and then cooled to room temperature. Water (10 mL) was added to the mixture to obtain precipitation. The precipitate was filtered, washed with water and recrystallized from EtOH to give compound **4** as white crystals (164 mg, 59%). ¹H NMR (400 MHz, CDCl₃) δ 7.59 (d, *J* = 8.9 Hz, 4H), 6.95 (d, *J* = 8.9 Hz, 4H), 4.21 (t, *J* = 6.0 Hz, 4H), 2.37 – 2.27 (m, 2H). ¹³C NMR (101 MHz, CDCl₃) δ 162.09, 134.19, 119.26, 115.29, 104.39, 64.56, 28.96.

4,4'-((heptane-1,7-diylbis(oxy))dibenzonitrile (5) Following the procedure as described above for compound **4**, using 1,7-dibromoheptane (0.60 mL, 3.5 mmol), afforded compound **5** (1.17 g, quant.). ¹H NMR (400 MHz, CDCl₃) δ 7.56 (d, *J* = 8.8 Hz, 4H), 6.92 (d, *J* = 8.8 Hz, 4H), 3.99 (t, *J* = 6.4 Hz, 4H), 1.89 – 1.76 (m, 4H), 1.55 – 1.40 (m, 6H). ¹³C NMR (101 MHz, CDCl₃) δ 162.49, 134.09, 119.42, 115.26, 103.82, 68.38, 29.14, 29.03, 26.00.

4,4'-((octane-1,8-diylbis(oxy))dibenzonitrile (6) Following the procedure as described above for compound **4**, using 1,8-dibromooctane (0.64 mL, 3.5 mmol), afforded compound **6** (1.10 g, 90%). ¹H NMR (400 MHz, CDCl₃) δ 7.57 (d, *J* = 8.9 Hz, 4H), 6.93 (d, *J* = 8.9 Hz, 4H), 3.99 (t, *J* = 6.5 Hz, 4H), 1.84 – 1.77 (m, 4H), 1.51 – 1.43 (m, 4H), 1.43 – 1.35 (m, 4H). ¹³C NMR (101 MHz, CDCl₃) δ 162.54, 134.12, 119.45, 115.29, 103.86, 68.46, 29.37, 29.11, 26.04.

4,4'-((nonane-1,9-diylbis(oxy))dibenzonitrile (7) Following the procedure as described above for compound **4**, using 1,9-dibromononane (0.71 mL, 3.5 mmol), afforded compound **7** (1.26 g, 99%). ¹H NMR (400 MHz, CDCl₃) δ 7.57 (d, *J* = 8.9 Hz, 4H), 6.93 (d, *J* = 8.8 Hz, 4H), 3.99 (t, *J* = 6.5

Hz, 4H), 1.86 – 1.75 (m, 4H), 1.51 – 1.41 (m, 4H), 1.40 – 1.30 (m, 6H). ¹³C NMR (101 MHz, CDCl₃) δ 162.55, 134.11, 119.46, 115.29, 103.82, 68.49, 29.56, 29.39, 29.11, 26.07.

4,4'-(undecane-1,11-diylbis(oxy))dibenzonitrile (8) Following the procedure as described above for compound **4**, using 1,11-dibromoundecane (0.82 mL, 3.5 mmol), afforded compound **8** (1.24 g, 92%). ¹H NMR (400 MHz, CDCl₃) δ 7.57 (d, J = 8.9 Hz, 4H), 6.93 (d, J = 8.9 Hz, 4H), 3.99 (t, J = 6.5 Hz, 4H), 1.84 – 1.75 (m, 4H), 1.49 – 1.40 (m, 4H), 1.39 – 1.28 (m, 10H). ¹³C NMR (101 MHz, CDCl₃) δ 162.57, 134.11, 119.47, 115.30, 103.80, 68.53, 29.65, 29.63, 29.46, 29.12, 26.08.

4,4'-(propane-1,3-diylbis(oxy))dibenzimidamide/propamidine (9) Following the procedure as described above for pentamidine (**1**), using compound **4** (60 mg, 0.2 mmol). After LCMS analysis of the reaction mixture at 48 hours, LHMDS (0.2 mL, 1 M THF solution, 1 eq) was added. The HCl quench was therefore also increased (4 mL, 4 M dioxane solution, 75 eq). Compound **9** was obtained after HPLC purification (33 mg, 49%). ¹H NMR (400 MHz, DMSO-*d*₆) δ 9.15 (d, J = 9.4 Hz, 8H), 7.82 (d, J = 8.9 Hz, 4H), 7.18 (d, J = 8.9 Hz, 4H), 4.27 (t, J = 6.2 Hz, 4H), 2.24 (p, J = 6.2 Hz, 2H). ¹³C NMR (101 MHz, DMSO) δ 164.73, 162.82, 130.22, 119.76, 114.84, 64.84, 28.26. HRMS (ESI): calculated for C₁₇H₂₀N₄O₂ [M+H]⁺ 313.1664, found 313.1662.

4,4'-(heptane-1,7-diylbis(oxy))dibenzimidamide/heptamidine (10) Following the procedure as described above for compound **3**, using compound **5** (100 mg, 0.3 mmol), LHMDS (1.5 mL, 1 M THF solution, 5 eq.) and HCl (5 mL, 4 M dioxane solution, 67 eq.), afforded compound **10** (95.3 mg, 86%). ¹H NMR (400 MHz, DMSO-*d*₆) δ 9.13 (d, J = 17.8 Hz, 8H), 7.81 (d, J = 8.9 Hz, 4H), 7.14 (d, J = 9.0 Hz, 4H), 4.08 (t, J = 6.5 Hz, 4H), 1.81 – 1.69 (m, 4H), 1.49 – 1.36 (m, 6H). ¹³C NMR (101 MHz, DMSO) δ 164.80, 163.12, 130.21, 119.50, 114.82, 68.14, 28.51, 28.47, 25.43. HRMS (ESI): calculated for C₂₁H₂₈N₄O₂ [M+H]⁺ 369.2290, found 369.2290.

4,4'-(octane-1,8-diylbis(oxy))dibenzimidamide/octamidine (11) Following the procedure as described above for compound **3**, using compound **6** (100 mg, 0.29 mmol). After LCMS analysis of the reaction mixture at 48 hours, LHMDS (0.3 mL, 1 M THF solution, 1 eq) was added, bringing the total of equivalents to 5. After an acidic quench with HCl (5 mL, 4 M dioxane solution, 69 eq.) the reaction was stirred overnight. HPLC purification afforded the product **11** (41 mg, 41%). ¹H NMR (400 MHz, DMSO-*d*₆) δ 8.95 (br, 8H), 7.78 (d, J = 8.9 Hz, 4H), 7.13 (d, J = 8.9 Hz, 4H), 4.06 (t, J = 6.5 Hz, 4H), 1.79 – 1.67 (m, 4H), 1.46 – 1.31 (m, 8H). ¹³C NMR (101 MHz, DMSO) δ 164.75, 163.19, 130.29, 119.49, 114.88, 68.22, 28.81, 28.55, 25.50. HRMS (ESI): calculated for C₂₂H₃₀N₄O₂ [M+H]⁺ 383.2447, found 383.2446.

4,4'-(undecane-1,11-diylbis(oxy))dibenzimidamide/undecamidine (12) Following the procedure as described above for compound **3**, using compound **8** (98 mg, 0.25 mmol), LHMDS (1 mL, 1 M THF solution, 4 eq.) and HCl (2 mL, 4M dioxane solution, 32 eq.), afforded the product **12** (68 mg, 64%). ¹H NMR (400 MHz, DMSO-*d*₆) δ 8.96 (br, 8H), 7.79 (d, J = 8.8 Hz, 4H), 7.14 (d, J = 8.9 Hz, 4H), 4.07 (t, J = 6.5 Hz, 4H), 1.78 – 1.67 (m, 4H), 1.44 – 1.26 (m, 14H). ¹³C NMR (101 MHz, DMSO) δ 164.81, 163.12, 130.20, 119.48, 114.81, 68.15, 29.06, 29.02, 28.82, 28.52, 25.48. HRMS (ESI): calculated for C₂₅H₃₆N₄O₂ [M+H]⁺ 425.2916, found 425.2919.

4-(2-bromoethoxy)benzonitrile (13) Protocol as described in literature.⁶⁹ 1,2-dibromoethane (4.3 mL, 50 mmol, 5 eq.), 4-cyanophenol (1.2 g, 10 mmol) and K₂CO₃ (4.2 g, 30 mmol, 3 eq.) were suspended in dry DMF (20 mL) under argon atmosphere. The mixture was stirred at 100 °C for 5 hours, cooled to room temperature and EtOAc and

water were added. The organic layer was separated, washed with brine, dried over Na₂SO₄ and concentrated in vacuo. The crude product was purified by column chromatography (petroleum ether/EtOAc = 9:1) to afford compound **13** (0.97 g, 43%). ¹H NMR (400 MHz, CDCl₃) δ 7.60 (d, J = 9.0 Hz, 2H), 6.96 (d, J = 8.9 Hz, 2H), 4.33 (t, J = 6.1 Hz, 2H), 3.66 (t, J = 6.1 Hz, 2H). ¹³C NMR (101 MHz, CDCl₃) δ 161.44, 134.24, 119.11, 115.44, 104.88, 68.08, 28.47.

4,4'-((thiobis(ethane-2,1-diyl))bis(oxy))dibenzonitrile (14**)** Protocol as described in literature.³² Compound **13** (0.96 g, 4.3 mmol, 2 eq.) and Na₂S·9H₂O (0.51 g, 2.1 mmol) were dissolved in DMSO (5 mL) and the mixture was stirred at 115 °C under argon atmosphere. After 1 hour, the mixture was poured into ice water (25 mL) and left for 24 hours in the fridge. The precipitate was filtered, washed with cold water and recrystallized from EtOH to obtain compound **14** (0.65 g, 93%). ¹H NMR (400 MHz, CDCl₃) δ 7.58 (d, J = 8.9 Hz, 4H), 6.94 (d, J = 8.9 Hz, 4H), 4.23 (t, J = 6.4 Hz, 4H), 3.05 (t, J = 6.4 Hz, 4H). ¹³C NMR (101 MHz, CDCl₃) δ 161.73, 134.20, 119.15, 115.31, 104.61, 68.35, 31.71.

4,4'-((thiobis(ethane-2,1-diyl))bis(oxy))dibenzimidamide (15**)** Following the procedure as described above for compound **3**, using compound **14** (100 mg, 0.31 mmol), LHMDS (1.55 mL, 1 M THF solution, 5 eq.) and quenched with and HCl (5.2 mL, 4 M dioxane solution, 67 eq.), afforded the product **15** (71 mg, 64%). ¹H NMR (400 MHz, DMSO-*d*₆) δ 9.00 (s, 6H), 7.81 (d, J = 8.9 Hz, 4H), 7.18 (d, J = 8.9 Hz, 4H), 4.29 (t, J = 6.4 Hz, 4H), 3.04 (t, J = 6.4 Hz, 4H). ¹³C NMR (101 MHz, DMSO) δ 164.61, 162.61, 130.24, 119.80, 114.86, 68.01, 30.54. HRMS (ESI): calculated for C₁₈H₂₂N₄O₂S [M+H]⁺ 359.1541, found 359.1541.

4,4'-((sulfonylbis(ethane-2,1-diyl))bis(oxy))dibenzimidamide (16**)** Compound **15** (100 mg, 0.22 mmol) was dissolved in dry DCM (10 mL) under argon atmosphere. The solution was cooled to 0 °C using an ice bath and *m*-CPBA (54 mg, 77% aqueous solution, 1.1 eq.) was added. The mixture was stirred at 0 °C for 2 hours and then concentrated in vacuo. After HPLC purification with a 0-100% gradient in 30 minutes to obtain compound **16** (27 mg, 32%). ¹H NMR (400 MHz, DMSO-*d*₆) δ 9.18 (s, 4H), 8.99 (s, 4H), 7.83 (d, J = 8.9 Hz, 4H), 7.21 (d, J = 9.0 Hz, 4H), 4.52 (t, J = 5.5 Hz, 4H), 3.79 (t, J = 5.5 Hz, 4H). ¹³C NMR (101 MHz, DMSO) δ 164.65, 162.00, 130.29, 120.39, 114.94, 62.19, 53.38. HRMS (ESI): calculated for C₁₈H₂₂N₄O₄S [M+H]⁺ 391.1441, found 391.1434.

4,4'-((1,2-phenylenebis(methylene))bis(oxy))dibenzonitrile (17**)** Following the procedure as described above for compound **4**, using 1,2-bis(bromomethyl)benzene (1.0 g, 3.8 mmol), afforded the title compound as crude product. No precipitation occurred upon addition of water. Therefore the mixture was concentrated under reduced pressure and the crude product was purified by column chromatography (petroleum ether/EtOAc = 19:1) to obtain compound **17** (1.2 g, 96%). ¹H NMR (400 MHz, CDCl₃) δ 7.59 (d, J = 8.0 Hz, 4H), 7.46 (dd, 4H), 6.99 (d, J = 8.0 Hz, 4H), 5.21 (s, 4H). ¹³C NMR (101 MHz, CDCl₃) δ 161.76, 134.26, 134.12, 129.56, 129.27, 119.12, 115.57, 104.79, 68.46.

4,4'-((1,3-phenylenebis(methylene))bis(oxy))dibenzonitrile (18**)** Following the procedure as described above for compound **4**, using 1,3-bis(bromomethyl)benzene (0.92 g, 3.5 mmol), afforded compound **18** (0.94 g, 79%). ¹H NMR (400 MHz, CDCl₃) δ 7.59 (d, J = 8.8 Hz, 4H), 7.50 – 7.37 (m, 4H), 7.02 (d, J = 8.8 Hz, 4H), 5.13 (s, 4H). ¹³C NMR (101 MHz, CDCl₃) δ 161.92, 136.51, 134.19, 129.37, 127.60, 126.52, 119.21, 115.66, 104.54, 70.09.

4,4'-((1,4-phenylenebis(methylene))bis(oxy))dibenzonitrile (19**)** Following the procedure as described above for compound **4**, using 1,4-bis(bromomethyl)benzene (0.92 g, 3.5 mmol), afforded compound **19** as a crude product. The crude product was not

recrystallized due to insolubility issues and was used in the next step without further purification based on a purity assessment (NMR) (1.2 g, 97%). ¹H NMR (400 MHz, DMSO-*d*₆) δ 7.78 (d, *J* = 8.8 Hz, 4H), 7.48 (s, 4H), 7.18 (d, *J* = 8.9 Hz, 4H), 5.22 (s, 4H). ¹³C NMR (101 MHz, DMSO) δ 161.74, 136.11, 134.24, 128.08, 119.13, 115.92, 103.05, 69.36.

4,4'-((2-benzylpropane-1,3-diyl)bis(oxy))dibenzonitrile (20) Following the procedure as described above for compound **4**, using 2,7-bis(bromomethyl)naphthalene (0.20 g, 0.64 mmol), afforded compound **20** as a crude product. The crude product was not recrystallized due to insolubility issues and was used in the next step without further purification based on a purity assessment (NMR) (0.25 g, quant.). ¹H NMR (400 MHz, CDCl₃) δ 7.90 (d, *J* = 8.5 Hz, 2H), 7.87 (s, 2H), 7.60 (d, *J* = 8.9 Hz, 4H), 7.54 (dd, *J* = 8.5, 1.7 Hz, 2H), 7.06 (d, *J* = 8.9 Hz, 4H), 5.29 (s, 4H). ¹³C NMR (101 MHz, CDCl₃) δ 134.23, 134.04, 133.08, 128.74, 126.61, 125.65, 119.26, 115.77, 104.56, 70.42.

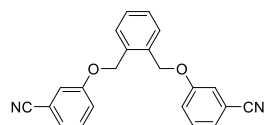
4,4'-((1,2-phenylenebis(methylene))bis(oxy))dibenzimidamide (21) Following the procedure as described above for compound **3**, using compound **17** (102 mg, 0.3 mmol), LHMDS (1.5 mL, 1 M THF solution, 5 eq.) and HCl (5.0 mL, 4 M dioxane solution, 67 eq.), afforded the product **21** (63 mg, 56%). ¹H NMR (400 MHz, DMSO-*d*₆) δ 9.14 (s, 4H), 9.04 (s, 4H), 7.81 (d, *J* = 8.9 Hz, 4H), 7.55 (dd, *J* = 5.6, 3.4 Hz, 2H), 7.40 (dd, *J* = 5.7, 3.3 Hz, 2H), 7.24 (d, *J* = 9.0 Hz, 4H), 5.38 (s, 4H). ¹³C NMR (101 MHz, DMSO) δ 164.70, 162.45, 134.57, 130.19, 128.82, 128.44, 120.04, 115.18, 67.51. HRMS (ESI): calculated for C₂₂H₂₂N₄O₂ [M+H]⁺ 375.1821, found 375.1821.

4,4'-((1,3-phenylenebis(methylene))bis(oxy))dibenzimidamide (22) Following the procedure as described above for compound **3**, using compound **18** (100 mg, 0.29 mmol), LHMDS (2.35 mL, 1 M THF solution, 8 eq.) and HCl (4.35 mL, 4 M dioxane solution, 60 eq.), afforded the product **22** (91 mg, 83%). ¹H NMR (400 MHz, DMSO-*d*₆) δ 9.13 (s, 4H), 8.85 (s, 4H), 7.80 (d, *J* = 8.9 Hz, 4H), 7.56 (s, 1H), 7.44 (d, *J* = 1.3 Hz, 3H), 7.23 (d, *J* = 9.0 Hz, 4H), 5.24 (s, 4H). ¹³C NMR (101 MHz, DMSO) δ 164.60, 162.61, 136.67, 130.24, 127.66, 127.19, 119.90, 115.15, 69.54. HRMS (ESI): calculated for C₂₂H₂₂N₄O₂ [M+H]⁺ 375.1821, found 375.1821.

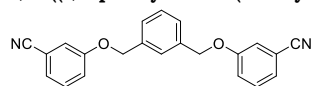
4,4'-((1,4-phenylenebis(methylene))bis(oxy))dibenzimidamide (23) Following the procedure as described above for compound **3**, using compound **19** (102 mg, 0.3 mmol), LHMDS (1.5 mL, 1 M THF solution, 5 eq.) and HCl (5 mL, 4 M dioxane solution, 67 eq.), afforded the product **23** (21 mg, 19%). ¹H NMR (400 MHz, DMSO-*d*₆) δ 9.15 (s, 4H), 9.04 (s, 4H), 7.81 (d, *J* = 8.9 Hz, 4H), 7.50 (s, 4H), 7.23 (d, *J* = 9.0 Hz, 4H), 5.25 (s, 4H). ¹³C NMR (101 MHz, DMSO) δ 164.71, 162.55, 136.21, 130.20, 128.05, 119.93, 115.19, 69.34. HRMS (ESI): calculated for C₂₂H₂₂N₄O₂ [M+H]⁺ 375.1821, found 375.1820.

4,4'-((naphthalene-2,7-diylbis(methylene))bis(oxy))dibenzimidamide (24) Following the procedure as described above for compound **3**, using compound **20** (117 mg, 0.3 mmol) and LHMDS (1.5 mL, 1 M THF solution, 5 eq.). After LCMS analysis of the reaction mixture at 48 hours, LHMDS (0.5 mL, 1 M THF solution, 1.7 eq) was added. The reaction was quenched using HCl (6 mL, 4M dioxane solution, 80 eq.). Compound **24** was obtained in a 26% yield (33 mg). ¹H NMR (400 MHz, DMSO-*d*₆) δ 9.14 (s, 4H), 9.07 (s, 4H), 8.04 – 7.95 (m, 4H), 7.82 (d, *J* = 9.0 Hz, 4H), 7.61 (dd, *J* = 8.4, 1.7 Hz, 2H), 7.29 (d, *J* = 9.0 Hz, 4H), 5.42 (s, 4H). ¹³C NMR (101 MHz, DMSO) δ 164.74, 162.58, 134.48, 132.52, 132.25, 130.21, 128.15, 126.59, 126.04, 119.98, 115.27, 69.68. HRMS (ESI): calculated for C₂₆H₂₄N₄O₂ [M+H]⁺ 425.1977, found 425.1977.

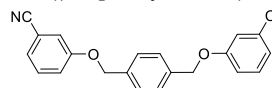
3,3'-((pentane-1,5-diylbis(oxy))dibenzonitrile (25)) Following the procedure as described above for compound **4**, using 1,5-dibromopentane (0.48 mL, 3.5 mmol) and 3-cyanophenol (1 g, 8.4 mmol), afforded compound **25** (0.68 g, 63%). ¹H NMR (400 MHz, CDCl₃) δ 7.39 – 7.34 (m, 2H), 7.25 – 7.21 (m, 2H), 7.15 – 7.10 (m, 4H), 4.00 (t, J = 6.3 Hz, 4H), 1.93 – 1.83 (m, 4H), 1.72 – 1.61 (m, 2H). ¹³C NMR (101 MHz, CDCl₃) δ 159.19, 130.48, 124.59, 119.92, 118.91, 117.46, 113.32, 68.20, 28.90, 22.79.



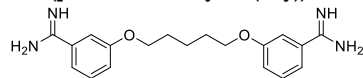
3,3'-((1,2-phenylenebis(methylene))bis(oxy))dibenzonitrile (26) Following the procedure as described above for compound **4**, using 1,2-bis(bromomethyl)benzene (1.0 g, 3.8 mmol) and 3-cyanophenol (1.1 g, 9.1 mmol, 2.4 eq.), afforded the title compound as a crude product. The crude product did not precipitate but had very high viscosity. During filtration a minimal amount of acetone was used to prevent clogging. The precipitate was collected and the filtrate was concentrated under reduced pressure to evaporate the acetone. The precipitate in the aqueous solution was filtered again with a minimal amount of acetone. This process was repeated three times to obtain compound **26** (1.1 g, 85%). ¹H NMR (400 MHz, CDCl₃) δ 7.53 – 7.47 (m, 2H), 7.45 – 7.35 (m, 4H), 7.28 – 7.27 (m, 1H), 7.26 – 7.25 (m, 1H), 7.20 – 7.16 (m, 4H), 5.18 (s, 4H). ¹³C NMR (101 MHz, CDCl₃) δ 158.65, 134.27, 130.67, 129.54, 129.22, 125.21, 120.18, 118.71, 117.74, 113.49, 68.55.



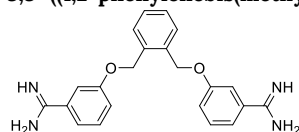
3,3'-((1,3-phenylenebis(methylene))bis(oxy))dibenzonitrile (27) Following the procedure as described above for compound **4**, using 1,3-bis(bromomethyl)benzene (0.92 g, 3.5 mmol) and 3-cyanophenol (1.0 g, 8.4 mmol, 2.4 eq.), afforded compound **27** as a crude product. The crude product was not recrystallized due to insolubility issues and was used in the next step without further purification based on a purity assessment (NMR) (1.2 g, quant.). ¹H NMR (400 MHz, CDCl₃) δ 7.51 – 7.34 (m, 6H), 7.28 – 7.24 (m, 2H), 7.23 – 7.17 (m, 4H), 5.11 (s, 4H). ¹³C NMR (101 MHz, CDCl₃) δ 158.73, 136.65, 130.56, 129.34, 127.48, 126.41, 125.02, 120.22, 118.77, 117.91, 113.38, 70.14.



3,3'-((1,4-phenylenebis(methylene))bis(oxy))dibenzonitrile (28) Following the procedure as described above for compound **4**, using 1,4-bis(bromomethyl)benzene (0.9 g, 4 mmol) and 3-cyanophenol (1.1 g, 9.6 mmol, 2.4 eq.), produced compound **28** (1.3 g, 97%). ¹H NMR (400 MHz, CDCl₃) δ 7.46 (s, 4H), 7.41 – 7.35 (m, 2H), 7.29 – 7.24 (m, 3H), 7.20 (m, 4H), 5.10 (s, 4H). ¹³C NMR (101 MHz, CDCl₃) δ 158.78, 136.21, 130.58, 127.96, 125.03, 120.27, 118.80, 117.93, 113.42, 70.08.



3,3'-((pentane-1,5-diylbis(oxy))dibenzimidamide (1b)) Following the procedure as described above for compound **3**, using compound **25** (92 mg, 0.3 mmol). LHMDS (1.5 mL, 1 M THF solution, 5 eq.) was added and after LCMS analysis of the reaction mixture at 48 hours, LHMDS (3.0 mL, 1 M THF solution, 10 eq.) was additionally added. A quench with HCl (5.0 mL, 4 M dioxane solution, 67 eq.), afforded the crude product. The crude product was purified using HPLC affording compound **1b** (93 mg, 91%). ¹H NMR (400 MHz, DMSO-*d*₆) δ 9.46 (s, 4H), 9.32 (s, 4H), 7.52 (t, J = 8.1 Hz, 2H), 7.38 (d, J = 6.6 Hz, 4H), 7.29 (d, J = 8.8 Hz, 2H), 4.09 (t, J = 6.3 Hz, 4H), 1.90 – 1.74 (m, 4H), 1.68 – 1.52 (m, 2H). ¹³C NMR (101 MHz, DMSO) δ 165.55, 158.72, 130.35, 129.48, 119.92, 113.80, 67.87, 28.29, 22.22. HRMS (ESI): calculated for C₁₉H₂₄N₄O₂ [M+H]⁺ 341.1977, found 341.1977.



3,3'-((1,2-phenylenebis(methylene))bis(oxy))dibenzimidamide (21b) Following the procedure as described above for compound **3**, using compound **26** (102 mg, 0.3 mmol). LHMDS (1.5 mL, 1 M THF solution, 5 eq.) was added and after LCMS analysis of the reaction mixture at 48 hours, LHMDS (3.0 mL, 1 M THF solution, 10 eq.) was additionally added. A quench with HCl (5.0 mL, 4 M dioxane solution, 67 eq.), afforded the crude product.

The crude product was purified using HPLC affording compound **21b** (80.4 mg, 72%). ¹H NMR (400 MHz, DMSO-*d*₆) δ 9.45 (s, 4H), 9.33 (s, 4H), 7.59 – 7.54 (m, 2H), 7.53 (s, 1H), 7.52 – 7.46 (m, 3H), 7.45 – 7.35 (m, 6H), 5.34 (s, 4H). ¹³C NMR (101 MHz, DMSO) δ 165.43, 158.25, 134.76, 130.37, 129.52, 128.84, 128.44, 120.46, 119.94, 114.63, 67.52. HRMS (ESI): calculated for C₂₂H₂₂N₄O₂ [M+H]⁺ 375.1821, found 375.1821.

3,3'-((1,3-phenylenebis(methylene))bis(oxy))dibenzimidamide (22b) Following the procedure as described above for compound **3**, using compound **27** (102 mg, 0.3 mmol). LHMDS (1.5 mL, 1 M THF solution, 5 eq.) was added and after LCMS analysis of the reaction mixture at 48 hours, LHMDS (2.0 mL, 1 M THF solution, 6.7 eq.) was additionally added. A quench with HCl (5.0 mL, 4 M dioxane solution, 67 eq.), afforded the crude product. The crude product was purified using HPLC affording compound **22b** (88 mg, 78%). ¹H NMR (400 MHz, DMSO-*d*₆) δ 9.46 (s, 4H), 9.34 (s, 4H), 7.62 – 7.52 (m, 3H), 7.50 (s, 2H), 7.47 (s, 3H), 7.44 – 7.36 (m, 4H), 5.23 (s, 4H). ¹³C NMR (101 MHz, DMSO) δ 165.44, 158.38, 136.84, 130.41, 129.52, 128.84, 127.59, 127.13, 120.41, 120.03, 114.43, 69.59. HRMS (ESI): calculated for C₂₂H₂₂N₄O₂ [M+H]⁺ 375.1821, found 375.1821.

3,3'-[1,4-Phenylenebis(methyleneoxy)]dibenzenecarboximidamide (23b) Following the procedure as described above for compound **3**, using compound **28** (102 mg, 0.3 mmol), LHMDS (2.4 mL, 1 M THF solution, 8 eq.) and HCl (4.5 mL, 4 M dioxane solution, 60 eq.) produced compound **23b** (114 mg, quant.). ¹H NMR (400 MHz, DMSO-*d*₆) δ 9.30 (d, J = 19.8 Hz, 8H), 7.54 – 7.38 (m, 8H), 7.38 – 7.26 (m, 4H), 5.16 (s, 4H). ¹³C NMR (101 MHz, DMSO) δ 165.40, 158.35, 136.33, 130.41, 129.51, 128.04, 120.40, 120.03, 114.47, 69.42. HRMS (ESI): calculated for C₂₂H₂₂N₄O₂ [M+H]⁺ 375.1821, found 375.1818.

2,2'-(pentane-1,5-diylbis(oxy))dibenzonitrile (29) Following the procedure as described above for compound **4**, using 1,5-dibromopentane (0.54 mL, 4 mmol) and 2-cyanophenol (1.14 g, 9.6 mmol, 2.4 eq.), afforded compound **29** (1.20 g, 97%). ¹H NMR (400 MHz, CDCl₃) δ 7.61 – 7.45 (m, 4H), 7.04 – 6.92 (m, 4H), 4.12 (t, J = 6.2 Hz, 4H), 1.95 (m, 4H), 1.85 – 1.69 (m, 2H). ¹³C NMR (101 MHz, CDCl₃) δ 160.85, 134.49, 133.85, 120.77, 116.70, 112.37, 102.08, 68.88, 28.58, 22.70.

2,2'-(1,2-phenylenebis(methylene))bis(oxy)dibenzonitrile (30) Following the procedure as described above for compound **4**, using 1,2-bis(bromomethyl)benzene (0.53 g, 2 mmol) and 2-cyanophenol (0.57 g, 4.8 mmol, 2.4 eq.), afforded compound **30** (0.56 g, 83%). ¹H NMR (400 MHz, CDCl₃) δ 7.62 – 7.46 (m, 6H), 7.45 – 7.36 (m, 2H), 7.15 (d, J = 8.4 Hz, 2H), 6.99 (td, J = 7.6, 0.9 Hz, 2H), 5.39 (s, 4H). ¹³C NMR (101 MHz, CDCl₃) δ 160.13, 134.72, 133.97, 133.87, 129.30, 129.05, 121.32, 116.66, 112.91, 102.09, 69.45.

2,2'-(1,3-phenylenebis(methylene))bis(oxy)dibenzonitrile (31) Following the procedure as described above for compound **4**, using 1,3-bis(bromomethyl)benzene (0.53 g, 2 mmol) and 2-cyanophenol (0.57 g, 4.8 mmol, 2.4 eq.), afforded compound **31** (0.60 g, 88%). ¹H NMR (400 MHz, CDCl₃) δ 7.58 (dd, J = 8.1, 1.7 Hz, 2H), 7.55 – 7.48 (m, 3H), 7.44 (m, 3H), 7.05 – 6.96 (m, 4H), 5.23 (s, 4H). ¹³C NMR (101 MHz, CDCl₃) δ 160.29, 136.37, 134.51, 134.00, 129.40, 127.02, 125.20, 121.31, 116.57, 111.95, 102.53, 77.48, 77.16, 76.84, 70.49.

2,2'-(1,4-phenylenebis(methylene))bis(oxy)dibenzonitrile (32) Following the procedure as described above for compound **4**, using 1,4-bis(bromomethyl)benzene (0.92 g, 3.5 mmol), 2-cyanophenol (1.1 g, 9.6 mmol, 2.6 eq.), and NaH (0.38 g, 60% dispersion in mineral oil, 2.6 eq.) afforded compound **32** (1.2 g, 99%). ¹H NMR (400 MHz, CDCl₃) δ 7.59 (dd, J = 7.6, 1.7 Hz, 2H), 7.55 – 7.44

(m, 6H), 7.08 – 6.95 (m, 4H), 5.22 (s, 4H). ^{13}C NMR (101 MHz, CDCl_3) δ 160.31, 135.86, 134.46, 134.04, 127.49, 121.30, 116.55, 112.99, 102.58, 70.37.

2,2'-(pentane-1,5-diylbis(oxy))dibenzimidamide (1c) These conditions were based on literature protocols.⁴² To a suspension of compound **29** (190 mg, 0.62 mmol) and DIPEA (0.56 mL, 3.2 mmol, 5 eq.) in EtOH (10 mL) was added $\text{NH}_2\text{OH}\cdot\text{HCl}$ (208 mg, 3 mmol, 4.8 eq.). The reaction mixture was stirred at 85 °C overnight. The mixture was concentrated in vacuo and the residue was dissolved in AcOH (4.2 mL) and Ac_2O (0.29 mL, 3 mmol, 4.8 eq.) was added. The reaction was stirred for 4 hours and then concentrated in vacuo. The residue was co-evaporated with toluene three times and then suspended in AcOH (7.5 mL) under argon atmosphere. Zinc powder (60 mg, 0.92 mmol, 1.5 eq.) was added and the mixture was stirred at 35 °C overnight. Upon completion, the reaction mixture was filtered through Celite®, the celite was rinsed with acetone and all collected fractions were concentrated in vacuo. The crude product purified by preparative HPLC (gradient 20–100%, 30 minutes) to afford the final compound **1c** (102 mg, 48%). ^1H NMR (400 MHz, $\text{DMSO}-d_6$) δ 9.32 (s, 4H), 9.12 (s, 4H), 7.60 (t, J = 7.9 Hz, 2H), 7.51 (d, J = 7.5 Hz, 2H), 7.25 (d, J = 8.4 Hz, 2H), 7.11 (t, J = 7.5 Hz, 2H), 4.09 (t, J = 6.4 Hz, 4H), 1.81 (p, J = 6.9 Hz, 4H), 1.56 (p, J = 7.6 Hz, 2H). ^{13}C NMR (101 MHz, DMSO) δ 164.64, 156.10, 133.82, 129.53, 120.35, 118.55, 113.07, 68.28, 28.01, 21.76. HRMS (ESI): calculated for $\text{C}_{19}\text{H}_{24}\text{N}_4\text{O}_2$ $[\text{M}+\text{H}]^+$ 341.1977, found 341.1972.

2,2'-((1,2-phenylenebis(methylene))bis(oxy))dibenzimidamide (21c) Following the procedure as described above for compound **1c**, using compound **30** (211 mg, 0.62 mmol), afforded compound **21c** (43 mg, 18%). ^1H NMR (400 MHz, $\text{DMSO}-d_6$) δ 9.46 (s, 4H), 9.24 (s, 4H), 7.67 – 7.58 (m, 4H), 7.55 (dd, J = 7.6, 1.7 Hz, 2H), 7.44 – 7.31 (m, 4H), 7.15 (td, J = 7.5, 0.8 Hz, 2H), 5.35 (s, 4H). ^{13}C NMR (101 MHz, DMSO) δ 164.75, 155.41, 134.33, 133.66, 129.61, 128.31, 128.22, 120.79, 119.07, 113.41, 67.37. HRMS (ESI): calculated for $\text{C}_{22}\text{H}_{22}\text{N}_4\text{O}_2$ $[\text{M}+\text{H}]^+$ 375.1821, found 375.1815.

2,2'-((1,3-phenylenebis(methylene))bis(oxy))dibenzimidamide (22c) Following the procedure as described above for compound **1c**, using compound **31** (210 mg, 0.62 mmol), afforded compound **22c** (49 mg, 21%). ^1H NMR (400 MHz, $\text{DMSO}-d_6$) δ 9.46 (s, 4H), 9.22 (s, 4H), 7.62 (ddd, J = 8.8, 7.4, 1.7 Hz, 2H), 7.58 – 7.42 (m, 6H), 7.33 (d, J = 8.4 Hz, 2H), 7.15 (td, J = 7.6, 0.8 Hz, 2H), 5.23 (s, 4H). ^{13}C NMR (101 MHz, DMSO) δ 164.69, 155.69, 136.70, 133.76, 129.65, 128.80, 127.31, 126.80, 120.77, 118.98, 113.46, 69.95. HRMS (ESI): calculated for $\text{C}_{22}\text{H}_{22}\text{N}_4\text{O}_2$ $[\text{M}+\text{H}]^+$ 375.1821, found 375.1816.

2,2'-((1,4-phenylenebis(methylene))bis(oxy))dibenzimidamide (23c) Following the procedure as described above for compound **1c**, using compound **32** (211 mg, 0.62 mmol), afforded compound **23c** (27 mg, 12%). ^1H NMR (400 MHz, $\text{DMSO}-d_6$) δ 9.33 (s, 4H), 9.21 (s, 4H), 7.62 (ddd, J = 8.8, 7.4, 1.8 Hz, 2H), 7.57 – 7.49 (m, 6H), 7.33 (d, J = 8.8 Hz, 2H), 7.14 (td, J = 7.6, 0.9 Hz, 2H), 5.23 (s, 4H). ^{13}C NMR (101 MHz, DMSO) δ 164.62, 155.66, 136.23, 133.75, 129.65, 127.79, 120.72, 118.92, 113.39, 69.75. HRMS (ESI): calculated for $\text{C}_{22}\text{H}_{22}\text{N}_4\text{O}_2$ $[\text{M}+\text{H}]^+$ 375.1821, found 375.1816.

(5-bromo-1,3-phenylene)dimethanol (33) Protocol as described in literature.⁴⁴ Dimethyl 5-bromoisophthalate (2.3 g, 8.3 mmol) was dissolved in dry DCM (25 mL) under argon atmosphere. The solution was then cooled to 0 °C using an ice bath and DIBALH (40 mL, 1 M hexane solution, 4.8 eq.) was added dropwise. The mixture was stirred from 0 °C to room temperature for 1 hour. The reaction was quenched with Rochelle salt (60 mL, sat. aq.) and the biphasic mixture was stirred at room temperature overnight. The layers were separated and the aqueous layer was two times extracted with diethyl ether. The organic layers were combined, washed with water and brine, dried over Na_2SO_4 and concentrated in vacuo. The crude product was purified using column chromatography (DCM/EtOAc = 1:1) and afforded

compound **33** (1.8 g, 96%). ¹H NMR (400 MHz, MeOD) δ 7.42 (s, 2H), 7.28 (s, 1H), 4.58 (s, 4H), 3.35 (s, 2H). ¹³C NMR (101 MHz, MeOD) δ 145.51, 129.42, 124.82, 123.31, 64.29.

1-bromo-3,5-bis(bromomethyl)benzene (34) Protocol as described in literature.⁴⁵ To a solution of compound **33** (1.0 g, 4.6 mmol) in dry DCM (50 mL) was added PPh₃ (2.5 g, 9.7 mmol, 2.1 eq.) and CBr₄ (3.2 g, 9.7 mmol, 2.1 eq.) and the mixture was stirred at room temperature for two hours under argon atmosphere. The reaction was quenched with water (30 mL) and the product was extracted from the aqueous layer with DCM three times. The combined organic layers were washed with water and brine, dried over Na₂SO₄ and concentrated in vacuo. The crude product was purified by column chromatography (petroleum ether 100%) to give compound **34** (0.87 g, 55%). ¹H NMR (400 MHz, CDCl₃) δ 7.51 – 7.45 (m, 2H), 7.34 (s, 1H), 4.53 (d, J = 4.0 Hz, 1H), 4.41 (d, J = 4.2 Hz, 3H). ¹³C NMR (101 MHz, CDCl₃) δ 140.42, 140.11, 132.11, 132.09, 131.64, 128.40, 127.90, 122.83, 44.89, 31.64, 31.59.

4,4'-(((5-bromo-1,3-phenylene)bis(methylene))bis(oxy))dibenzonitrile (35) Following the procedure as described above for compound **4**, using compound **34** (0.82 g, 2.4 mmol), afforded compound **35** as a crude product. The crude product was not recrystallized due to insolubility issues and was used in the next step without further purification based on a purity assessment (NMR) (1.0 g, quant.). ¹H NMR (400 MHz, CDCl₃) δ 7.66 – 7.57 (m, 4H), 7.57 – 7.53 (m, 1H), 7.04 – 6.96 (m, 4H), 5.15 – 5.05 (m, 4H). ¹³C NMR (101 MHz, CDCl₃) δ 161.57, 138.62, 134.25, 130.33, 124.72, 123.30, 119.09, 115.62, 104.87, 69.18.

4,4'-(((1,1'-biphenyl)-3,5-diylbis(methylene))bis(oxy))dibenzonitrile (36) Conditions were based on protocols described in literature.^{47,48} Dibenzonitrile intermediate **35** (0.30 g, 0.72 mmol) was dissolved in a 3:1 mixture of THF and 2 M Na₂CO₃ (aq.) of 8 mL, respectively. Phenylboronic acid (0.13 g, 1.1 mmol, 1.5 eq.) and Pd(dppf)Cl₂·DCM (58 mg, 0.07 mmol, 0.1 eq.) were added. The reaction mixture was heated to 65 °C for 18 hours and then partitioned between DCM and NaHCO₃ (sat. aq.). The aqueous layer was three times extracted with DCM, the organic layers were combined and dried over Na₂SO₄. The solvent was evaporated under reduced pressure and the crude product was purified using column chromatography (petroleum ether/EtOAc = 4:1) to obtain compound **36** (0.28 g, 94%). ¹H NMR (400 MHz, CDCl₃) δ 7.66 – 7.57 (m, 8H), 7.50 – 7.36 (m, 4H), 7.05 (d, J = 8.8 Hz, 4H), 5.19 (s, 4H). ¹³C NMR (101 MHz, CDCl₃) δ 161.90, 142.59, 140.22, 137.05, 134.21, 129.06, 128.03, 127.31, 126.40, 125.32, 119.19, 115.67, 104.57, 70.12.

4,4'-(((5-bromo-1,3-phenylene)bis(methylene))bis(oxy))dibenzimidamide (37) Following the procedure as described above for compound **3**, using compound **35** (126 mg, 0.3 mmol), LHMDS (3.0 mL, 1 M THF solution, 10 eq.) and HCl (10 mL, 4 M dioxane solution, 133 eq.), afforded the product **37** (23 mg, 17%). ¹H NMR (400 MHz, DMSO-*d*₆) δ 9.17 (s, 3H), 9.09 (s, 3H), 7.83 (d, J = 8.9 Hz, 4H), 7.67 (d, J = 1.1 Hz, 2H), 7.58 (s, 1H), 7.24 (d, J = 9.0 Hz, 4H), 5.27 (s, 4H). ¹³C NMR (101 MHz, DMSO) δ 164.78, 162.35, 139.43, 130.28, 130.05, 125.93, 121.85, 120.20, 115.20, 68.57. HRMS (ESI): calculated for C₂₂H₂₁BrN₄O₂ [M+H]⁺ 453.0926, found 453.0924.

4,4'-(((1,1'-biphenyl)-3,5-diylbis(methylene))bis(oxy))dibenzimidamide (38) Following the procedure as described above for compound **3**, using compound **36** (0.28 g, 0.67 mmol), LHMDS (5.4 mL, 1 M THF solution, 8 eq.) and HCl (10 mL, 4 M dioxane solution, 60 eq.). HPLC purification using a 30–100% gradient for 30 minutes afforded compound **38** (0.23 g, 74%). ¹H NMR (400 MHz, DMSO-*d*₆) δ 9.15 (d, J = 15.3 Hz, 8H), 7.83 (d, J = 9.0 Hz, 4H), 7.76 (s, 2H), 7.69 (d, J = 7.2 Hz, 2H), 7.58 (s, 1H), 7.50 (t, J = 7.6

Hz, 2H), 7.40 (t, $J = 7.3$ Hz, 1H), 7.27 (d, $J = 9.0$ Hz, 4H), 5.33 (s, 4H). ^{13}C NMR (101 MHz, DMSO) δ 164.83, 162.61, 140.77, 139.54, 137.54, 130.26, 129.14, 127.94, 126.84, 126.19, 126.03, 120.04, 115.25, 69.51. HRMS (ESI): calculated for $\text{C}_{28}\text{H}_{26}\text{N}_4\text{O}_2$ $[\text{M}+\text{H}]^+$ 451.2135, found 451.2130.

(4-bromo-1,2-phenylene)dimethanol (39) Conditions were based on protocol reported in literature.⁴⁹ LAH (15 mL, 1 M THF solution, 2 eq.) and ZnCl_2 (0.61 g, 4.5 mmol, 0.6 eq.) were suspended in dry THF (30 mL) and cooled to 0 °C, then 4-bromophthalic anhydride (1.7 g, 7.5 mmol) was slowly added. The mixture was stirred at room temperature for 6 hours under argon atmosphere. The mixture was cooled to 0 °C and quenched with Rochelle salt (30 mL, sat. aq.) and the biphasic mixture was stirred at room temperature overnight. The layers were separated and the aqueous layer was extracted with diethyl ether two times and the combined organic layers were washed with water and brine, dried over Na_2SO_4 and concentrated in vacuo. The crude product was purified by column chromatography (DCM/EtOAc = 1:1) to give compound **39** (1.5 g, 95%). ^1H NMR (400 MHz, CDCl_3) δ 7.48 (d, $J = 2.1$ Hz, 1H), 7.42 (dd, $J = 8.0, 2.1$ Hz, 1H), 7.18 (d, $J = 8.0$ Hz, 1H), 4.62 (d, $J = 2.6$ Hz, 4H), 3.20 (s, 2H). ^{13}C NMR (101 MHz, CDCl_3) δ 141.49, 138.18, 129.88, 128.77, 127.92, 122.30, 64.53, 64.40, 64.31, 63.49, 63.47, 31.08, 23.80.

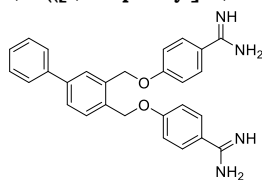
4-bromo-1,2-bis(bromomethyl)benzene (40) Following the procedure described for compound **34**, using compound **39** (1.5 g, 7.0 mmol) as starting material, afforded compound **40** (1.8 g, 74%). ^1H NMR (400 MHz, CDCl_3) δ 7.52 (d, $J = 2.1$ Hz, 1H), 7.43 (dd, $J = 8.2, 2.1$ Hz, 1H), 7.24 (d, $J = 8.2$ Hz, 1H), 4.59 (s, 2H), 4.58 (s, 2H). ^{13}C NMR (101 MHz, CDCl_3) δ 138.65, 135.67, 134.02, 132.69, 132.58, 131.24, 129.60, 123.17, 66.00, 42.46, 42.32, 30.14, 29.32, 29.12, 29.00, 28.83, 15.43.

4,4'-(((4-bromo-1,2-phenylene)bis(methylene))bis(oxy))dibenzonitrile (41) Following the procedure as described above for compound **4**, using compound **40** (0.80 g, 2.3 mmol), afforded compound **41** as a crude product. The crude product was not recrystallized due to insolubility issues and was used in the next step without further purification (1.1 g, quant.). ^1H NMR (400 MHz, CDCl_3) δ 7.67 (d, $J = 2.1$ Hz, 1H), 7.62 – 7.57 (m, 4H), 7.54 (dd, $J = 8.1, 2.1$ Hz, 1H), 7.37 (d, $J = 8.1$ Hz, 1H), 6.99 (dd, $J = 8.9, 4.6$ Hz, 4H), 5.15 (d, $J = 6.0$ Hz, 4H). ^{13}C NMR (101 MHz, CDCl_3) δ 161.46, 136.30, 134.29, 134.27, 132.83, 132.15, 132.10, 131.05, 129.52, 129.23, 123.21, 118.99, 115.52, 105.06, 104.99, 67.83, 67.51.

4,4'-(((1,1'-biphenyl)-3,4-diylbis(methylene))bis(oxy))dibenzonitrile (42) Following the procedure as described above for compound **36**, using compound **41** (0.33 g, 0.79 mmol), a 3:1 mixture of THF and 2M Na_2CO_3 (aq.) (8.0 mL), phenylboronic acid (0.13 g, 1.1 mmol, 1.5 eq.) and $\text{Pd}(\text{dppf})\text{Cl}_2\text{-DCM}$ (58 mg, 0.07 mmol, 0.1 eq) afforded compound **42** (0.28 g, 84%). ^1H NMR (400 MHz, CDCl_3) δ 7.72 (s, 1H), 7.66 – 7.57 (m, 8H), 7.49 – 7.44 (m, 2H), 7.41 – 7.36 (m, 1H), 7.04 – 7.00 (m, 4H), 5.25 (d, $J = 7.1$ Hz, 4H). ^{13}C NMR (101 MHz, CDCl_3) δ 161.76, 142.35, 140.07, 134.61, 134.27, 132.94, 130.17, 129.54, 129.26, 129.09, 128.37, 128.04, 127.82, 127.27, 119.11, 115.58, 104.84, 104.80, 68.55, 68.27.

4,4'-(((4-bromo-1,2-phenylene)bis(methylene))bis(oxy))dibenzimidamide (43) Following the procedure as described above for compound **1c**, using compound **41** (172 mg, 0.41 mmol), affording compound **43** (72 mg, 39%). ^1H NMR (400 MHz, $\text{DMSO}-d_6$) δ 9.14 (d, $J = 18.5$ Hz, 8H), 7.82 (dd, $J = 9.0, 3.2$ Hz, 4H), 7.77 (d, $J = 2.1$ Hz, 1H), 7.62 (dd, $J = 8.2, 2.1$ Hz, 1H), 7.51 (d, $J = 8.3$ Hz, 1H), 7.33 – 7.20 (m, 4H), 5.37 (d, $J = 10.1$ Hz, 4H). ^{13}C NMR (101 MHz, $\text{DMSO}-d_6$) δ 164.76, 164.74, 162.24, 162.17, 137.22, 133.96, 131.16, 131.01, 130.76, 130.25, 130.21, 121.48, 120.32, 120.23, 115.22, 66.83, 66.59, 40.15, 39.94, 39.73, 39.52, 39.31, 39.10, 38.89. HRMS (ESI): calculated for $\text{C}_{22}\text{H}_{21}\text{BrN}_4\text{O}_2$ $[\text{M}+\text{H}]^+$ 453.0926, found 453.0923.

4,4'-((([1,1'-biphenyl]-3,4-diylbis(methylene))bis(oxy))dibenzimidamide (44)



Following the procedure as described above for compound **3**, using compound **42** (0.28 g, 0.66 mmol), LHMDS (5.4 mL, 1 M THF solution, 8 eq.) and HCl (10 mL, 4 M dioxane solution, 60 eq.), afforded the crude product. The crude product was purified using HPLC with a 30–100% gradient for 30 minutes to obtain the pure compound **44** (35 mg, 12%). ¹H NMR (400 MHz, DMSO-*d*₆) δ 9.14 (d, *J* = 5.2 Hz, 4H), 9.00 (d, *J* = 4.8 Hz, 4H), 7.88 (d, *J* = 2.0 Hz, 1H), 7.81 (dd, *J* = 8.9, 3.2 Hz, 4H), 7.72 – 7.61 (m, 4H), 7.48 (t, *J* = 7.6 Hz, 2H), 7.39 (t, *J* = 7.3 Hz, 1H), 7.28 (t, *J* = 8.6 Hz, 4H), 5.44 (d, *J* = 10.4 Hz, 4H). ¹³C NMR (101 MHz, DMSO) δ 164.72, 162.49, 162.45, 140.20, 139.34, 135.20, 133.89, 130.25, 129.56, 129.11, 127.37, 126.75, 120.10, 120.08, 115.26, 115.23, 67.64, 67.31. HRMS (ESI): calculated for C₂₈H₂₆N₄O₂ [M+H]⁺ 451.2135, found 451.2129.

4.2. Antimicrobial assays

All compounds were screened for antimicrobial activity against *E. coli* BW25113. A select group of the pentamidine analogues was further tested against *E. coli* ATCC25922, *E. coli* W3110, *E. coli* 552060.1, *E. coli* BW25113 transformed with pGDP2-mcr-1 (the plasmid was a gift from Gerard Wright (Addgene plasmid # 118404; <http://n2t.net/addgene:118404>; RRID:Addgene_118404)⁶³), *E. coli* mcr-1, *E. coli* EQASmcr-1 (EQAS 2016 412016126), *E. coli* EQASmcr-2 (EQAS 2016 KP37), *E. coli* EQASmcr-3 (EQAS 2017 2013-SQ352), *E. coli* RC0089, *K. pneumoniae* ATCC13883, *P. aeruginosa* ATCC27853 and *A. baumannii* ATCC17978. The antimicrobial assay was performed according to CLSI guidelines. Bacteria were plated out directly from their glycerol stocks on blood agar plates, incubated overnight at 37 °C, and then kept in the fridge. The blood agar plates were only used for 2 weeks and then replaced.

4.3. MIC assays

A single colony from a blood agar plate was inoculated in Lysogeny Broth (LB) at 37 °C until a 0.5 optical density at 600nm (OD₆₀₀) was reached (compared to the sterility control of LB). The bacterial suspension was diluted in fresh LB to 2.0 × 10⁶ CFU/mL. The serial dilutions were prepared in polypropylene microtiter plates: a stock of the test compounds was prepared with a 2x final concentration in LB. 100 µl of the stock was added to the wells of the top row of which 50 µl was used for the serial dilution. The bottom row of each plate was used as the positive (50 µl of LB) and negative controls (100 µl of LB) (6 wells each). 50 µl of the 2.0 × 10⁶ CFU/mL bacterial stock was added to each well except for the negative controls, adding up to a total volume of 100 µl per well. The plates were sealed with a breathable seal and incubated for 20 hours at 37 °C and 600 rpm. The MIC was visually determined after centrifuging the plates for 2 minutes at 3000 rpm.

4.4. Checkerboard assays

Dilution series of both the test compound and antibiotic to be evaluated was prepared in LB media. To evaluate synergy, 25 µL of the test compound solutions were added to wells containing 25 µL of the antibiotic solution. This was replicated in three columns for each combination so as to obtain triplicates. To the resulting 50 µL volume of antibiotic + test compound was next added 50 µL of bacterial stock (See MIC assays) and the plates sealed. After incubation for 20 hours at 37 °C while shaking at 600 rpm, the breathable seals were removed and the plates shaken using a bench top shaker to ensure even suspension of the bacterial cells as established by visual inspection. The plates were then transferred to a Tecan Spark plate reader and following another brief shaking (20 seconds) the density of the bacterial suspensions measured at 600 nm (OD₆₀₀). The resulting OD₆₀₀ values were transformed to a 2D gradient to visualize the growth/no-growth results. The FICI was calculated using Equation 1, with an FICI ≤ 0.5 indicating synergy.²¹

$$FICI = \frac{MSC_{ant}}{MIC_{ant}} + \frac{MSC_{syn}}{MIC_{syn}} \quad (1)$$

Equation 1. Calculation of FICI. MSC_{ant} = MIC of antibiotic in combination with synergist; MIC_{ant} = MIC of antibiotic alone; MSC_{syn} = MIC of synergist in combination with antibiotic; MIC_{syn} = MIC of synergist alone. In cases where the MIC of the antibiotic or synergist was found to exceed the highest concentration tested, the next highest concentration in the dilution series was used in determining the FICI and the result reported as \leq the calculated value.

4.5. Hemolysis assays

The hemolytic activity of each analogue was assessed in triplicate. Red blood cells from defibrinated sheep blood obtained from Thermo Fisher were centrifuged (400 g for 15 minutes at 4°C) and washed with Phosphate-Buffered Saline (PBS) containing 0.002% Tween20 (buffer) for five times. Then, the red blood cells were normalized to obtain a positive control read-out between 2.5 and 3.0 at 415 nm to stay within the linear range with the maximum sensitivity. A serial dilution of the compounds (200 – 6.25 $\mu\text{g/mL}$, 75 μL) was prepared in a 96-well plate. The outer border of the plate was filled with 75 μL buffer. Each plate contained a positive control (0.1% Triton-X final concentration, 75 μL) and a negative control (buffer, 75 μL) in triplicate. The normalized blood cells (75 μL) were added and the plates were incubated at 37 °C for 1 hour or 20 hours while shaking at 500 rpm. A flat-bottom plate of polystyrene with 100 μL buffer in each well was prepared. After incubation, the plates were centrifuged (800 g for 5 minutes at room temperature) and 25 μL of the supernatant was transferred to their respective wells in the flat-bottom plate. The values obtained from a read-out at 415 nm were corrected for background (negative control) and transformed to a percentage relative to the positive control.

4.6. Membrane permeability assay using N-phenylnaphthalen-1-amine (NPN)

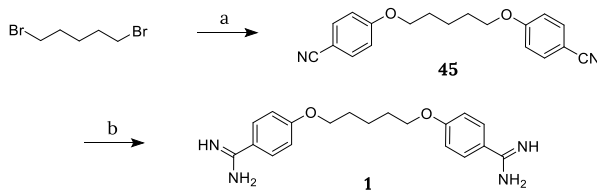
The assay was performed based on protocols adapted from those described in literature.^{67,68} Bacteria were inoculated overnight at 37 °C in LB, diluted the next day 50x in LB and grown to OD_{600} of 0.5. The bacterial suspension was then centrifuged for 10 minutes at 1000 g at 25 °C. The pellet of bacteria was suspended in 5 mM HEPES buffer containing 20mM glucose to a final concentration of OD_{600} of 1.0. The compounds were serially diluted (25 μL) in triplicate in a black ½ area clear-bottom 96-well plate. 100 $\mu\text{g/mL}$ final concentration of colistin in triplicate served as the positive control. Three wells were filled with 25 μL buffer to serve as the negative control. Additional controls of the compounds were made in triplicate using 25 μL of the highest concentration to detect interactions of the compounds with NPN in the absence of bacteria. A stock of 0.5 mM of NPN in acetone was prepared and diluted 12.5x in the buffer. 25 μL of the NPN solution was added to each well. 50 μL of the 1.0 OD_{600} bacterial stock was then added to each well except for the controls of the compounds with NPN. To these wells 50 μL of buffer was added. After 60 minutes the plate was measured using Tecan plate reader with λ_{ex} 355 nm \pm 20 nm and λ_{em} 420 nm \pm 20 nm. The fluorescence values obtained were then transformed into a NPN uptake percentage using the following equation 2:

$$\text{NPN uptake (\%)} = (F_{obs} - F_0) / (F_{100} - F_0) \times 100\%, \quad (2)$$

Equation 2: NPN uptake. The observed fluorescence (F_{obs}) is corrected for background using the negative control (F_0). This value is divided by the positive control corrected for background ($F_{100} - F_0$) and multiplied by 100% to obtain the percentage NPN uptake.^{68,75}

Supporting information

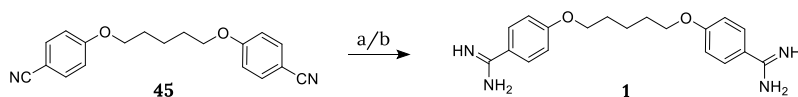
Synthesis



Scheme S1. Synthesis of pentamidine (**1**). Reagents and conditions: (a) 4-Cyanophenol, NaH, DMF, 80°C, 1h (78%); (b) i) LHMDs, THF, 48h, rt, ii) 4M HCl (dioxane), 0°C to rt, overnight (quant.).

4,4'-(pentane-1,5-diylbis(oxy))dibenzonitrile (45**)** 4-cyanophenol (1.14 g, 9.6 mmol, 2.4 eq.) was suspended in dry DMF (12 mL) under argon atmosphere. The suspension was cooled to 0 °C using an ice bath and NaH (384 mg, 60% dispersion in mineral oil, 2.4 eq.) was slowly added. The reaction was stirred until a clear solution appeared, the ice bath was removed and 1,5-dibromopentane (0.92 g, 4.0 mmol) was added. The reaction mixture was heated to 80 °C for 1 hour and then cooled to room temperature. Water (35 mL) was added to the mixture to obtain precipitation. The precipitate was filtered, washed with water and recrystallized from EtOH to give compound **45** as white crystals (0.95 g, 78%). ¹H NMR (400 MHz, CDCl₃) δ 7.57 (d, J = 8.9 Hz, 4H), 6.93 (d, J = 8.9 Hz, 4H), 4.03 (t, J = 6.3 Hz, 4H), 1.93 – 1.84 (m, 4H), 1.72 – 1.61 (m, 2H). ¹³C NMR (101 MHz, CDCl₃) δ 162.37, 134.09, 119.36, 115.24, 103.91, 68.14, 28.81, 22.73.

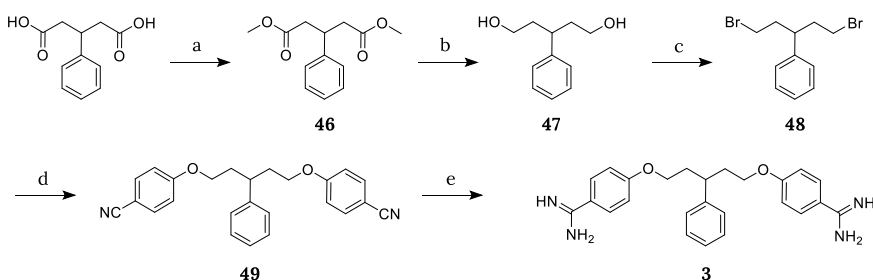
4,4'-(pentane-1,5-diylbis(oxy))dibenzimidamide (1**)** Compound **45** (94 mg, 0.3 mmol) was dissolved in dry THF (2 mL) under argon atmosphere and LHMDs (1.2 mL, 1 M THF solution, 4.0 eq.) was added. The reaction was stirred at room temperature for 48 hours or longer until complete conversion to the bis-amidine (monitored by LCMS). The solution was cooled to 0 °C and quenched with HCl (4.5 mL, 4 M dioxane solution, 60 eq.). The mixture was stirred at room temperature overnight, then diluted with diethyl ether and filtered. The precipitate was purified by preparative HPLC with the gradient 0–100% in 30 minutes. The samples were analyzed and the combined pure fractions were dried to give pentamidine (**1**) (120 mg, quant.). ¹H NMR (400 MHz, DMSO-*d*₆) δ 9.14 (s, 3H), 9.06 (s, 3H), 7.81 (d, J = 8.9 Hz, 4H), 7.15 (d, J = 8.9 Hz, 4H), 4.12 (t, J = 6.4 Hz, 4H), 1.88 – 1.75 (m, 4H), 1.65 – 1.52 (m, 2H). ¹³C NMR (101 MHz, DMSO) δ 164.70, 163.06, 130.19, 119.50, 114.79, 68.05, 28.21, 22.09. HRMS (ESI): calculated for C₁₉H₂₄N₄O₂ [M+H]⁺ 341.1977, found 341.1977.



Scheme S2. Exploration of the optimal acidic quench. Reagents and conditions: (a) i) LHMDs, THF, 48h, ii) 2M HCl (aq), 0°C to rt, overnight (68%) or (b) i) LHMDs, THF, 48h, ii) sat. ethanolic HCl, 0°C to rt, overnight (9%).

4,4'-(pentane-1,5-diylbis(oxy))dibenzimidamide (1) using 2M HCl (aq) Following the procedure as described for compound **1** except for using 2 M HCl (aq) (20 mL) as acidic quench afforded pentamidine (**1**) (71 mg, 68%). ¹H NMR (400 MHz, DMSO-*d*₆) δ 9.14 (s, 4H), 9.06 (s, 4H), 7.81 (d, *J* = 8.9 Hz, 4H), 7.15 (d, *J* = 8.9 Hz, 4H), 4.12 (t, *J* = 6.4 Hz, 4H), 1.88 – 1.75 (m, 4H), 1.65 – 1.52 (m, 2H). ¹³C NMR (101 MHz, DMSO) δ 164.70, 163.06, 130.19, 119.50, 114.79, 68.05, 28.21, 22.09. HRMS (ESI): calculated for C₁₉H₂₄N₄O₂ [M+H]⁺ 341.1977, found 341.1977.

4,4'-(pentane-1,5-diylbis(oxy))dibenzimidamide (1) using sat. ethanolic HCl Following the procedure as described for compound **1** except for using freshly prepared sat. ethanolic HCl (20 mL) as acidic quench afforded pentamidine (**1**) (9 mg, 9%). ¹H NMR (400 MHz, DMSO-*d*₆) δ 9.14 (s, 4H), 9.06 (s, 4H), 7.81 (d, *J* = 8.9 Hz, 4H), 7.15 (d, *J* = 8.9 Hz, 4H), 4.12 (t, *J* = 6.4 Hz, 4H), 1.88 – 1.75 (m, 4H), 1.65 – 1.52 (m, 2H). ¹³C NMR (101 MHz, DMSO) δ 164.70, 163.06, 130.19, 119.50, 114.79, 68.05, 28.21, 22.09. HRMS (ESI): calculated for C₁₉H₂₄N₄O₂ [M+H]⁺ 341.1977, found 341.1977.



Scheme S3. Synthesis of 4,4'-((3-phenylpentane-1,5-diyl)bis(oxy))dibenzimidamide (**3**). Reagents and conditions: (a) H₂SO₄, MeOH, 70°C, overnight (91%); (b) DIBAL-H, DCM, 0°C, 1 hour (quant.); (c) NBS, PPh₃, DCM, 0°C to rt, 2 hours (62%) (d) 4-Cyanophenol, NaH, DMF, 80°C, 1h (89%); (e) i) LHMDs, THF, 48h, ii) 4M HCl (dioxane), 0°C to rt, overnight (23%).

Dimethyl 3-phenylpentanedioate (46) 3-phenylpentanedioic acid (1.04 g, 5 mmol) was dissolved in MeOH (20 mL) and a few drops of H₂SO₄ were added to the solution. The reaction mixture was refluxed at 70 °C overnight, concentrated in vacuo and redissolved in DCM (50 mL). The organic layer was washed with water (4 mL) five times. The organic layer was then washed with brine, dried over Na₂SO₄ and concentrated in vacuo. The crude product was purified using column chromatography (petroleum ether/EtOAc = 17:3) to give dimethyl ester **46** (1.08 g, 92%). ¹H NMR (400 MHz, CDCl₃) δ 7.33 – 7.26 (m, 2H), 7.25 – 7.18 (m, 3H), 3.70 – 3.61 (m, 1H), 3.59 (s, 6H), 2.73 (dd, *J* = 15.6, 7.2 Hz, 2H), 2.65 (dd, *J* = 15.6, 7.9 Hz, 2H). ¹³C NMR (101 MHz, CDCl₃) δ 172.19, 142.67, 128.74, 127.28, 127.10, 51.75, 40.53, 38.36.

3-phenylpentane-1,5-diol (47) Dimethyl ester **46** (1.07 mg, 4.5 mmol) was dissolved in dry DCM (12.5 mL) under argon atmosphere. The mixture was cooled to 0 °C using an ice bath. DIBAL-H (21.7 mL, 1M dioxane solution, 4.8 eq.) was added dropwise to the cooled solution and stirred for 1 hour. The reaction was quenched with Rochelle salt (30 mL, sat. aq.) and the biphasic mixture was stirred at room temperature overnight. The layers were separated and the aqueous layer was extracted two times with diethyl ether. The organic layers were combined, washed with water and brine, dried over Na₂SO₄ and concentrated in vacuo. The diol **47** (863 mg, quant.) was used in the next step without further purification. ¹H NMR (400 MHz, CDCl₃) δ 7.34 – 7.27 (m, 2H), 7.24 – 7.15 (m, 3H), 3.62 – 3.52 (m, 2H), 3.52 – 3.43 (m, 2H), 2.98

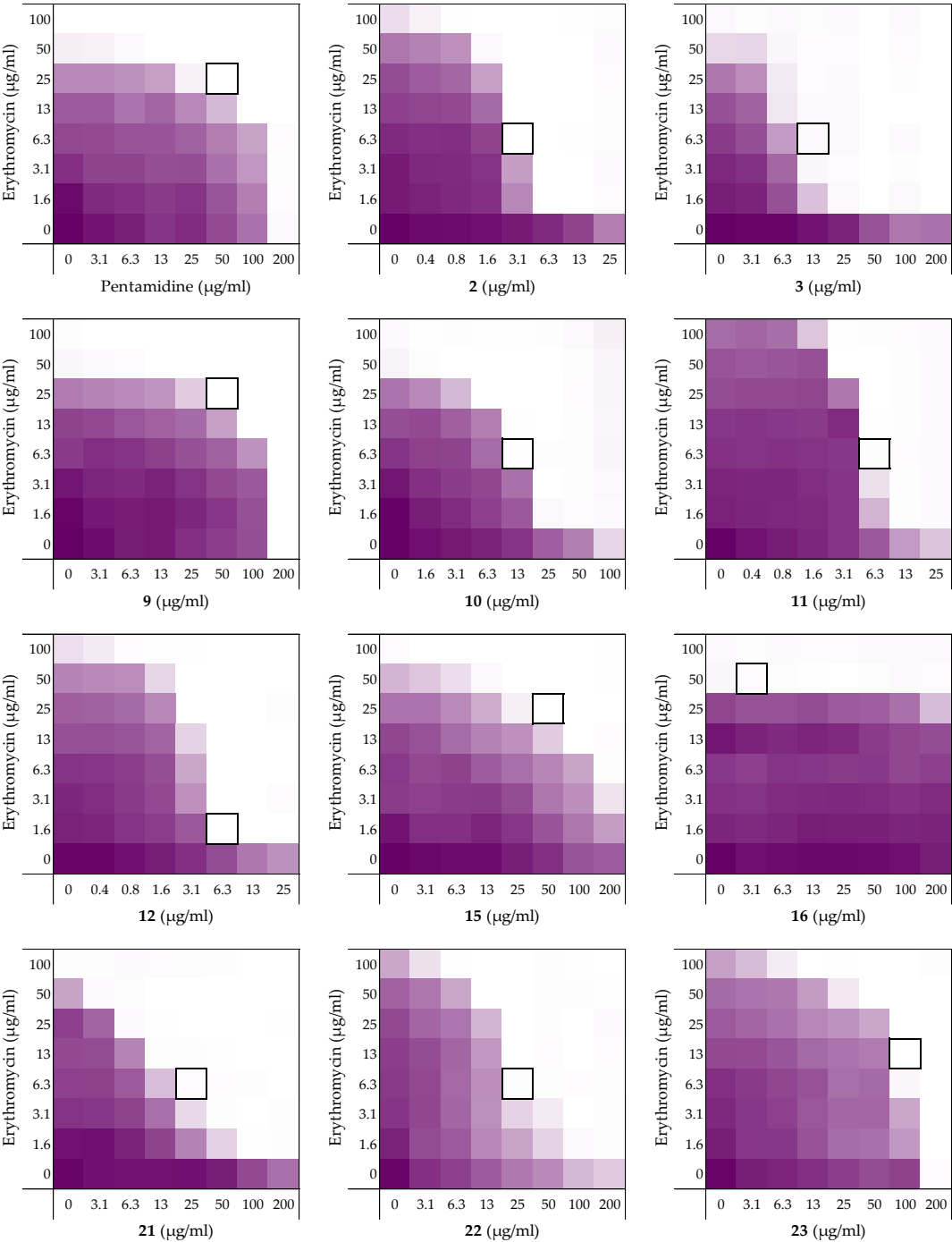
– 2.84 (m, 1H), 2.01 – 1.79 (m, 4H). ^{13}C NMR (101 MHz, CDCl_3) δ 144.48, 128.80, 127.73, 126.63, 61.04, 39.55, 38.94.

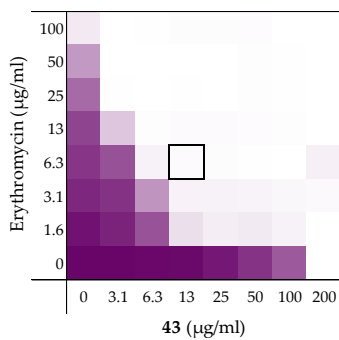
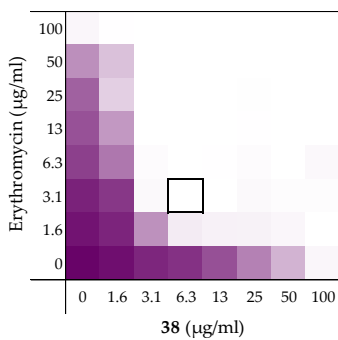
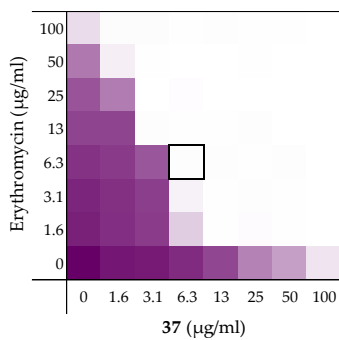
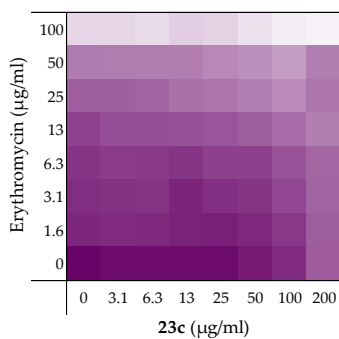
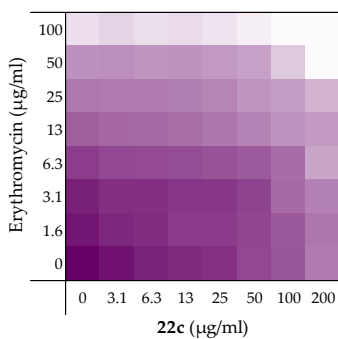
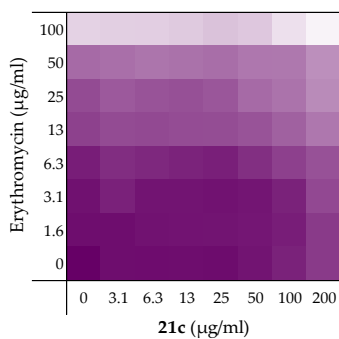
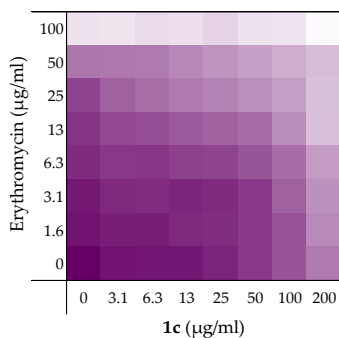
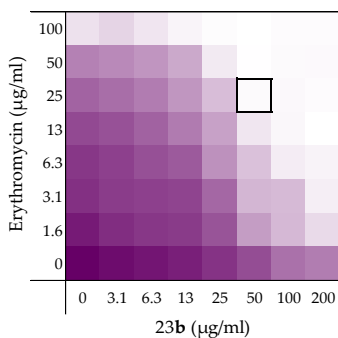
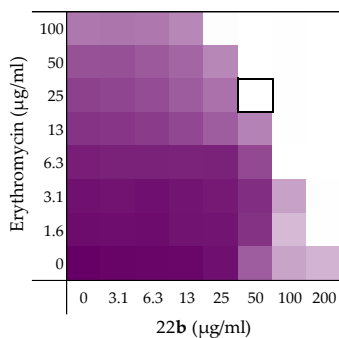
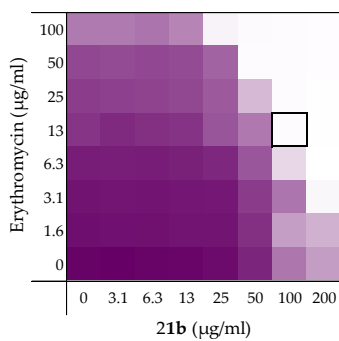
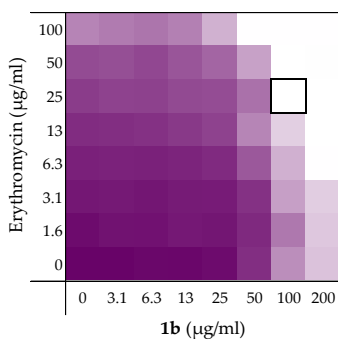
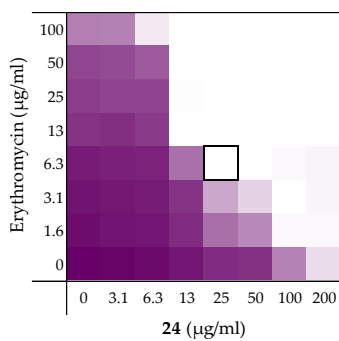
(1,5-dibromopentane-3-yl)benzene (48) Compound **47** (400 mg, 2.2 mmol) was dissolved in dry DCM (10 mL), PPh_3 (1.46 g, 5.5 mmol, 2.5 eq.) was added, and the mixture under argon was cooled to 0 °C using an ice bath. N-bromosuccinimide (0.65 g, 5.5 mmol, 2.5 eq.) was added portion wise. After the addition, the ice bath was removed and the reaction was stirred at room temperature for 2 hours. The reaction mixture was concentrated under reduced pressure and the crude product was purified by column chromatography (petroleum ether/EtOAc = 99:1) to give compound **48** (415 mg, 62%). ^1H NMR (400 MHz, CDCl_3) δ 7.34 – 7.33 (m, 3H), 7.22 – 7.16 (m, 2H), 3.28 (ddd, J = 10.0, 6.6, 5.5 Hz, 2H), 3.21 – 2.94 (m, 3H), 2.20 – 2.13 (m, 4H). ^{13}C NMR (101 MHz, CDCl_3) (including $\text{PPh}_3=\text{O}$ peaks) δ 134.00, 133.81, 132.37, 132.27, 129.09, 129.05, 128.78, 128.74, 128.67, 127.88, 127.23, 42.79, 39.34, 31.54.

4,4'-((3-phenylpentane-1,5-diyl)bis(oxy))dibenzonitrile (49) Following the procedure as described above for compound **45**, using compound **48** (500 mg, 1.6 mmol), afforded crude compound **49** (546 mg, 89%). The crude product was used in the next step without further purification. ^1H NMR (400 MHz, CDCl_3) δ 7.51 – 7.40 (m, 5H), 7.24 – 7.24 (m, 2H), 7.12 – 7.08 (m, 2H), 6.82 – 6.67 (m, 4H), 3.81 (ddd, J = 9.4, 6.6, 4.9 Hz, 2H), 3.72 (ddd, J = 9.4, 8.1, 6.0 Hz, 2H), 3.11 – 2.96 (m, 1H), 2.24 – 2.12 (m, 2H), 2.09 – 1.98 (m, 2H). ^{13}C NMR (101 MHz, CDCl_3) δ 162.23, 142.69, 137.35, 137.24, 134.08, 133.96, 133.77, 128.84, 128.66, 128.59, 127.69, 127.13, 119.34, 115.25, 104.02, 66.21, 39.00, 36.00, 29.84.

4,4'-((3-phenylpentane-1,5-diyl)bis(oxy))dibenzimidamide (3) Compound **49** (109 mg, 0.28 mmol) was dissolved in the LHMDS solution (1.1 mL, 1 M THF solution, 4.0 eq.) under argon atmosphere. The reaction was stirred at room temperature for 48 hours or longer until complete conversion to the bis-amidine (monitored by LCMS). The solution was cooled to 0 °C and quenched with HCl (4.5 mL, 4 M dioxane solution, 60 eq.). The mixture was stirred at room temperature overnight, then diluted with diethyl ether and filtered. The precipitate was purified by preparative HPLC with the gradient 20–100% in 30 minutes. The samples were analyzed and the combined pure fractions were dried to give compound **3** (27.4 mg, 23%). ^1H NMR (400 MHz, $\text{DMSO}-d_6$) δ 9.11 (d, J = 12.6 Hz, 8H), 7.77 (d, J = 8.9 Hz, 4H), 7.34 – 7.16 (m, 5H), 7.05 (d, J = 9.0 Hz, 4H), 4.00 – 3.90 (m, 2H), 3.83 (dd, J = 15.0, 8.9 Hz, 2H), 3.14 – 3.04 (m, 1H), 2.29 – 2.16 (m, 2H), 2.13 – 2.00 (m, 2H). ^{13}C NMR (101 MHz, DMSO) δ 164.81, 162.92, 143.38, 130.21, 128.62, 127.69, 126.58, 119.64, 66.21, 38.31, 35.10. HRMS (ESI): calculated for $\text{C}_{25}\text{H}_{28}\text{N}_4\text{O}_2$ $[\text{M}+\text{H}]^+$ 417.2291, found 417.2287.

Checkerboard assays and FICI data against *E. coli* BW25113 with erythromycin





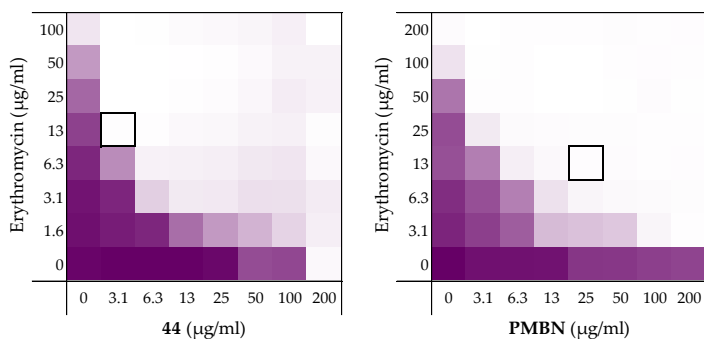
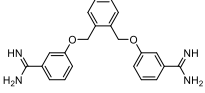
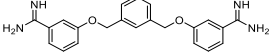
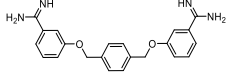
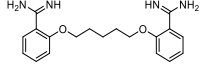
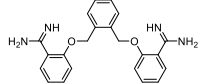
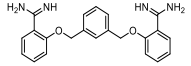
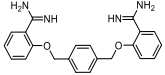
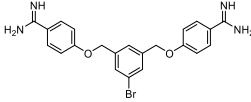
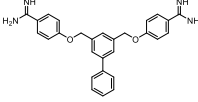
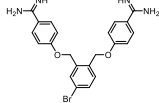
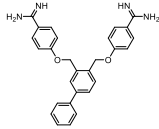


Figure S1. Checkerboard assays of the compounds and PMBN in combination with erythromycin versus *E. coli* BW25113. OD600 values were measured using a plate reader and transformed to a gradient: purple represents growth, white represents no growth. In each case, the bounded box in the checkerboard assays indicates the minimal synergistic concentration (MSC) of compound and antibiotic resulting in the lowest FICI.

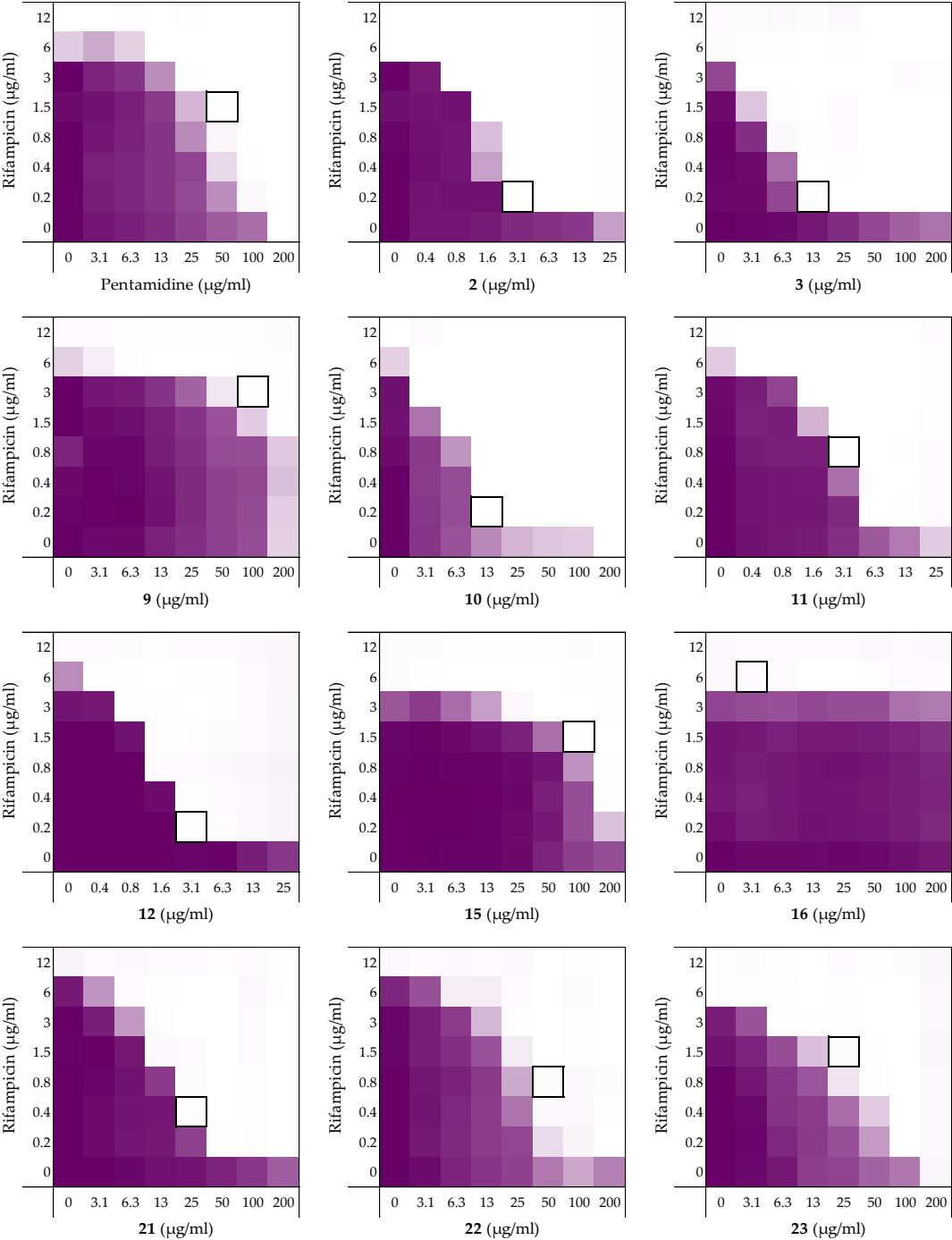
Table S1. Synergistic data of compounds and PMBN of the checkerboard assays with erythromycin as shown in Figure S1. All minimal inhibitory concentrations (MICs) and minimal synergistic concentrations (MSCs) are in $\mu\text{g/mL}$.

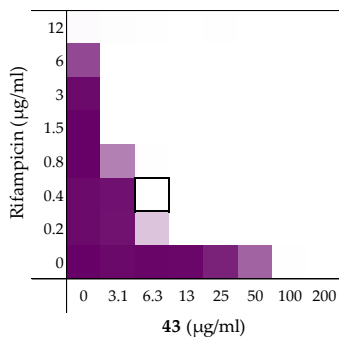
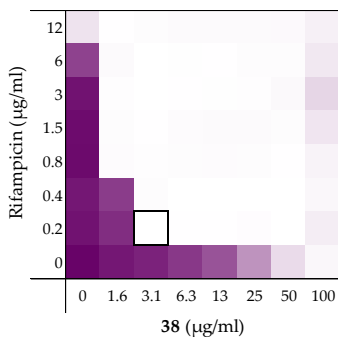
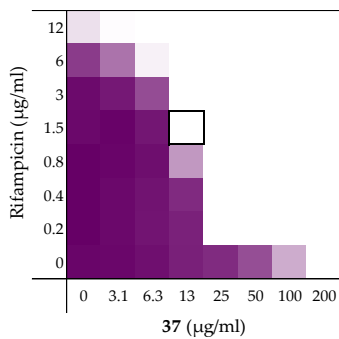
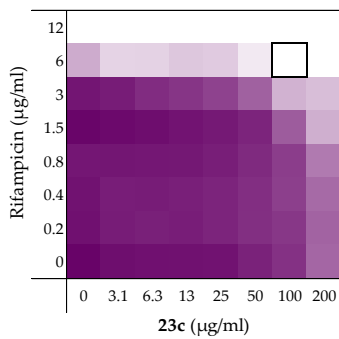
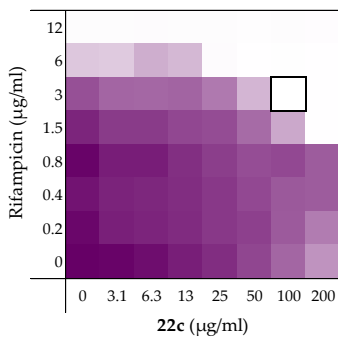
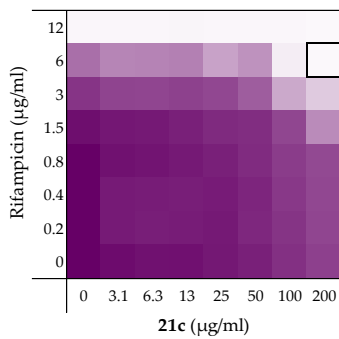
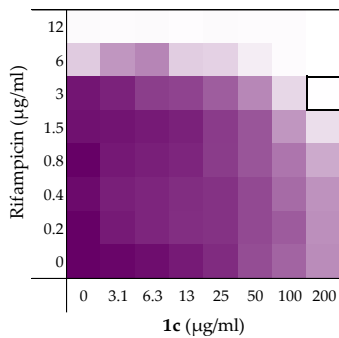
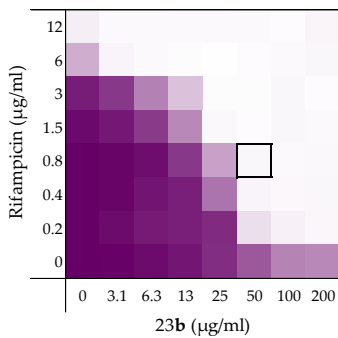
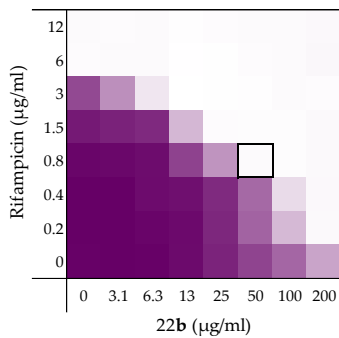
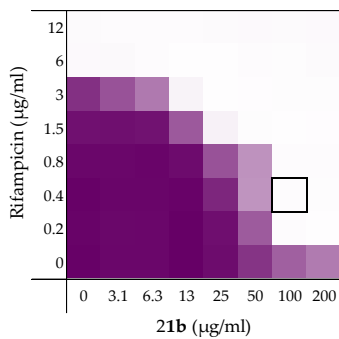
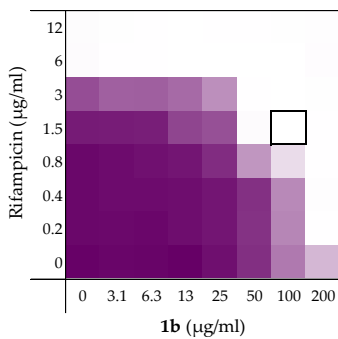
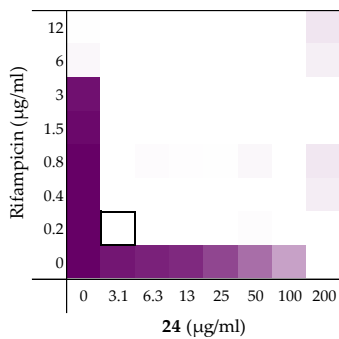
	Structures	MIC	MSC	MIC ery	MSC ery	FICI
1		200	50	100	25	0.500
2		>25	3.13	>100	6.25	≤ 0.094
3		>200	12.5	>100	6.25	≤ 0.063
9		200	50	100	25	0.500
10		>100	12.5	100	6.25	≤ 0.125
11		>25	6.25	>100	6.25	≤ 0.156
12		>25	6.25	>100	1.56	≤ 0.133
15		>200	50	100	25	≤ 0.375
16		>200	3.13	50	50	$>0.5^a$
21		>200	25	100	6.25	≤ 0.125
22		>200	25	>100	6.25	≤ 0.094
23		>200	100	>100	12.5	≤ 0.313
24		>200	25	>100	6.25	≤ 0.094
1b		>200	100	>100	25	≤ 0.375

21b		>200	100	>100	12.5	≤0.313
22b		>200	50	>100	25	≤0.250
23b		>200	50	>100	25	≤0.250
1c		>200	nd.	>100	nd.	>0.5 ^a
21c		>200	nd.	>100	nd.	>0.5 ^a
22c		>200	nd.	>100	nd.	>0.5 ^a
23c		>200	nd.	>100	nd.	>0.5 ^a
37		>100	6.25	>100	6.25	≤0.063
38		>100	6.25	>100	3.13	≤0.047
43		200	12.5	>100	6.25	≤0.094
44		200	3.13	>100	12.5	≤0.078
PMBN		>200	25	200	12.5	≤0.125

^a Synergy is defined as FICI ≤0.5.²¹

Checkerboard assays and FICI data against *E. coli* BW25113 with rifampicin





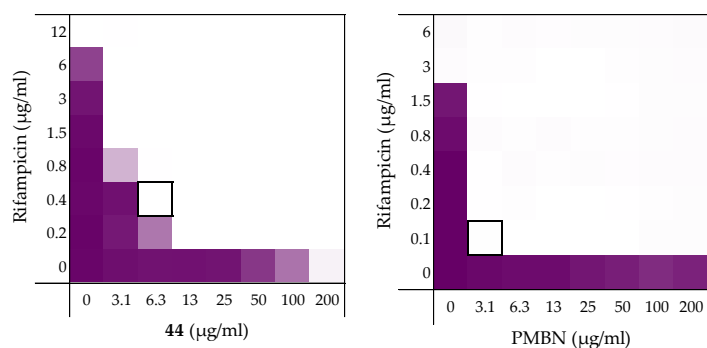
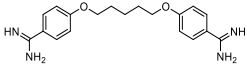
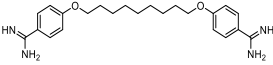
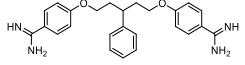
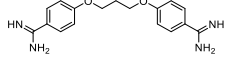
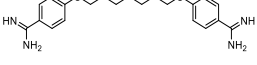
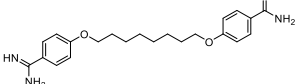
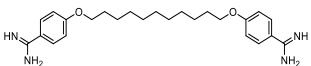
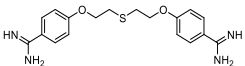
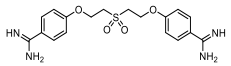
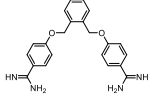
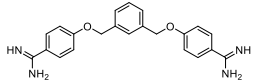
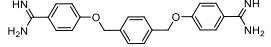
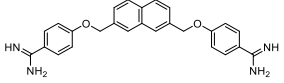
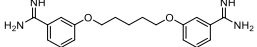
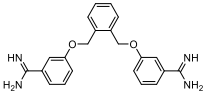
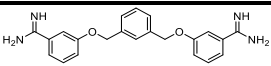
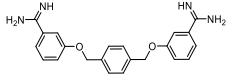
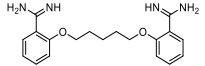
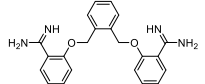
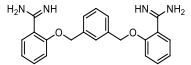
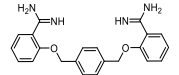
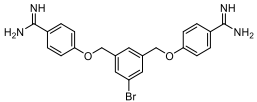
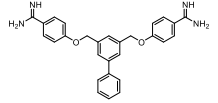
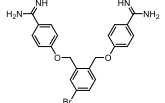
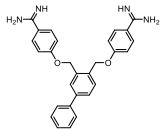


Figure S2. Checkerboard assays of the compounds and PMBN in combination with rifampicin versus *E. coli* BW25113. OD600 values were measured using a plate reader and transformed to a gradient: purple represents growth, white represents no growth. In each case, the bounded box in the checkerboard assays indicates the minimal synergistic concentration (MSC) of compound and antibiotic resulting in the lowest FICI.

Table S2. Synergistic data of compounds and PMBN of the checkerboard assays with rifampicin as shown in Figure S2. All minimal inhibitory concentrations (MICs) and minimal synergistic concentrations (MSCs) are in $\mu\text{g/mL}$.

	Structures	MIC	MSC	MIC rif	MSC rif	FICI
1		200	50	12	1.5	0.375
2		>25	3.13	6	0.19	≤ 0.094
3		>200	12.5	6	0.19	≤ 0.063
9		>200	100	12	3	≤ 0.500
10		200	12.5	12	0.19	0.078
11		>25	3.13	12	0.75	≤ 0.125
12		>25	3.13	12	0.19	≤ 0.078
15		>200	100	6	1.5	≤ 0.500
16		>200	3.13	6	6	$>0.5^a$
21		>200	25	12	0.38	≤ 0.094
22		>200	50	12	0.75	≤ 0.188
23		200	25	6	1.5	0.375
24		200	3.13	12	0.19	0.031
1b		>200	100	12	1.5	≤ 0.375
21b		>200	100	6	0.38	≤ 0.313

22b		>200	50	6	0.75	≤0.250
23b		>200	50	>12	0.75	≤0.156
1c		>200	nd.	12	nd.	>0.5 ^a
21c		>200	nd.	12	nd.	>0.5 ^a
22c		>200	nd.	12	nd.	>0.5 ^a
23c		>200	nd.	12	nd.	>0.5 ^a
37		200	12.5	>12	1.5	≤0.125
38		100	3.13	>12	0.19	≤0.039
43		100	6.25	12	0.38	0.094
44		>200	6.25	12	0.38	≤0.047
PMBN		>200	3.125	3	0.09	≤0.039

^a Synergy is defined as FICI ≤0.5.²¹

Checkerboard assays and FICI data against *E. coli* BW25113 with novobiocin

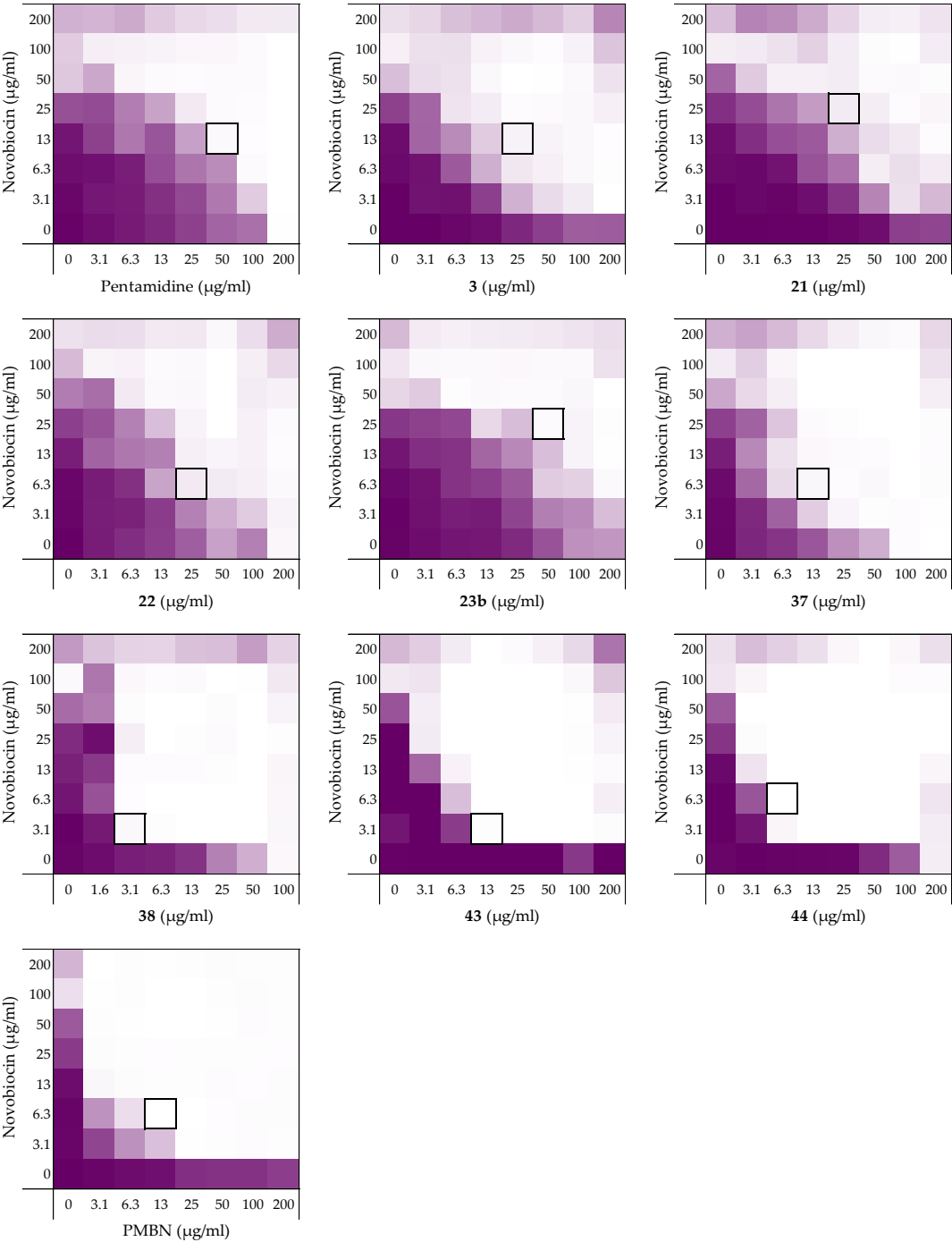
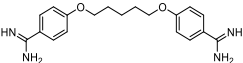
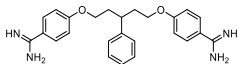
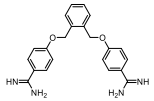
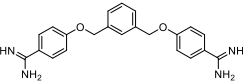
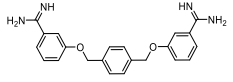
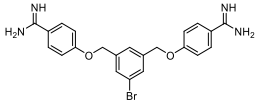
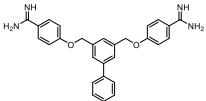
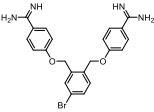
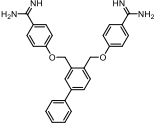


Figure S3. Checkerboard assays of compounds **1**, **3**, **21**, **22**, **23b**, **37**, **38**, **43**, **44**, and PMBN in combination with novobiocin versus *E. coli* BW25113. OD₆₀₀ values were measured using a plate reader and transformed to a gradient: purple represents growth, white represents no growth. In each case, the bounded box in the checkerboard assays indicates the minimal synergistic concentration (MSC) of compound and antibiotic resulting in the lowest FICI.

Table S3. Synergistic data of compounds **1**, **3**, **21**, **22**, **23b**, **37**, **38**, **43**, **44**, and PMBN of the checkerboard results for *E. coli* BW25113 with novobiocin as shown in Figure S3. All minimal inhibitory concentrations (MICs) and minimal synergistic concentrations (MSCs) are in µg/mL.

	Structures	MIC	MSC	MIC nov	MSC nov	FICI
1		200	50	>200	12.5	≤0.281
3		>200	25	>200	12.5	≤0.094
21		>200	25	>200	25	≤0.125
22		>200	25	>200	6.25	≤0.078
23b		>200	50	>200	25	≤0.188
37		200	12.5	>200	6.25	≤0.078
38		100	3.13	>200	3.13	≤0.039
43		>200	12.5	>200	3.13	≤0.039
44		>200	6.25	>200	6.25	≤0.031
PMBN		>200	12.5	>200	6.25	≤0.047

Checkerboard assays and FICI data against *E. coli* BW25113 with vancomycin

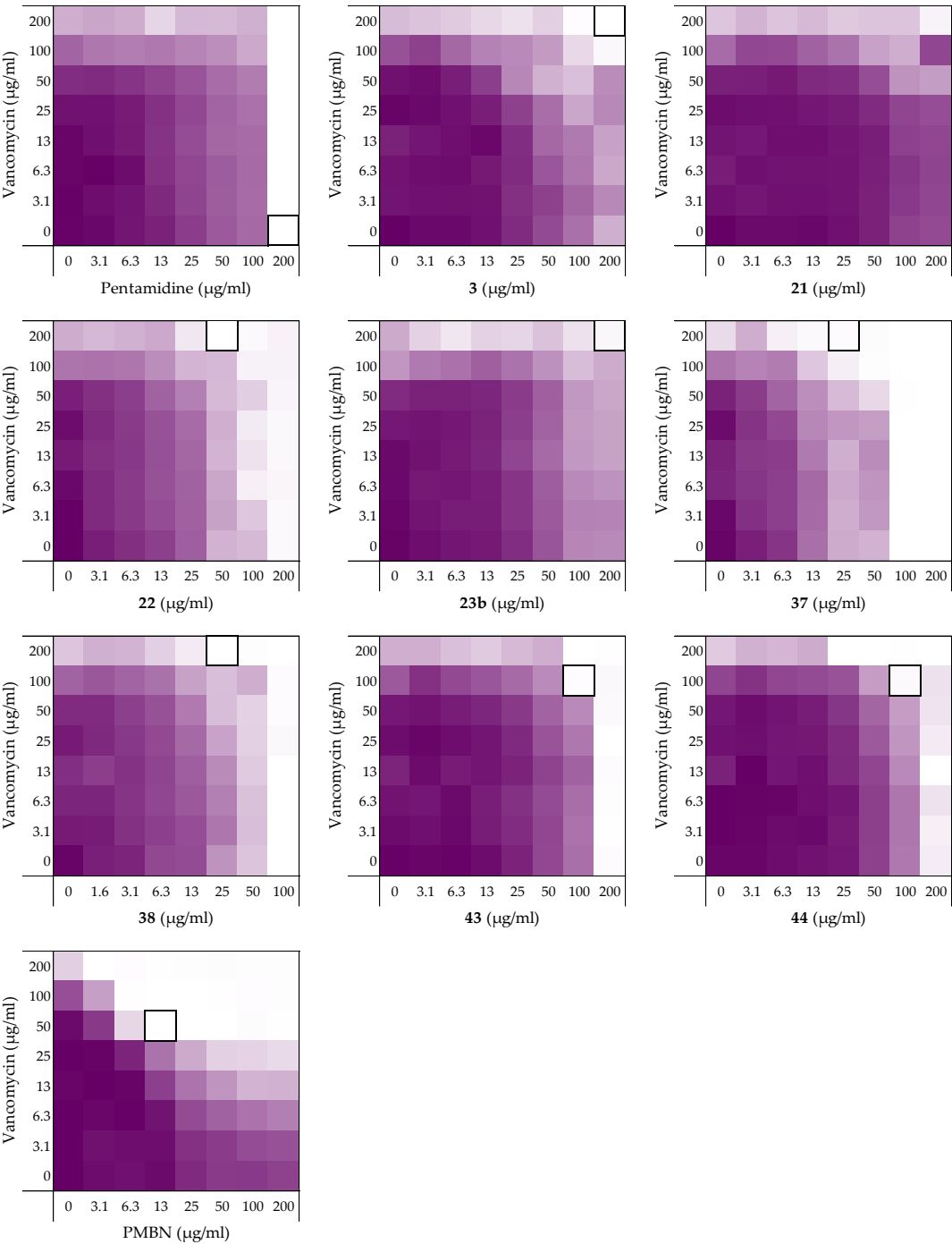
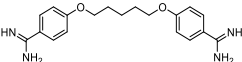
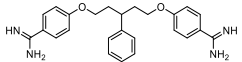
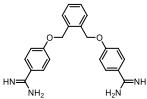
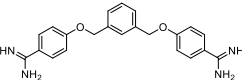
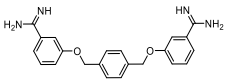
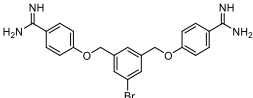
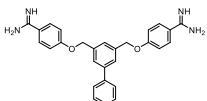
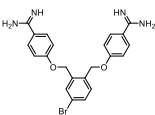
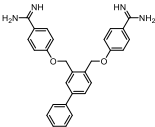


Figure S4. Checkerboard assays of compounds **1**, **3**, **21**, **22**, **23b**, **37**, **38**, **43**, **44**, and PMBN in combination with vancomycin versus *E. coli* BW25113. OD₆₀₀ values were measured using a plate reader and transformed to a gradient: purple represents growth, white represents no growth. In each case, the bounded box in the checkerboard assays indicates the minimal synergistic concentration (MSC) of compound and antibiotic resulting in the lowest FICI.

Table S4. Synergistic data of compounds **1**, **3**, **21**, **22**, **23b**, **37**, **38**, **43**, **44**, and PMBN of the checkerboard results for *E. coli* BW25113 with vancomycin as shown in Figure S4. All minimal inhibitory concentrations (MICs) and minimal synergistic concentrations (MSCs) are in µg/mL.

	Structures	MIC	MSC	MIC van	MSC van	FICI
1		200	200	>200	-	>0.5 ^a
3		>200	200	>200	200	>0.5 ^a
21		>200	>200	>200	>200	>0.5 ^a
22		>200	50	>200	200	>0.5 ^a
23b		>200	200	>200	200	>0.5 ^a
37		100	25	>200	200	>0.5 ^a
38		100	25	>200	200	>0.5 ^a
43		200	100	>200	100	>0.5 ^a
44		>200	100	>200	100	≤0.500
PMBN		>200	12.5	>200	50	≤0.156

^a Synergy is defined as FICI ≤ 0.5.²¹

Checkerboard assays and FICI data against *E. coli* ATCC25922 with rifampicin

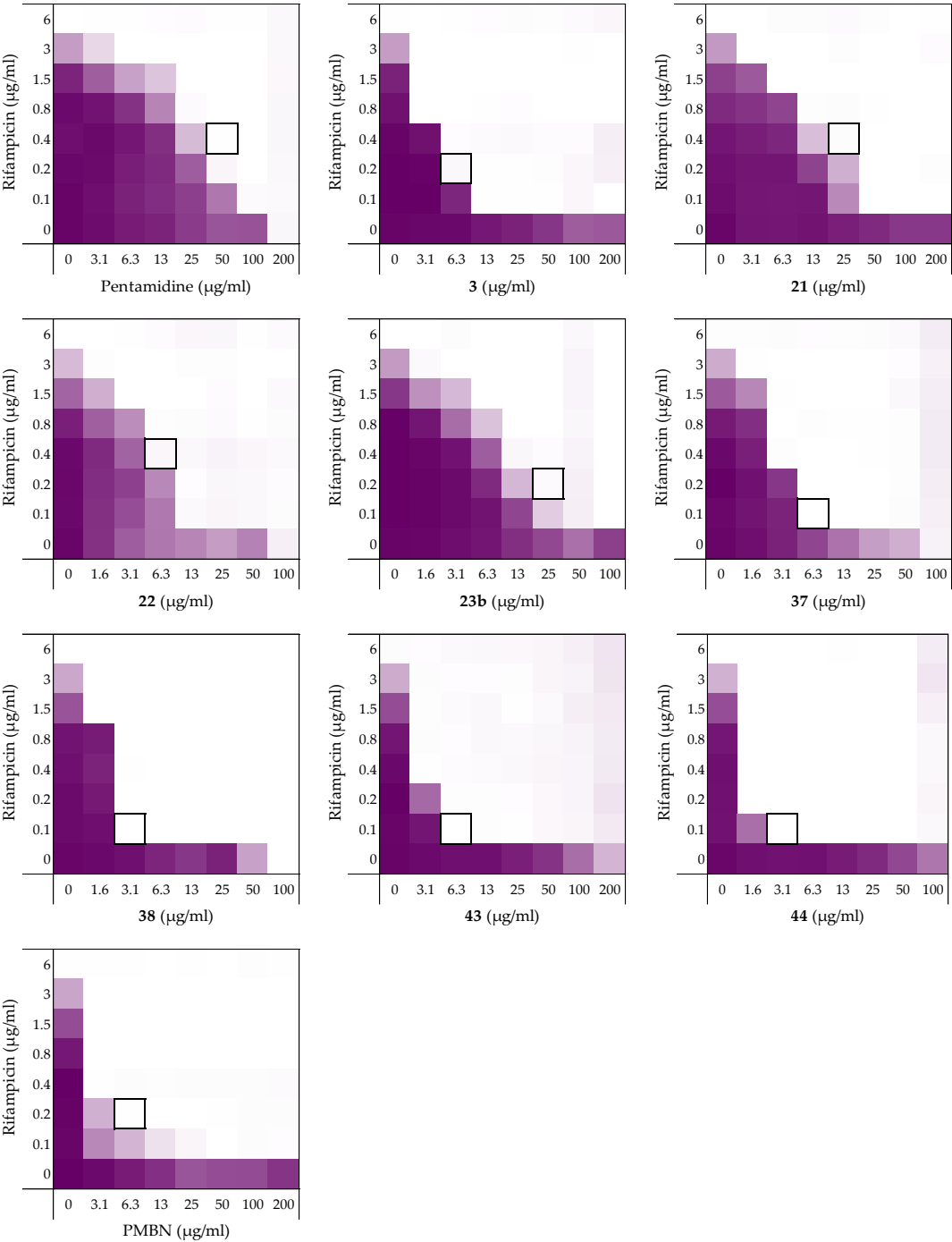
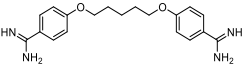
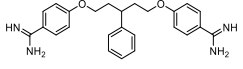
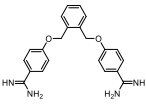
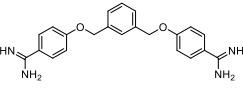
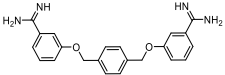
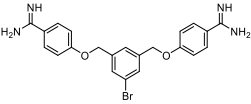
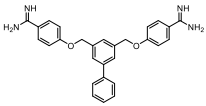
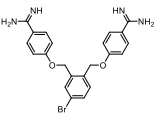
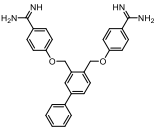


Figure S5. Checkerboard assays of compounds **1**, **3**, **21**, **22**, **23b**, **37**, **38**, **43**, **44**, and PMBN in combination with rifampicin versus *E. coli* ATCC25922. OD₆₀₀ values were measured using a plate reader and transformed to a gradient: purple represents growth, white represents no growth. In each case, the bounded box in the checkerboard assays indicates the minimal synergistic concentration (MSC) of compound and antibiotic resulting in the lowest FICI.

Table S5. Synergistic data of compounds **1**, **3**, **21**, **22**, **23b**, **37**, **38**, **43**, **44**, and PMBN of the checkerboard results for *E. coli* ATCC25922 with rifampicin as shown in Figure S5. All minimal inhibitory concentrations (MICs) and minimal synergistic concentrations (MSCs) are in µg/mL.

	Structures	MIC	MSC	MIC rif	MSC rif	FICI
1		200	50	6	0.38	0.313
3		>200	6.25	6	0.19	≤0.047
21		>200	25	6	0.38	≤0.125
22		200	6.25	6	0.38	0.094
23b		200	25	6	0.19	0.156
37		100	6.25	6	0.09	0.078
38		100	3.13	6	0.09	0.047
43		>200	6.25	6	0.09	≤0.031
44		200	3.13	6	0.09	0.031
PMBN		>200	6.25	6	0.19	≤0.047

Checkerboard assays and FICI data against *E. coli* W3110 with rifampicin

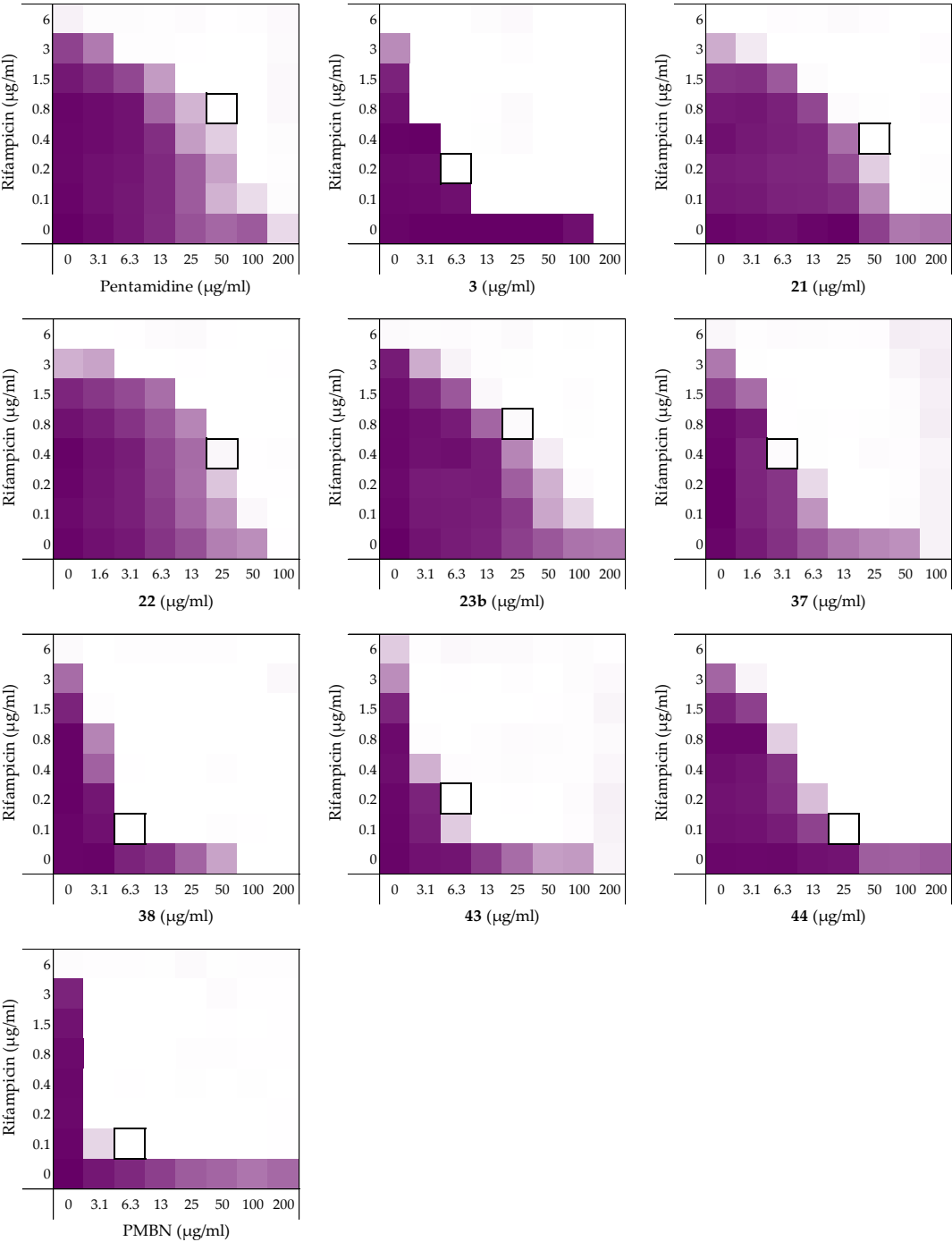
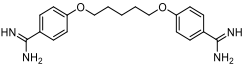
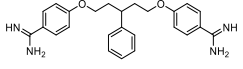
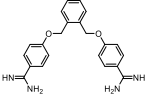
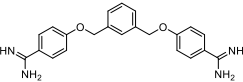
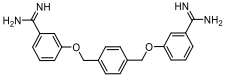
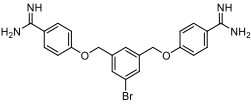
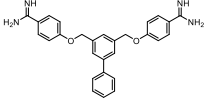
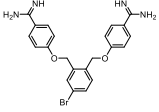
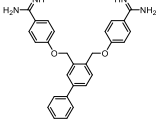


Figure S6. Checkerboard assays of compounds **1**, **3**, **21**, **22**, **23b**, **37**, **38**, **43**, **44**, and PMBN in combination with rifampicin versus *E. coli* W3110. OD₆₀₀ values were measured using a plate reader and transformed to a gradient: purple represents growth, white represents no growth. In each case, the bounded box in the checkerboard assays indicates the minimal synergistic concentration (MSC) of compound and antibiotic resulting in the lowest FICI.

Table S6. Synergistic data of compounds **1**, **3**, **21**, **22**, **23b**, **37**, **38**, **43**, **44**, and PMBN of the checkerboard results for *E. coli* W3110 with rifampicin as shown in Figure S6. All minimal inhibitory concentrations (MICs) and minimal synergistic concentrations (MSCs) are in µg/mL.

	Structures	MIC	MSC	MIC rif	MSC rif	FICI
1		>200	50	>6	0.75	≤0.188
3		200	6.25	6	0.19	0.063
21		>200	50	6	0.38	≤0.188
22		100	25	6	0.38	0.313
23b		>200	25	6	0.75	≤0.188
37		100	3.13	>6	0.38	≤0.063
38		100	6.25	>6	0.09	≤0.070
43		200	6.25	>6	0.19	≤0.047
44		>200	25	6	0.09	≤0.078
PMBN		>200	6.25	6	0.09	≤0.031

Checkerboard assays and FICI data against *E. coli* 552060.1 with rifampicin

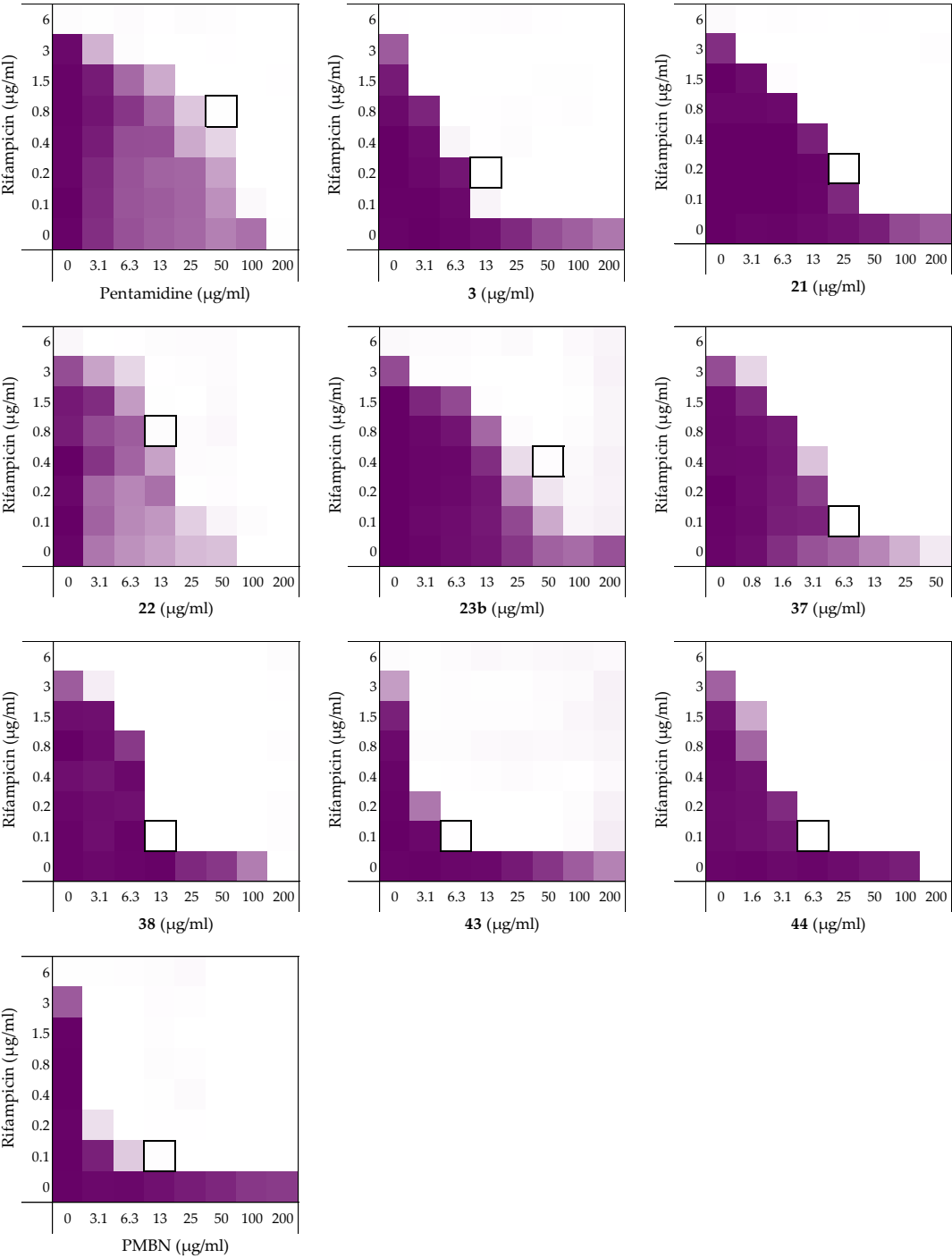
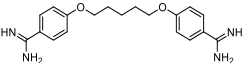
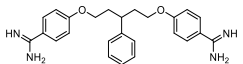
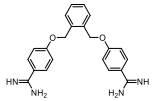
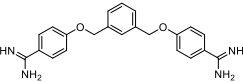
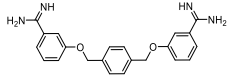
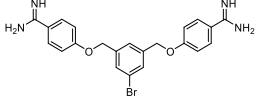
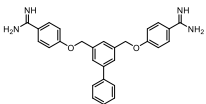
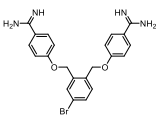
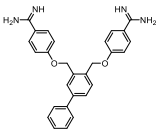


Figure S7. Checkerboard assays of compounds **1**, **3**, **21**, **22**, **23b**, **37**, **38**, **43**, **44**, and PMBN in combination with rifampicin versus *E. coli* 552060.1. OD₆₀₀ values were measured using a plate reader and transformed to a gradient: purple represents growth, white represents no growth. In each case, the bounded box in the checkerboard assays indicates the minimal synergistic concentration (MSC) of compound and antibiotic resulting in the lowest FICI.

Table S7. Synergistic data of compounds **1**, **3**, **21**, **22**, **23b**, **37**, **38**, **43**, **44**, and PMBN of the checkerboard results for *E. coli* 552060.1 with rifampicin as shown in Figure S7. All minimal inhibitory concentrations (MICs) and minimal synergistic concentrations (MSCs) are in µg/mL.

	Structures	MIC	MSC	MIC rif	MSC rif	FICI
1		200	50	6	0.75	0.375
3		>200	12.5	6	0.19	≤0.063
21		>200	25	6	0.19	≤0.094
22		100	12.5	6	0.75	0.250
23b		>200	50	6	0.38	≤0.188
37		100	6.25	6	0.09	0.078
38		200	12.5	6	0.09	0.078
43		>200	6.25	6	0.09	≤0.031
44		200	6.25	6	0.09	0.047
PMBN		>200	12.5	6	0.09	≤0.047

Checkerboard assays and FICI data against *E. coli* BW25113 *mcr-1* with rifampicin

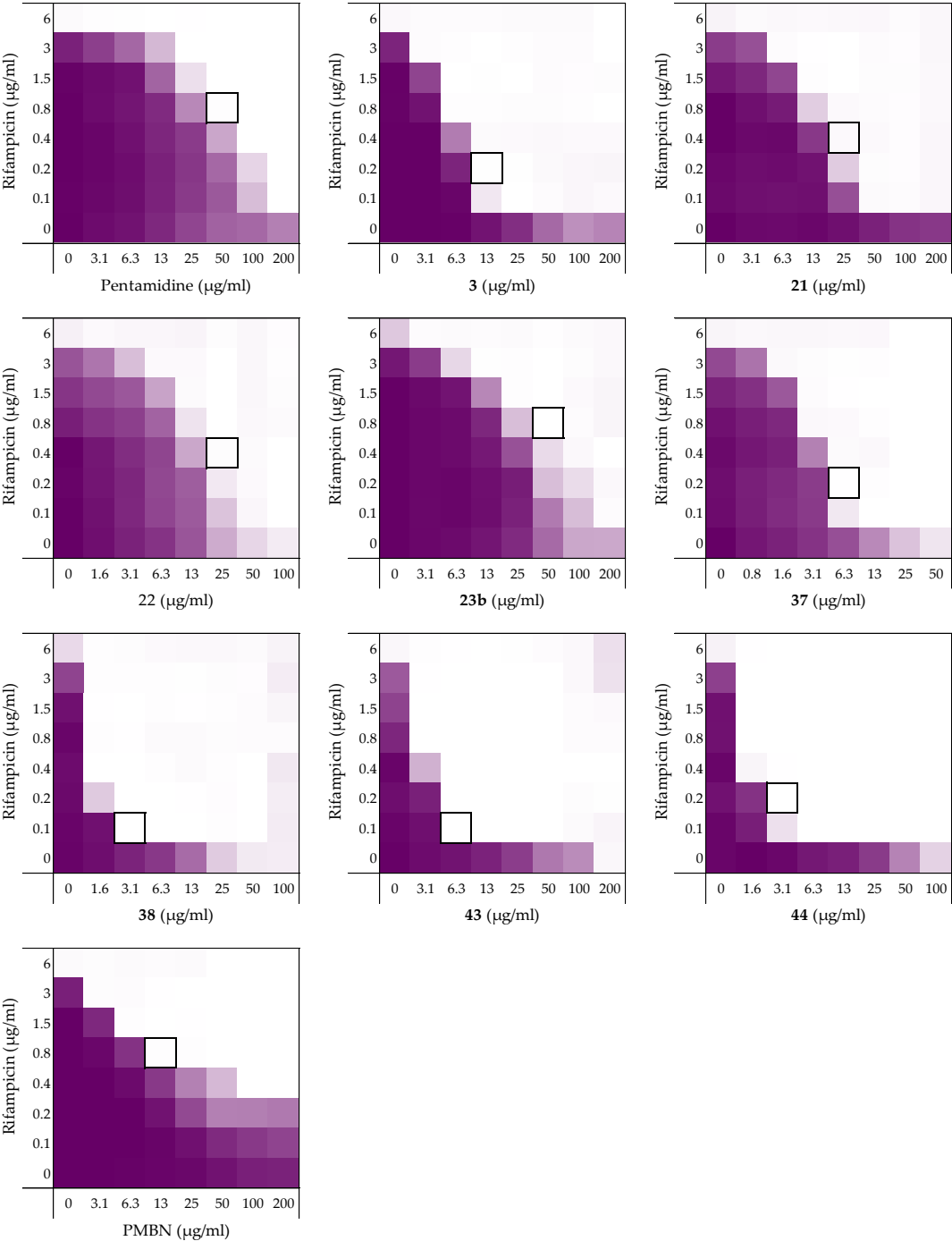
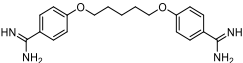
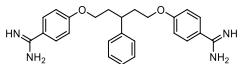
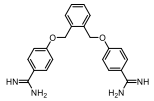
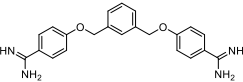
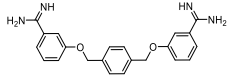
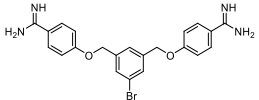
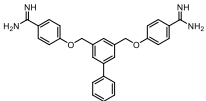
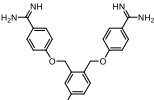
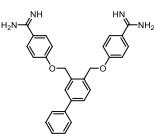


Figure S8. Checkerboard assays of compounds **1**, **3**, **21**, **22**, **23b**, **37**, **38**, **43**, **44**, and PMBN in combination with rifampicin versus *E. coli* BW25113 mcr-1. OD₆₀₀ values were measured using a plate reader and transformed to a gradient: purple represents growth, white represents no growth. In each case, the bounded box in the checkerboard assays indicates the minimal synergistic concentration (MSC) of compound and antibiotic resulting in the lowest FICI.

Table S8. Synergistic data of compounds **1**, **3**, **21**, **22**, **23b**, **37**, **38**, **43**, **44**, and PMBN of the checkerboard results for *E. coli* BW25113 mcr-1 with rifampicin as shown in Figure S8. All minimal inhibitory concentrations (MICs) and minimal synergistic concentrations (MSCs) are in µg/mL.

	Structures	MIC	MSC	MIC rif	MSC rif	FICI
1		>200	50	6	0.75	≤0.250
3		>200	12.5	6	0.19	≤0.063
21		>200	25	>6	0.38	≤0.094
22		>100	25	>6	0.38	≤0.156
23b		>200	50	>6	0.75	≤0.188
37		>50	6.25	>6	0.19	≤0.078
38		100	3.13	>6	0.09	≤0.039
43		200	6.25	>6	0.09	≤0.039
44		>100	3.13	>6	0.19	≤0.031
PMBN		>200	12.5	6	0.75	≤0.156

Checkerboard assays and FICI data against *E. coli* mcr-1 with rifampicin

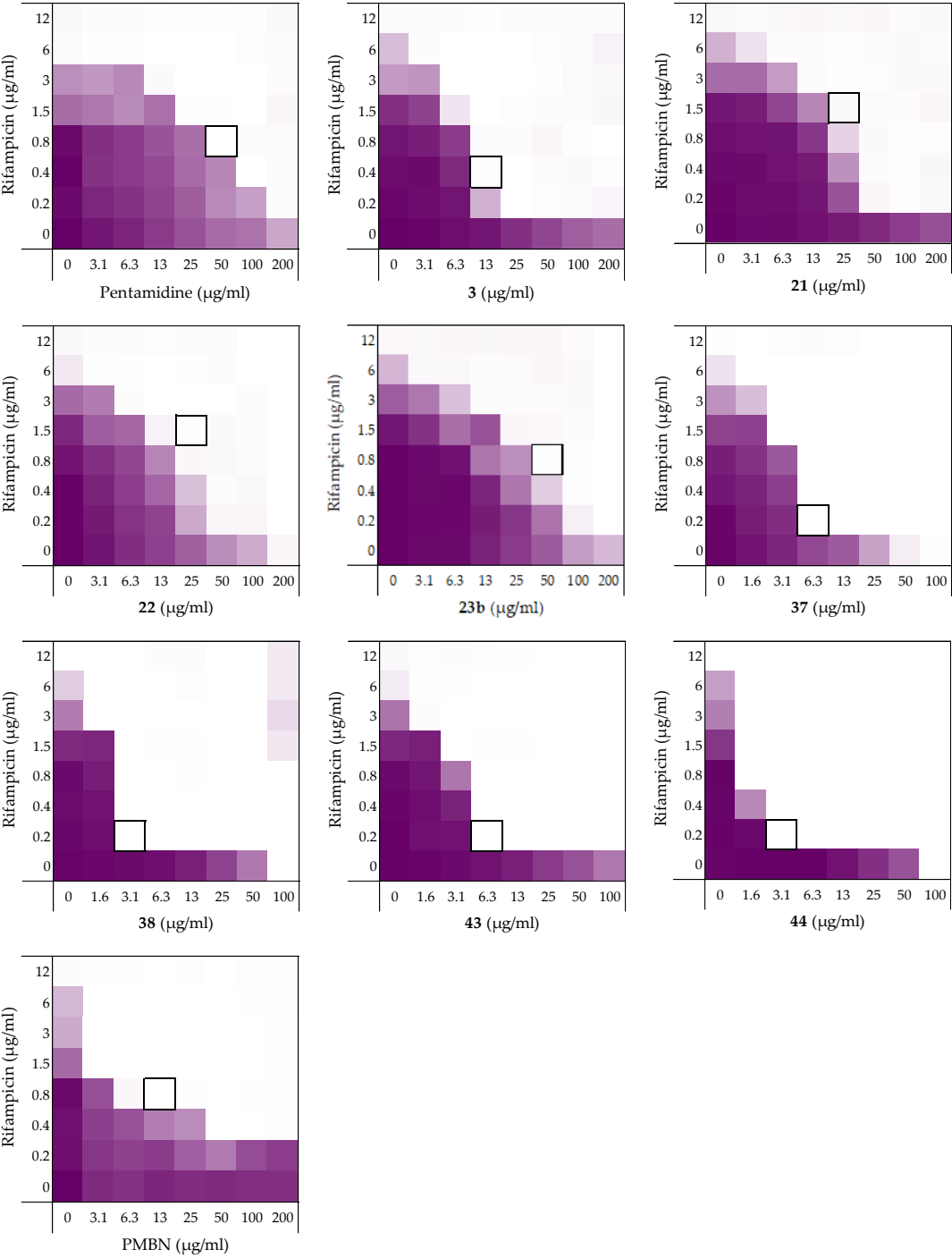
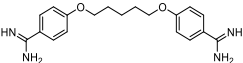
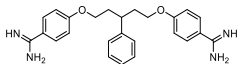
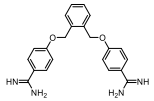
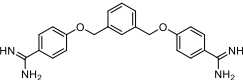
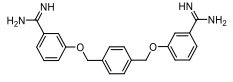
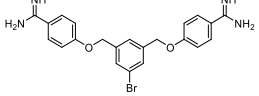
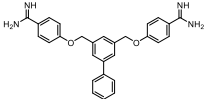
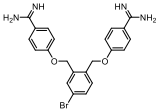
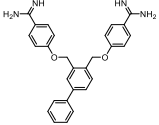


Figure S9. Checkerboard assays of compounds **1**, **3**, **21**, **22**, **23b**, **37**, **38**, **43**, **44**, and PMBN in combination with rifampicin versus *E. coli* mcr-1. OD₆₀₀ values were measured using a plate reader and transformed to a gradient: purple represents growth, white represents no growth. In each case, the bounded box in the checkerboard assays indicates the minimal synergistic concentration (MSC) of compound and antibiotic resulting in the lowest FICI.

Table S9. Synergistic data of compounds **1**, **3**, **21**, **22**, **23b**, **37**, **38**, **43**, **44**, and PMBN of the checkerboard results for *E. coli* mcr-1 with rifampicin as shown in Figure S9. All minimal inhibitory concentrations (MICs) and minimal synergistic concentrations (MSCs) are in µg/mL.

	Structures	MIC	MSC	MIC rif	MSC rif	FICI
1		>200	50	12	0.75	≤0.188
3		>200	12.5	12	0.38	≤0.063
21		>200	25	12	1.5	≤0.188
22		>200	25	12	1.5	≤0.188
23b		>200	50	12	0.75	≤0.188
37		100	6.25	12	0.19	0.078
38		100	3.13	12	0.19	0.047
43		>100	6.25	12	0.19	≤0.047
44		100	3.13	12	0.19	0.047
PMBN		>200	12.5	12	0.75	≤0.094

Checkerboard assays and FICI data against *E. coli* EQASmc^r-1 with rifampicin

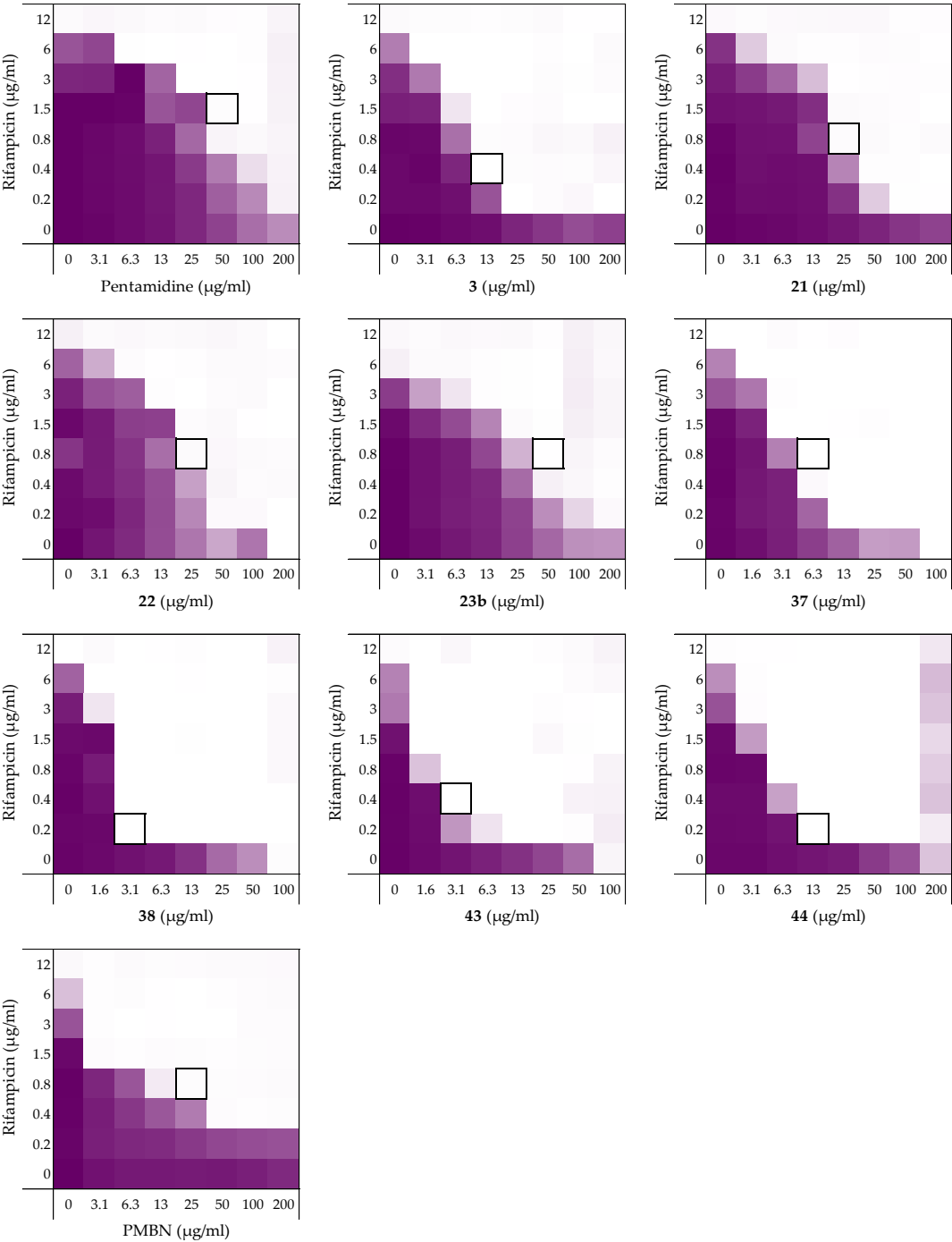
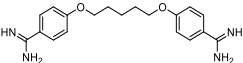
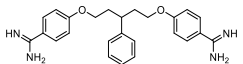
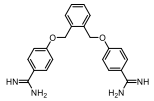
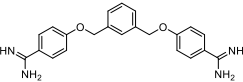
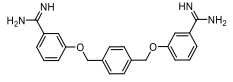
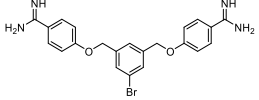
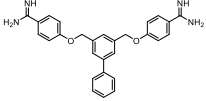
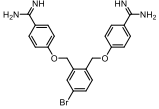
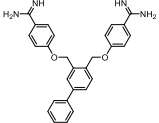


Figure S10. Checkerboard assays of compounds **1**, **3**, **21**, **22**, **23b**, **37**, **38**, **43**, **44**, and PMBN in combination with rifampicin versus *E. coli* EQASmc^r-1. OD₆₀₀ values were measured using a plate reader and transformed to a gradient: purple represents growth, white represents no growth. In each case, the bounded box in the checkerboard assays indicates the minimal synergistic concentration (MSC) of compound and antibiotic resulting in the lowest FICI.

Table S10. Synergistic data of compounds **1**, **3**, **21**, **22**, **23b**, **37**, **38**, **43**, **44**, and PMBN of the checkerboard results for *E. coli* EQASmc^r-1 with rifampicin as shown in Figure S10. All minimal inhibitory concentrations (MICs) and minimal synergistic concentrations (MSCs) are in µg/mL.

	Structures	MIC	MSC	MIC rif	MSC rif	FICI
1		>200	50	12	1.5	≤0.250
3		>200	12.5	12	0.38	≤0.063
21		>200	25	12	0.75	≤0.125
22		200	25	12	0.75	0.188
23b		>200	50	12	0.75	≤0.188
37		100	6.25	12	0.75	0.125
38		100	3.13	12	0.19	0.047
43		100	3.13	12	0.38	0.063
44		200	12.5	12	0.19	0.078
PMBN		>200	25	12	0.75	≤0.125

Checkerboard assays and FICI data against *E. coli* EQASmc-2 with rifampicin

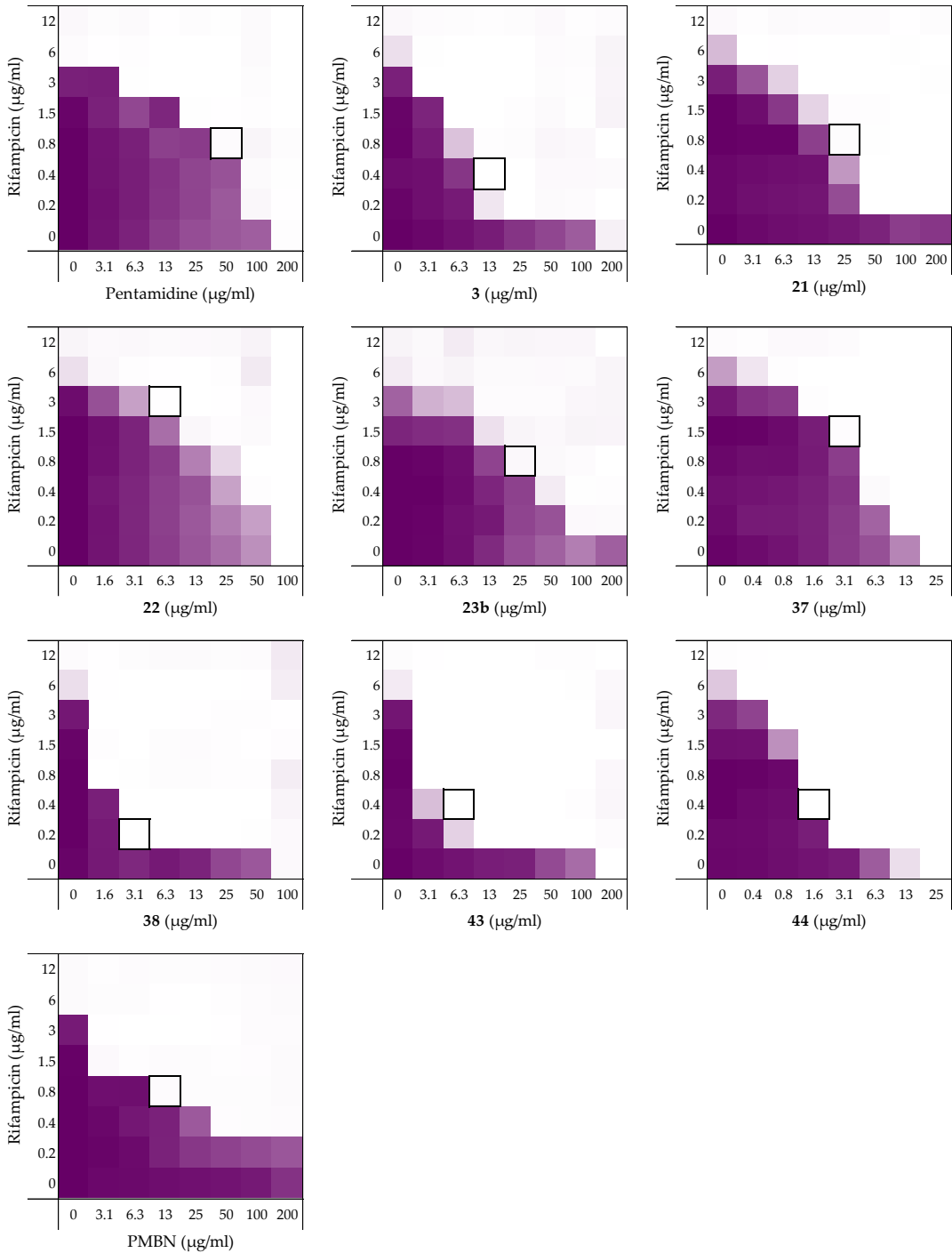
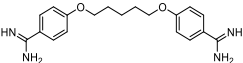
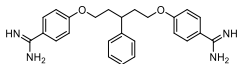
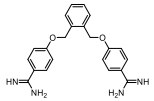
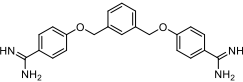
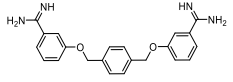
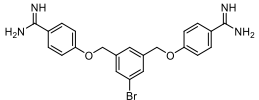
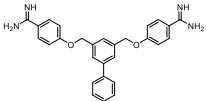
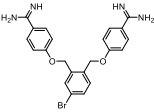
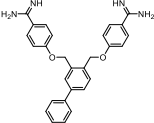


Figure S11. Checkerboard assays of compounds **1**, **3**, **21**, **22**, **23b**, **37**, **38**, **43**, **44**, and PMBN in combination with rifampicin versus *E. coli* EQASmc^r-2. OD₆₀₀ values were measured using a plate reader and transformed to a gradient: purple represents growth, white represents no growth. In each case, the bounded box in the checkerboard assays indicates the minimal synergistic concentration (MSC) of compound and antibiotic resulting in the lowest FICI.

Table S11. Synergistic data compounds **1**, **3**, **21**, **22**, **23b**, **37**, **38**, **43**, **44**, and PMBN of the checkerboard results for *E. coli* EQASmc^r-2 with rifampicin as shown in Figure S11. All minimal inhibitory concentrations (MICs) and minimal synergistic concentrations (MSCs) are in µg/mL.

	Structures	MIC	MSC	MIC rif	MSC rif	FICI
1		200	50	6	0.75	0.375
3		>200	12.5	12	0.38	≤0.063
21		>200	25	12	0.75	≤0.125
22		100	6.25	12	3	0.313
23b		>200	25	12	0.75	≤0.125
37		25	3.13	12	1.5	0.250
38		100	3.13	12	0.19	0.047
43		200	6.25	12	0.38	0.063
44		25	1.56	12	0.38	0.094
PMBN		>200	12.5	6	0.75	≤0.156

Checkerboard assays and FICI data against *E. coli* EQASmc-3 with rifampicin

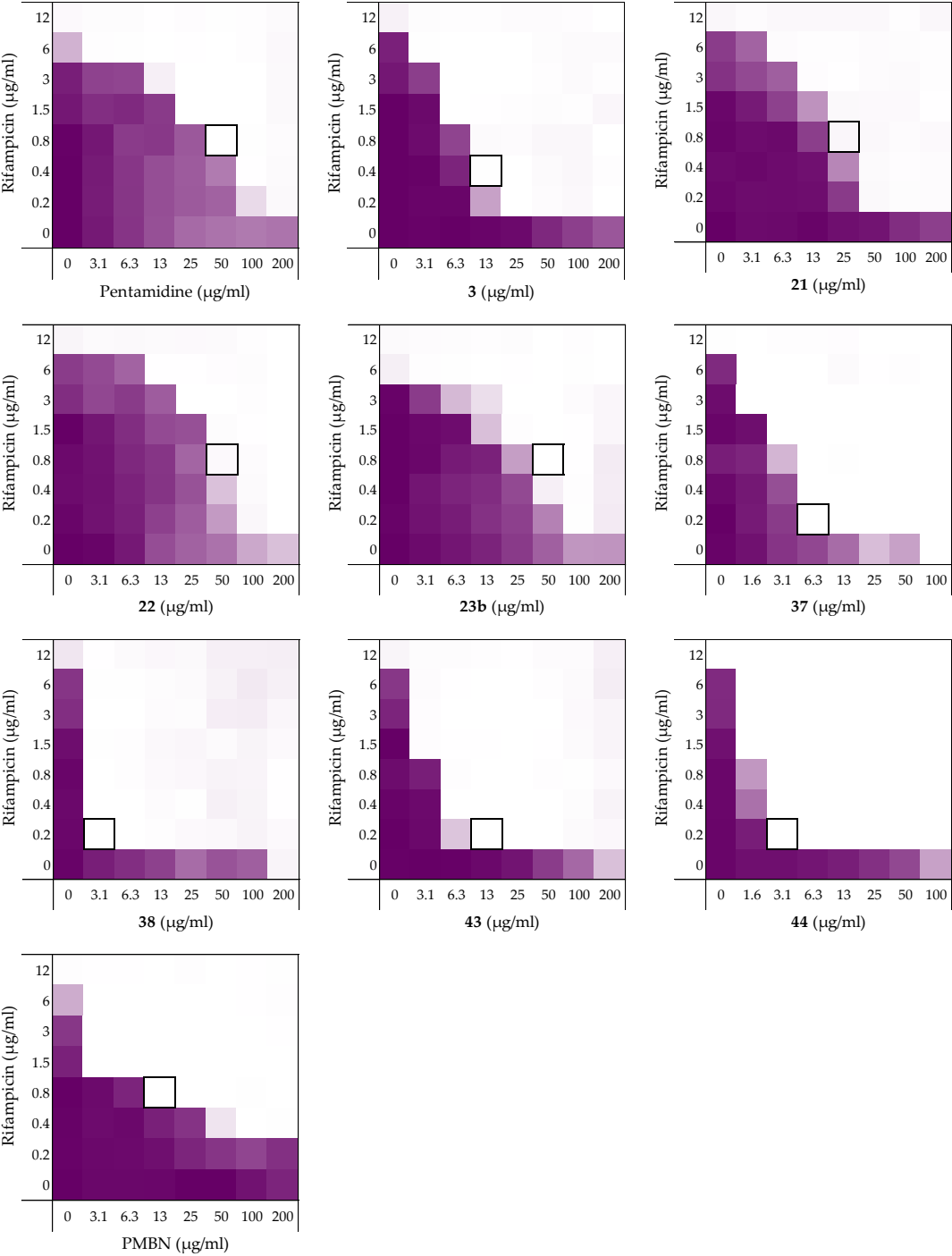
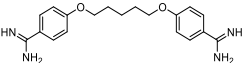
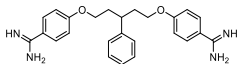
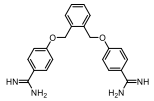
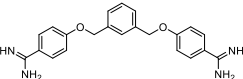
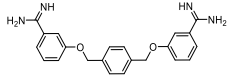
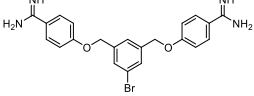
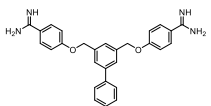
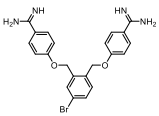
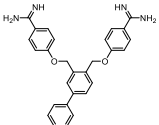


Figure S12. Checkerboard assays of compounds **1**, **3**, **21**, **22**, **23b**, **37**, **38**, **43**, **44**, and PMBN in combination with rifampicin versus *E. coli* EQASmc^r-3. OD₆₀₀ values were measured using a plate reader and transformed to a gradient: purple represents growth, white represents no growth. In each case, the bounded box in the checkerboard assays indicates the minimal synergistic concentration (MSC) of compound and antibiotic resulting in the lowest FICI.

Table S12. Synergistic data of compounds **1**, **3**, **21**, **22**, **23b**, **37**, **38**, **43**, **44**, and PMBN of the checkerboard results for *E. coli* EQASmc^r-3 with rifampicin as shown in Figure S12. All minimal inhibitory concentrations (MICs) and minimal synergistic concentrations (MSCs) are in µg/mL.

	Structures	MIC	MSC	MIC rif	MSC rif	FICI
1		>200	50	12	0.75	≤0.188
3		>200	12.5	12	0.38	≤0.063
21		>200	25	12	0.75	≤0.125
22		>200	50	12	0.75	≤0.188
23b		>200	50	12	0.75	≤0.188
37		100	6.25	12	0.19	0.078
38		200	3.13	12	0.19	0.031
43		>200	12.5	12	0.19	≤0.047
44		>100	3.13	12	0.19	≤0.031
PMBN		>200	12.5	12	0.75	≤0.094

Checkerboard assays and FICI data against *E. coli* RC00089 with rifampicin

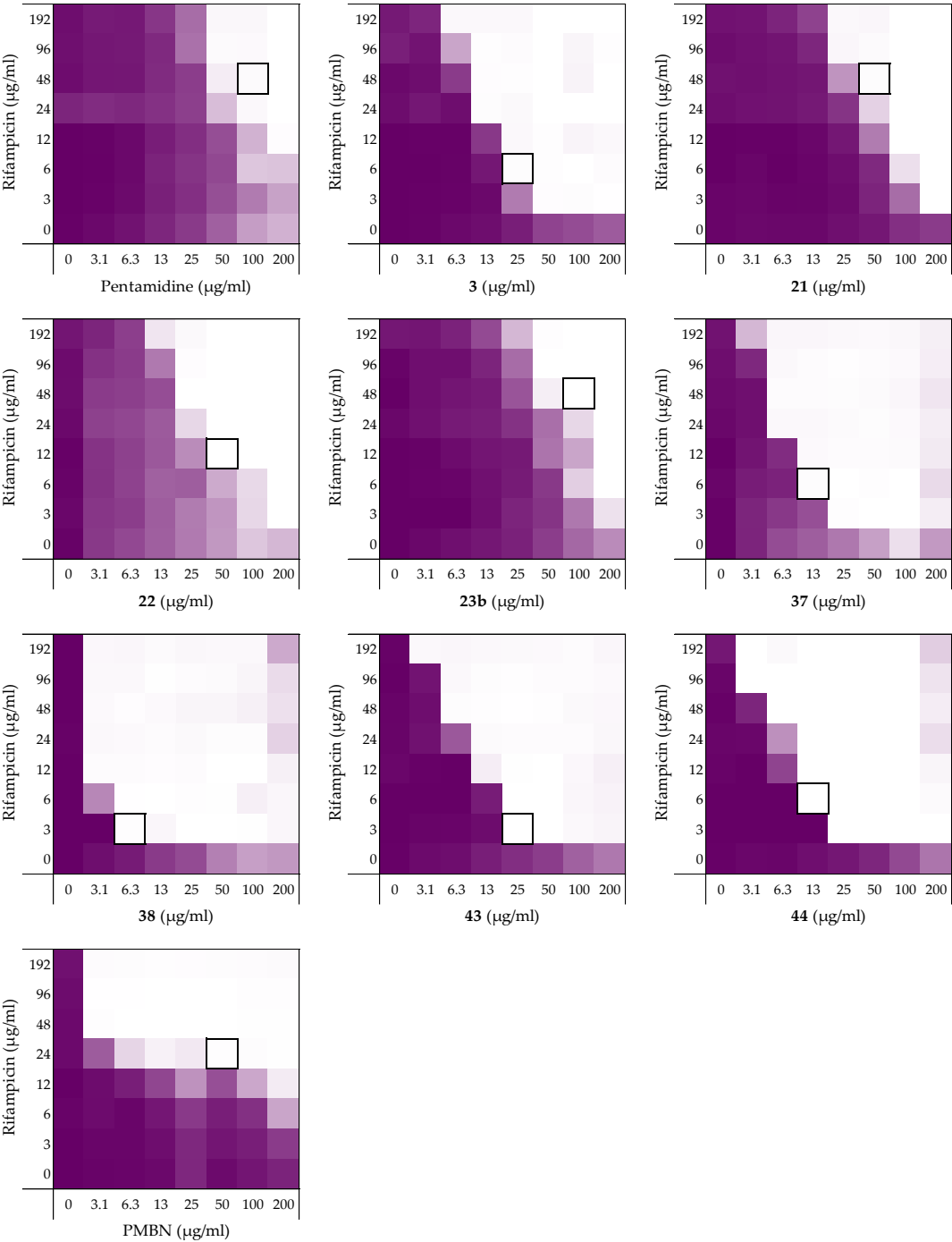
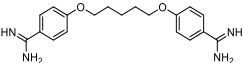
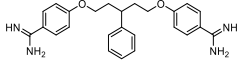
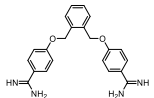
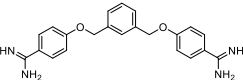
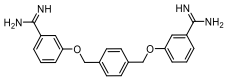
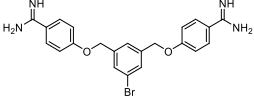
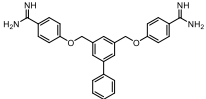
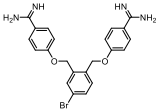
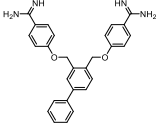


Figure S13. Checkerboard assays of compounds **1**, **3**, **21**, **22**, **23b**, **37**, **38**, **43**, **44**, and PMBN in combination with rifampicin versus *E. coli* RC00089. OD₆₀₀ values were measured using a plate reader and transformed to a gradient: purple represents growth, white represents no growth. In each case, the bounded box in the checkerboard assays indicates the minimal synergistic concentration (MSC) of compound and antibiotic resulting in the lowest FICI.

Table S13. Synergistic data of compounds **1**, **3**, **21**, **22**, **23b**, **37**, **38**, **43**, **44**, and PMBN of the checkerboard results for *E. coli* RC00089 with rifampicin as shown in Figure S13. All minimal inhibitory concentrations (MICs) and minimal synergistic concentrations (MSCs) are in µg/mL.

	Structures	MIC	MSC	MIC rif	MSC rif	FICI
1		>200	100	>192	48	≤0.375
3		>200	25	>192	6	≤0.078
21		>200	50	>192	48	≤0.250
22		>200	50	>192	12	≤0.156
23b		>200	100	>192	48	≤0.375
37		>200	12.5	>192	6	≤0.047
38		>200	6.25	>192	3	≤0.023
43		>200	25	>192	3	≤0.070
44		>200	12.5	>192	6	≤0.047
PMBN		>200	50	>192	24	≤0.188

Checkerboard assays and FICI data against *A. baumannii* ATCC17978 with rifampicin

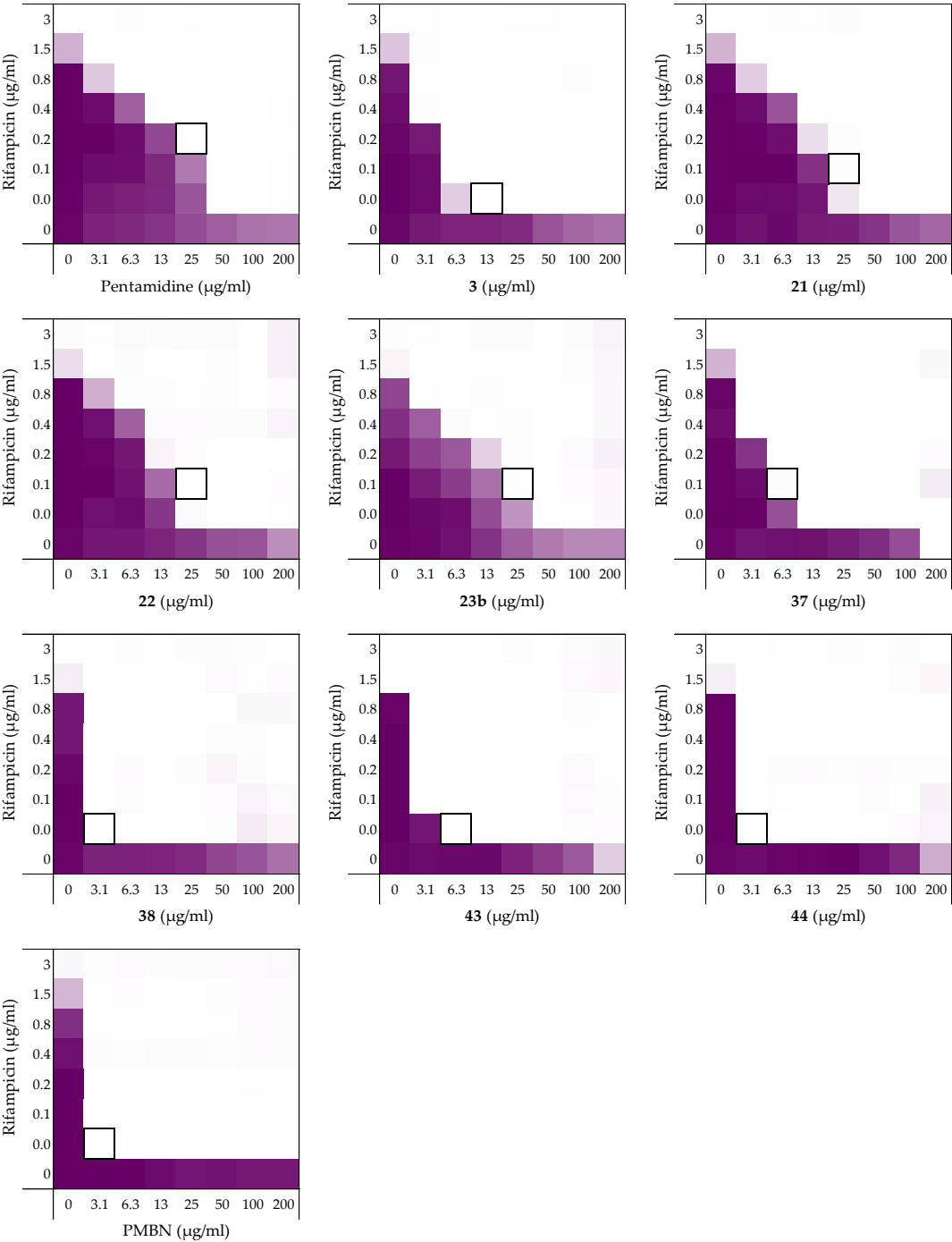
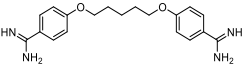
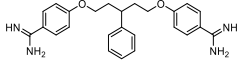
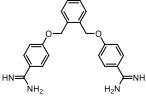
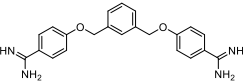
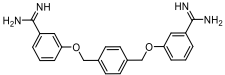
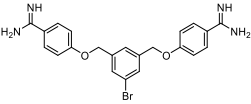
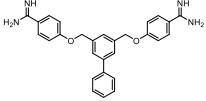
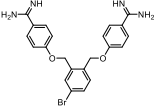
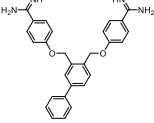


Figure S14. Checkerboard assays of compounds **1**, **3**, **21**, **22**, **23b**, **37**, **38**, **43**, **44**, and PMBN in combination with rifampicin versus *A. baumannii* ATCC17978. OD₆₀₀ values were measured using a plate reader and transformed to a gradient: purple represents growth, white represents no growth. In each case, the bounded box in the checkerboard assays indicates the minimal synergistic concentration (MSC) of compound and antibiotic resulting in the lowest FICI.

Table S14. Synergistic data of compounds **1**, **3**, **21**, **22**, **23b**, **37**, **38**, **43**, **44**, and PMBN of the checkerboard results for *A. baumannii* ATCC17978 with rifampicin as shown in Figure S14. All minimal inhibitory concentrations (MICs) and minimal synergistic concentrations (MSCs) are in µg/mL.

	Structures	MIC	MSC	MIC rif	MSC rif	FICI
1		>200	25	3	0.19	≤0.125
3		>200	12.5	3	0.05	≤0.047
21		>200	25	3	0.09	≤0.094
22		>200	25	3	0.09	≤0.094
23b		>200	25	3	0.09	≤0.094
37		>200	6.25	3	0.09	≤0.047
38		>200	3.13	3	0.05	≤0.023
43		>200	6.25	1.5	0.05	≤0.047
44		>200	3.13	3	0.05	≤0.023
PMBN		>200	3.13	3	0.05	≤0.023

Checkerboard assays and FICI data against *K. pneumoniae* ATCC13883 with rifampicin

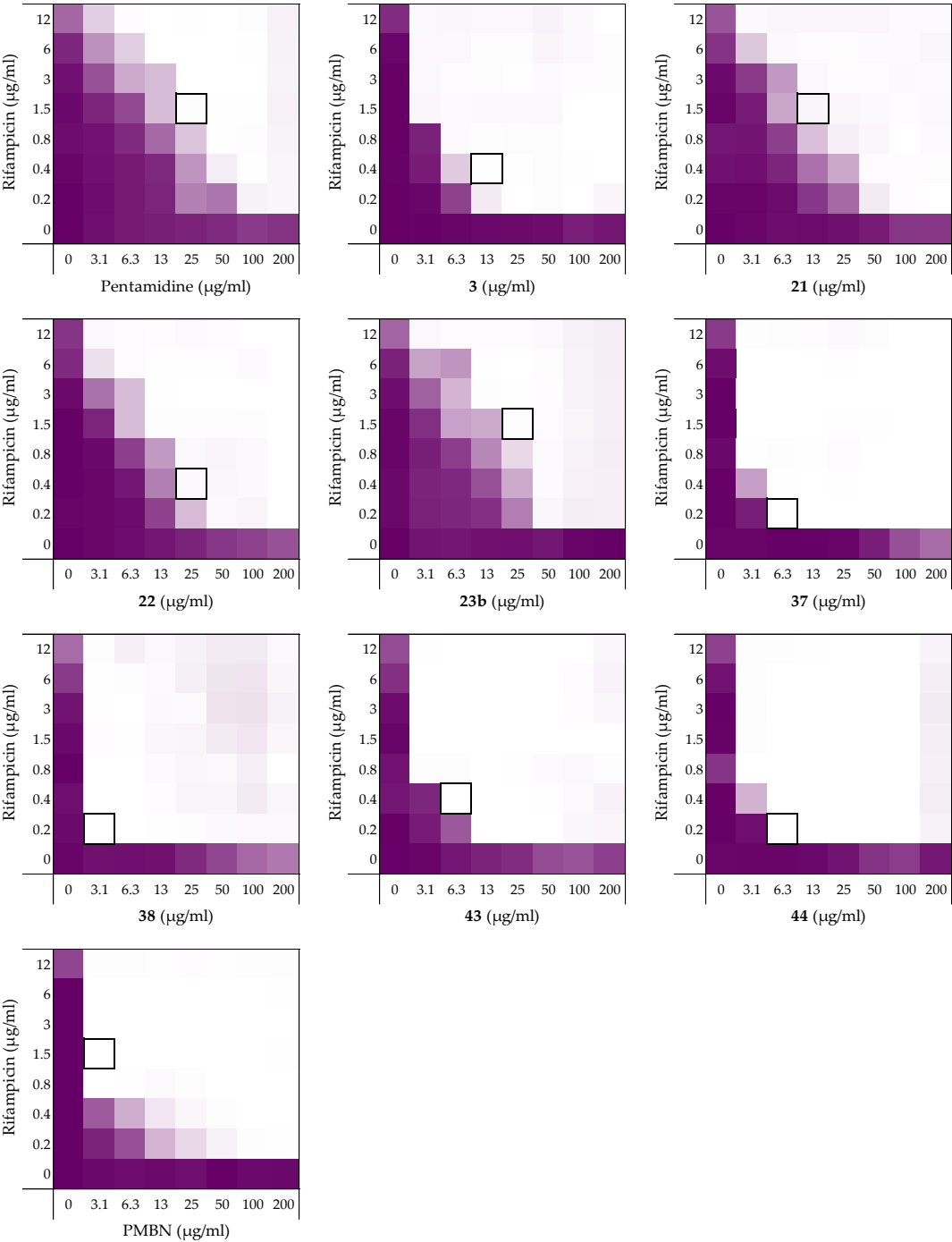
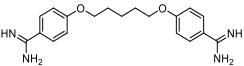
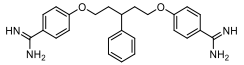
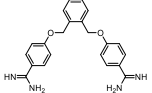
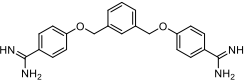
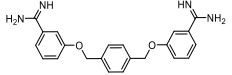
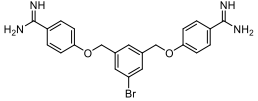
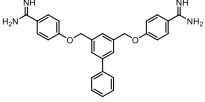
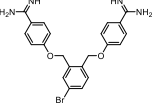
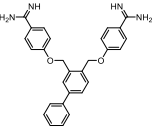


Figure S15. Checkerboard assays of compounds **1**, **3**, **21**, **22**, **23b**, **37**, **38**, **43**, **44**, and PMBN in combination with rifampicin versus *K. pneumoniae* ATCC13883. OD₆₀₀ values were measured using a plate reader and transformed to a gradient: purple represents growth, white represents no growth. In each case, the bounded box in the checkerboard assays indicates the minimal synergistic concentration (MSC) of compound and antibiotic resulting in the lowest FICI.

Table S15. Synergistic data of compounds **1**, **3**, **21**, **22**, **23b**, **37**, **38**, **43**, **44**, and PMBN of the checkerboard results for *K. pneumoniae* ATCC13883 with rifampicin as shown in Figure S15. All minimal inhibitory concentrations (MICs) and minimal synergistic concentrations (MSCs) are in µg/mL.

	Structures	MIC	MSC	MIC rif	MSC rif	FICI
1		>200	25	>12	1.5	≤0.125
3		>200	12.5	>12	0.38	≤0.047
21		>200	12.5	>12	1.5	≤0.094
22		>200	25	>12	0.38	≤0.078
23b		>200	25	>12	1.5	≤0.125
37		>200	6.25	>12	0.19	≤0.023
38		>200	3.13	>12	0.19	≤0.016
43		>200	6.25	>12	0.38	≤0.031
44		>200	6.25	>12	0.19	≤0.023
PMBN		>200	3.13	>12	1.5	≤0.070

Checkerboard assays and FICI data against *P. aeruginosa* ATCC27853 with rifampicin

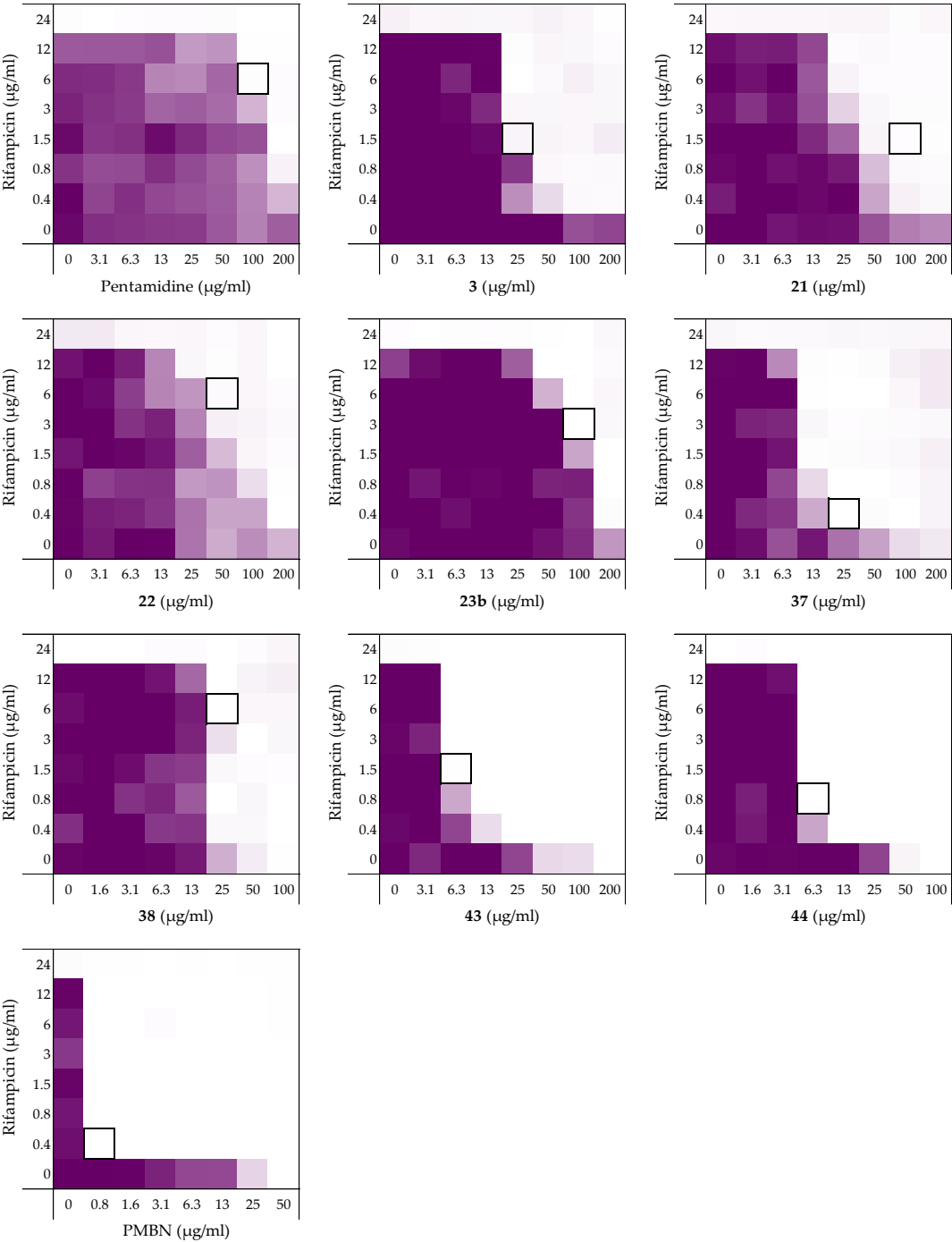
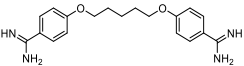
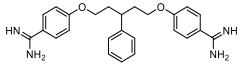
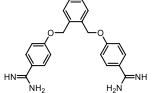
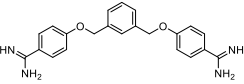
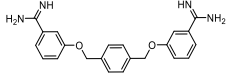
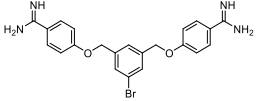
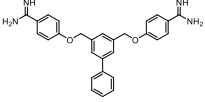
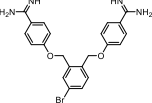
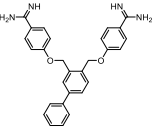


Figure S16. Checkerboard assays of compounds **1**, **3**, **21**, **22**, **23b**, **37**, **38**, **43**, **44**, and PMBN in combination with rifampicin versus *P. aeruginosa* ATCC27853. OD₆₀₀ values were measured using a plate reader and transformed to a gradient: purple represents growth, white represents no growth. In each case, the bounded box in the checkerboard assays indicates the minimal synergistic concentration (MSC) of compound and antibiotic resulting in the lowest FICI.

Table S16. Synergistic data of compounds **1**, **3**, **21**, **22**, **23b**, **37**, **38**, **43**, **44**, and PMBN of the checkerboard results for *P. aeruginosa* ATCC27853 with rifampicin as shown in Figure S16. All minimal inhibitory concentrations (MICs) and minimal synergistic concentrations (MSCs) are in µg/mL.

	Structures	MIC	MSC	MIC rif	MSC rif	FICI
1		>200	100	24	6	≤0.500
3		>200	25	24	1.5	≤0.125
21		>200	100	24	1.5	≤0.313
22		>200	50	>24	6	≤0.250
23b		>200	100	24	3	≤0.375
37		>200	25	24	0.38	≤0.078
38		100	25	24	6	0.500
43		200	6.25	24	1.5	0.094
44		100	6.25	24	0.75	0.094
PMBN		50	0.78	24	0.38	0.031

Hemolysis assay

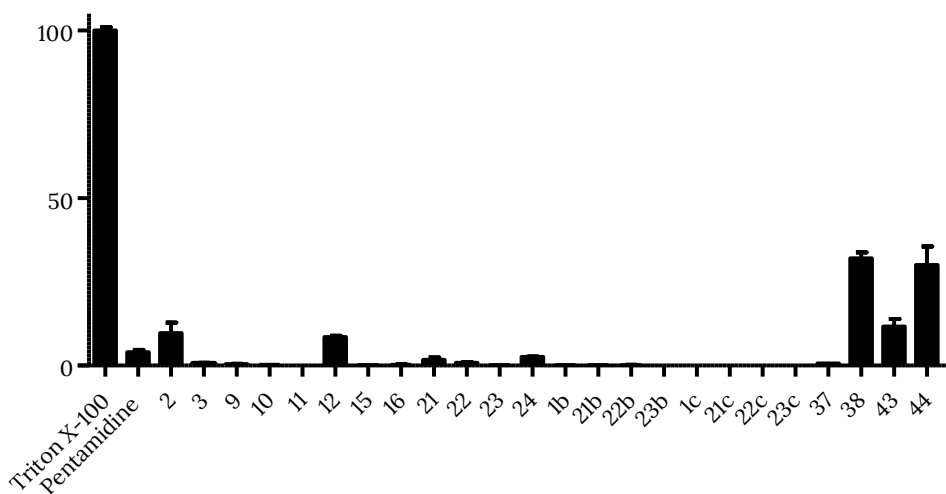


Figure S17. Hemolytic activity of all compounds (200 $\mu\text{g/mL}$) after 1 hour of incubation. The hemolysis assay was performed as described in materials and methods. Values below 10% were defined as non-hemolytic.⁷⁶ Error bars represent the standard deviation based on n=3 technical replicates.

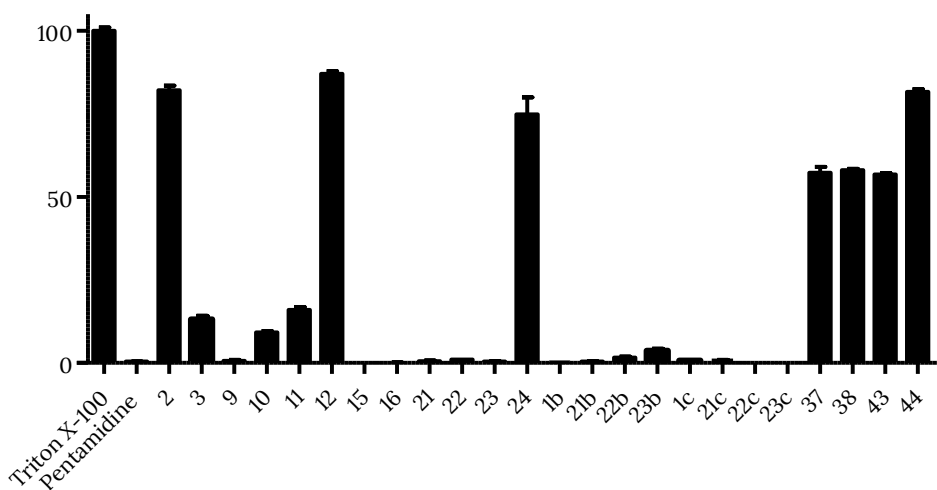
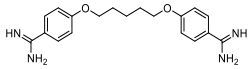
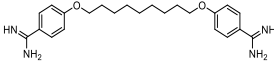
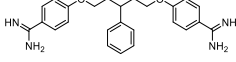
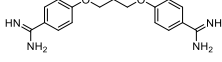
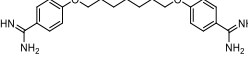
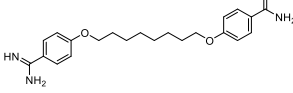
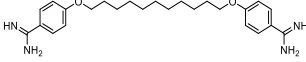
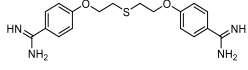
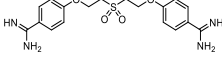
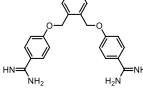
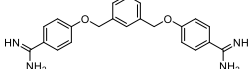
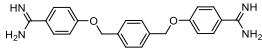
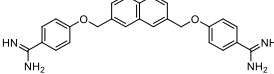
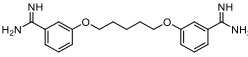
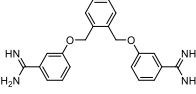


Figure S18. Hemolytic activity of all compounds (200 $\mu\text{g/mL}$) after 20 hours of incubation. The hemolysis assay was performed as described in materials and methods. Values below 10% were defined as non-hemolytic.⁷⁶ Error bars represent the standard deviation based on n=3 technical replicates.

Table S17. Hemolytic activity of all compounds (200 µg/mL). The hemolysis assay was performed as described in materials and methods. Values <10% were defined as non-hemolytic.⁷⁶

	Structures	Hemolysis 1 hour (%)	Hemolysis 20 hours (%)
1		4.0	0.4
2		9.7	82
3		0.5	13
9		0.4	0.6
10		0.3	9.2
11		0.0	16
12		8.5	87
15		0.2	0.0
16		0.2	0.1
21		1.7	0.5
22		0.9	11
23		0.2	0.4
24		2.6	75
1b		0.1	0.1
21b		0.1	0.4

22b		0.2	1.6
23b		0.0	3.7
1c		0.0	0.7
21c		0.0	0.4
22c		0.0	0.0
23c		0.0	0.0
37		0.6	57
38		32	58
43		12	57
44		30	82

Outer membrane permeability assay

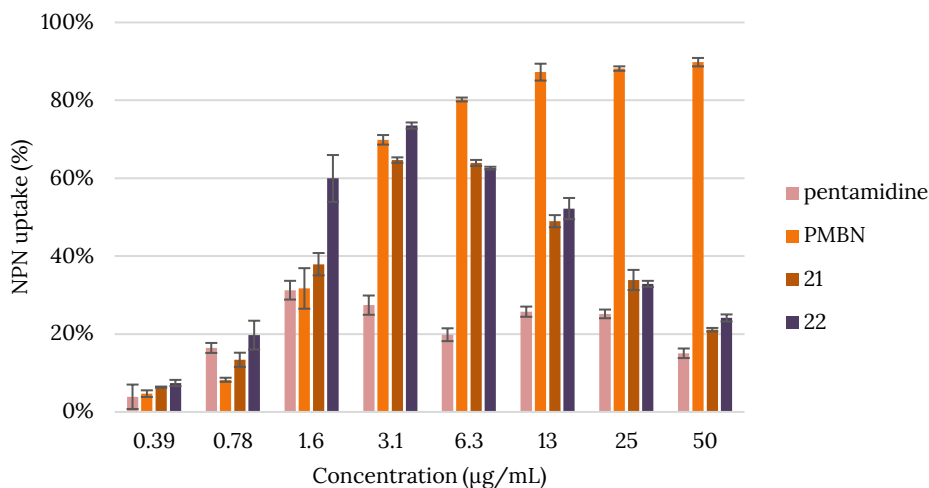


Figure S19. Outer membrane permeabilization assay of compounds **1**, **21**, **22**, and PMBN with *E. coli* BW25113 using *N*-phenyl-napthalen-1-amine (NPN) (at 0.01 mM) as fluorescent probe. The read-out was performed using a plate reader with λ_{ex} 355 nm and λ_{em} 420 nm. The NPN uptake values shown are relative to the uptake signal obtained upon treating the cells with 100 µg/mL colistin as previously reported.⁶⁸ Error bars represent the standard deviation based on $n=3$ technical replicates. Of note is the maximum NPN fluorescence measured for pentamidine and bis-amidines **21** and **22** at 3.1 µg/mL (0.01 mM). At higher bis-amidines concentrations, NPN fluorescence decreases, an effect not observed for PMBN.

References

- (1) Amann, S.; Neef, K.; Kohl, S. Antimicrobial Resistance (AMR). *European Journal of Hospital Pharmacy* **2019**, 26 (3), 175–177. <https://doi.org/10.1136/ejpharm-2018-001820>.
- (2) UN Interagency Coordination Group on Antimicrobial Resistance. No Time to Wait: Securing the Future from Drug-Resistant Infections; Report to the Secretary-General of the United Nations. Geneva, WHO. **2019**. <https://www.who.int/antimicrobial-resistance/interagency-coordination-group/final-report/en/>.
- (3) WHO. Prioritization of pathogens to guide discovery, research and development of new antibiotics for drug-resistant bacterial infections including tuberculosis (WHO/EKP/IAU/2017.12), Geneva, WHO. **2017**
- (4) Macnair, C. R.; Brown, E. D. Outer Membrane Disruption Overcomes Intrinsic, Acquired, and Spontaneous Antibiotic Resistance. *mBio* **2020**, 11 (5), 1–15. <https://doi.org/10.1128/mBio.01615-20>.
- (5) Nikaido, H. The Role of Outer Membrane and Efflux Pumps in the Resistance of Gram-Negative Bacteria. Can We Improve Drug Access? *Drug Resistance Updates*. Churchill Livingstone January 1, 1998, pp 93–98. [https://doi.org/10.1016/S1368-7646\(98\)80023-X](https://doi.org/10.1016/S1368-7646(98)80023-X).
- (6) Vaara, M.; Vaara, T. Sensitization of Gram-Negative Bacteria to Antibiotics and Complement by a Nontoxic Oligopeptide. *Nature* **1983**, 303 (5917), 526–528. <https://doi.org/10.1038/303526a0>.
- (7) Stokes, J. M.; Macnair, C. R.; Ilyas, B.; French, S.; Côté, J. P.; Bouwman, C.; Farha, M. A.; Sieron, A. O.; Whitfield, C.; Coombes, B. K.; Brown, E. D. Pentamidine Sensitizes Gram-Negative Pathogens to Antibiotics and Overcomes Acquired Colistin Resistance. *Nature Microbiology* **2017**, 2. <https://doi.org/10.1038/nmicrobiol.2017.28>.
- (8) Stokes, J. M.; Davis, J. H.; Mangat, C. S.; Williamson, J. R.; Brown, E. D. Discovery of a Small Molecule That Inhibits Bacterial Ribosome Biogenesis. *eLife* **2014**, 3, e03574. <https://doi.org/10.7554/eLife.03574>.
- (9) Stokes, J. M.; French, S.; Ovchinnikova, O. G.; Bouwman, C.; Whitfield, C.; Brown, E. D. Cold Stress Makes Escherichia Coli Susceptible to Glycopeptide Antibiotics by Altering Outer Membrane Integrity. *Cell Chemical Biology* **2016**, 23 (2), 267–277. <https://doi.org/10.1016/j.chembiol.2015.12.011>.
- (10) Bean, D. C.; Wareham, D. W. Pentamidine: A Drug to Consider Re-Purposing in the Targeted Treatment of Multi-Drug Resistant Bacterial Infections? *Journal of Laboratory and Precision Medicine* **2017**, 2, 49–49. <https://doi.org/10.21037/jlpm.2017.06.18>.
- (11) Waller, D. G.; Sampson, A. P. Chemotherapy of Infections. In *Medical pharmacology and therapeutics*; Elsevier, 2018; pp 581–629. <https://doi.org/10.1016/B978-0-7020-7167-6.00051-8>.
- (12) Sands, M.; Kron, M. A.; Brown, R. B. Pentamidine: A Review. *Reviews of infectious diseases* **1985**, 7 (5), 625–634. <https://doi.org/10.1093/clinids/7.5.625>.
- (13) Goa, K. L.; Campoli-Richards, D. M. Pentamidine Isethionate: A Review of Its Antiprotozoal Activity, Pharmacokinetic Properties and Therapeutic Use in Pneumocystis Carinii Pneumonia. *Drugs* **1987**, 33 (3), 242–258. <https://doi.org/10.2165/00003495-198733030-00002>.
- (14) Libman, M. D.; Miller, M. A.; Richards, G. K. Antistaphylococcal Activity of Pentamidine. *Antimicrobial Agents and Chemotherapy* **1990**, 34 (9), 1795–1796. <https://doi.org/10.1128/AAC.34.9.1795>.
- (15) Maciejewska, D.; Zabiński, J.; Kaźmierczak, P.; Wójciuk, K.; Kruszewski, M.; Kruszewska, H. In Vitro Screening of Pentamidine Analogs against Bacterial and Fungal Strains. *Bioorganic and Medicinal Chemistry Letters* **2014**, 24 (13), 2918–2923. <https://doi.org/10.1016/j.bmcl.2014.04.075>.

- (16) Edwards, K. J.; Jenkins, T. C.; Neidle, S. Crystal Structure of a Pentamidine–Oligonucleotide Complex: Implications for DNA–Binding Properties. *Biochemistry* **1992**, 31 (31), 7104–7109. <https://doi.org/10.1021/bi00146a011>.
- (17) Sun, T.; Zhang, Y. Pentamidine Binds to tRNA through Non-Specific Hydrophobic Interactions and Inhibits Aminoacylation and Translation. *Nucleic Acids Research* **2008**, 36 (5), 1654–1664. <https://doi.org/10.1093/nar/gkm1180>.
- (18) Malkawi, R.; Iyer, A.; Parmar, A.; Lloyd, D. G.; Tze, E.; Goh, L.; Taylor, E. J.; Sarmad, S.; Maddar, A.; Lakshminarayanan, R.; Singh, I.; Yang, H.; Wierzbicki, M.; Bois, D. R. Du; Nowick, J. S.; Lee, H.; Song, W. Y.; Kim, M.; Lee, M. W.; Kim, S.; Park, Y. S.; Kwak, K.; Oh, M. H.; Kim, H. J.; Acedo, J. Z.; Chiorean, S.; Vederas, J. C.; Belkum, M. J. Van; Enterobacteriaceae, C.; Brennan-krohn, T.; Pironti, A.; Kirby, E.; Paracini, N.; Clifton, L. A.; Skoda, M. W. A.; Lakey, J. H.; Scherer, K. M.; Spille, J.; Sahl, H.; Grein, F.; Kubitscheck, U.; Brenna, E.; Cannavale, F.; Crotti, M.; Vitis, V. De; Gatti, F. G.; Migliazza, G.; Molinari, F.; Parmeggiani, F.; Romano, D.; Santangelo, S.; Cebrero-cangueiro, T.; Álvarez-marin, R.; Labrador-herrera, G.; Tomas, M.; Wiese, J.; Imhoff, J. F. Liquid Crystalline Bacterial Outer Membranes Are Critical for Antibiotic Susceptibility. *Biophysj* **2018**, 108 (August), 8–12. <https://doi.org/10.1002/ddr.21482>.
- (19) Cavalier, M. C.; Ansari, M. I.; Pierce, A. D.; Wilder, P. T.; McKnight, L. E.; Raman, E. P.; Neau, D. B.; Bezawada, P.; Alasady, M. J.; Charpentier, T. H.; Varney, K. M.; Toth, E. A.; MacKerell, A. D.; Coop, A.; Weber, D. J. Small Molecule Inhibitors of Ca²⁺-S100B Reveal Two Protein Conformations. *Journal of Medicinal Chemistry* **2016**, 59 (2), 592–608. <https://doi.org/10.1021/acs.jmedchem.5b01369>.
- (20) Lam, C.; Hildebrandt, J.; Schütze, E.; Wenzel, A. F. Membrane-Disorganizing Property of Polymyxin B Nonapeptide. *Journal of Antimicrobial Chemotherapy* **1986**, 18 (1), 9–15. <https://doi.org/10.1093/jac/18.1.9>.
- (21) Odds, F. C. Synergy, Antagonism, and What the Checkerboard Puts between Them. *Journal of Antimicrobial Chemotherapy* **2003**, 52 (1), 1–1. <https://doi.org/10.1093/jac/dkg301>.
- (22) Gromyko, A. V.; Popov, K. V.; Mosoleva, A. P.; Streltsov, S. A.; Grokhovsky, S. L.; Oleinikov, V. A.; Zhuze, A. L. DNA Sequence-Specific Ligands: XII. Synthesis and Cytological Studies of Dimeric Hoechst 33258 Molecules. *Russian Journal of Bioorganic Chemistry* **2005**, 31 (4), 344–351. <https://doi.org/10.1007/s11171-005-0047-z>.
- (23) Turner, A. D.; Pizzo, S. V.; Porter, N. A.; Rozakis, G. Photoreactivation of Irreversibly Inhibited Serine Proteinases. *Journal of the American Chemical Society* **1988**, 110 (1), 244–250. <https://doi.org/10.1021/ja00209a040>.
- (24) Tidwell, R. R.; Jones, S. K.; Geratz, J. D.; Ohemeng, K. A.; Cory, M.; Hall, J. E. Analogues of 1,5-Bis(4-Amidinophenoxy)Pentane (Pentamidine) in the Treatment of Experimental Pneumocystis Carinii Pneumonia. *Journal of Medicinal Chemistry* **1990**, 33 (4), 1252–1257. <https://doi.org/10.1021/jm00166a026>.
- (25) Stolić, I.; Avdičević, M.; Bregović, N.; Piantanida, I.; Glavaš-Obrovac, L.; Bajić, M. Synthesis, DNA Interactions and Anticancer Evaluation of Novel Diamidine Derivatives of 3,4-Ethylenedioxythiophene. *Croatica Chemica Acta* **2012**, 85 (4), 457–467. <https://doi.org/10.5562/cca2141>.
- (26) Ewins, A. J.; Barber, H. J.; Newbery, G.; Ashley, J. N.; Self, A. D. H. Verfahren Zur Herstellung von Diamidinderivaten. German patent DE 844897 C, 1952.
- (27) Roger, R.; Neilson, D. G. The Chemistry of Imidates. *Chemical Reviews* **2002**, 61 (2), 179–211. <https://doi.org/10.1021/CR60210A003>.
- (28) Bruncko, M.; McClellan, W. J.; Wendt, M. D.; Sauer, D. R.; Geyer, A.; Dalton, C. R.; Kaminski, M. A.; Weitzberg, M.; Gong, J.; Dellaria, J. F.; Mantel, R.; Zhao, X.; Nienaber, V. L.; Stewart, K.; Klinghofer, V.; Bouska, J.; Rockway, T. W.; Giranda, V. L. Naphthamidine Urokinase Plasminogen Activator Inhibitors with Improved Pharmacokinetic Properties. *Bioorganic*

- and *Medicinal Chemistry Letters* **2005**, 15 (1), 93–98. <https://doi.org/10.1016/j.bmcl.2004.10.026>.
- (29) Zhang, J.; Qian, K.; Yan, C.; He, M.; Jassim, B. A.; Ivanov, I.; Zheng, Y. G. Discovery of Decamidine as a New and Potent PRMT1 Inhibitor. *MedChemComm* **2017**, 8 (2), 440–444. <https://doi.org/10.1039/c6md00573j>.
- (30) Wendt, M. D.; Rockway, T. W.; Geyer, A.; McClellan, W.; Weitzberg, M.; Zhao, X.; Mantei, R.; Nienaber, V. L.; Stewart, K.; Klinghofer, V.; Giranda, V. L. Identification of Novel Binding Interactions in the Development of Potent, Selective 2-Naphthamidine Inhibitors of Urokinase. Synthesis, Structural Analysis, and SAR of N-Phenyl Amide 6-Substitution. *Journal of Medicinal Chemistry* **2004**, 47 (2), 303–324. <https://doi.org/10.1021/jm0300072>.
- (31) Abou-Elkhair, R. A. I.; Hassan, A. E. A.; Boykin, D. W.; Wilson, W. D. Lithium Hexamethyldisilazane Transformation of Transiently Protected 4-Aza/Benzimidazole Nitriles to Amidines and Their Dimethyl Sulfoxide Mediated Imidazole Ring Formation. *Organic Letters* **2016**, 18 (18), 4714–4717. <https://doi.org/10.1021/acs.orglett.6b02359>.
- (32) Maciejewska, D.; Zabinski, J.; Kaźmierczak, P.; Rezler, M.; Krassowska-Świebicka, B.; Collins, M. S.; Cushion, M. T. Analogs of Pentamidine as Potential Anti-Pneumocystis Chemotherapeutics. *European Journal of Medicinal Chemistry* **2012**, 48, 164–173. <https://doi.org/10.1016/j.ejmech.2011.12.010>.
- (33) Amin, K.; Dannenfelser, R.-M. In Vitro Hemolysis: Guidance for the Pharmaceutical Scientist. *Journal of Pharmaceutical Sciences* **2006**, 95 (6), 1173–1176. <https://doi.org/10.1002/JPS.20627>.
- (34) Wang, B.; Boykin, D.; Choudhary, M.; Kumar, A.; Yu, B.; Zhu, M. Amidines and Amidine Analogs for the Treatment of Bacterial Infections and Potentiation Antibiotics. World patent WO 2019/241566 A1, 2019.
- (35) Geratz, J. D.; Cheng, M. C. F.; Tidwell, R. R. Novel Bis(Benzamidino) Compounds with an Aromatic Central Link. Inhibitors of Thrombin, Pancreatic Kallikrein, Trypsin, and Complement. *Journal of Medicinal Chemistry* **1976**, 19 (5), 634–639. <https://doi.org/10.1021/jm00227a011>.
- (36) Vanden Eynde, J. J.; Mayence, A.; Huang, T. L.; Collins, M. S.; Rebholz, S.; Walzer, P. D.; Cushion, M. T. Novel Bisbenzamidines as Potential Drug Candidates for the Treatment of Pneumocystis Carinii Pneumonia. *Bioorganic and Medicinal Chemistry Letters* **2004**, 14 (17), 4545–4548. <https://doi.org/10.1016/j.bmcl.2004.06.034>.
- (37) Chauhan, P. M. S.; Niyer, R.; Bhakuni, D. S.; Shankhdhar, V.; Guru, P. Y.; Sen, A. B. Antiparasitic Agents: Part VI - Synthesis of 1,2-, 1,3- and 1,4-Bis(4-Substituted Aryloxy)Benzenes and Their Biological Activities. *Indian Journal of Chemistry - Section B Organic and Medicinal Chemistry* **1988**, 27 (1–12), 38–42.
- (38) Patrick, D. A.; Bakunov, S. A.; Bakunova, S. M.; Suresh Kumar, E. V. K.; Chen, H.; Jones, S. K.; Wenzler, T.; Barzecz, T.; Werbovetz, K. A.; Brun, R.; Tidwell, R. R. Synthesis and Antiprotozoal Activities of Dicationic Bis(Phenoxymethyl)Benzenes, Bis(Phenoxymethyl)Naphthalenes, and Bis(Benzyloxy)Naphthalenes. *European Journal of Medicinal Chemistry* **2009**, 44 (9), 3543–3551. <https://doi.org/10.1016/j.ejmech.2009.03.014>.
- (39) Bakunova, S. M.; Bakunov, S. A.; Patrick, D. A.; Kumar, E. V. K. S.; Ohemeng, K. A.; Bridges, A. S.; Wenzler, T.; Barszcz, T.; Jones, S. K.; Werbovetz, K. A.; Brun, R.; Tidwell, R. R. Structure-Activity Study of Pentamidine Analogues as Antiprotozoal Agents. *Journal of medicinal chemistry* **2009**, 52 (7), 2016–2035. <https://doi.org/10.1021/jm801547t>.
- (40) Ashley, J. N.; Barber, H. J.; Ewins, A. J.; Newbery, G.; Self, A. D. H. A Chemotherapeutic Comparison of the Trypanocidal Action of Some Aromatic Diamidines. *Journal of the Chemical Society (Resumed)* **1942**, No. 0, 103–116. <https://doi.org/10.1039/jr9420000103>.
- (41) Hamano, S.; Kanazawa, T.; Kitamura, S.-I. Bis-(Meta-Amidinophenoxy)-Compounds and Pharmacologically Acceptable Acid Addition Salts Thereof. U.S. patent US 4034010 A, 1977.

- (42) Goswami, R.; Mukherjee, S.; Wohlfahrt, G.; Ghadiyaram, C.; Nagaraj, J.; Chandra, B. R.; Sistla, R. K.; Satyam, L. K.; Samiulla, D. S.; Moilanen, A.; Subramanya, H. S.; Ramachandra, M. Discovery of Pyridyl Bis(Oxy)Dibenzimidamide Derivatives as Selective Matriptase Inhibitors. *ACS Medicinal Chemistry Letters* **2013**, 4 (12), 1152–1157. <https://doi.org/10.1021/ml400213v>.
- (43) Cavallo, G.; Metrangolo, P.; Milani, R.; Pilati, T.; Priimagi, A.; Resnati, G.; Terraneo, G. The Halogen Bond. *Chemical Reviews* **2016**, 116 (4), 2478–2601. <https://doi.org/10.1021/acs.chemrev.5b00484>.
- (44) Kong, N.; Liu, E. A.; Vu, B. T. Cis-Imidazolines. U.S. patent US 6617346 B1, 2003.
- (45) Huang, H.; Li, H.; Martásek, P.; Roman, L. J.; Poulos, T. L.; Silverman, R. B. Structure-Guided Design of Selective Inhibitors of Neuronal Nitric Oxide Synthase. *Journal of Medicinal Chemistry* **2013**, 56 (7), 3024–3032. <https://doi.org/10.1021/jm4000984>.
- (46) Suzuki, A. Organoborane Coupling Reactions (Suzuki Coupling). *Proceedings of the Japan Academy. Series B, Physical and Biological Sciences* **2004**, 80 (8), 359.
- (47) Martino, G.; Muzio, L.; Riva, N.; Gornati, D.; Seneci, P.; Eleuteri, S. Aminoguanidine Hydrazones as Retromer Stabilizers Useful for Treating Neurological Diseases. World patent WO 2020/201326 A1, 2020.
- (48) Innocenti, P.; Woodward, H.; O'Fee, L.; Hoelder, S. Expanding the Scope of Fused Pyrimidines as Kinase Inhibitor Scaffolds: Synthesis and Modification of Pyrido[3,4-d]Pyrimidines. *Organic & Biomolecular Chemistry* **2014**, 13 (3), 893–904. <https://doi.org/10.1039/C4OB02238F>.
- (49) García, D.; Foubelo, F.; Yus, M. Selective Lithiation of 4- and 5-Halophthalans. *Heterocycles* **2009**, 77 (2), 991–1005. [https://doi.org/10.3987/COM-08-S\(F\)85](https://doi.org/10.3987/COM-08-S(F)85).
- (50) Washington, J. A.; Wilson, W. R. Erythromycin: A Microbial and Clinical Perspective after 30 Years of Clinical Use (First of Two Parts). *Mayo Clinic Proceedings* **1985**, 60 (3), 189–203. [https://doi.org/10.1016/S0025-6196\(12\)60219-5](https://doi.org/10.1016/S0025-6196(12)60219-5).
- (51) Washington, J. A.; Wilson, W. R. Erythromycin: A Microbial and Clinical Perspective after 30 Years of Clinical Use (Second of Two Parts). *Mayo Clinic Proceedings* **1985**, 60 (4), 271–278. [https://doi.org/10.1016/S0025-6196\(12\)60322-X](https://doi.org/10.1016/S0025-6196(12)60322-X).
- (52) Farr, B.; Mandell, G. L. Rifampin. *Medical Clinics of North America* **1982**, 66 (1), 157–168. [https://doi.org/10.1016/S0025-7125\(16\)31449-3](https://doi.org/10.1016/S0025-7125(16)31449-3).
- (53) Levine, J. F. Vancomycin: A Review. *Medical Clinics of North America* **1987**, 71 (6), 1135–1145. [https://doi.org/10.1016/S0025-7125\(16\)30801-X](https://doi.org/10.1016/S0025-7125(16)30801-X).
- (54) Kirby, W. M. M.; Hudson, D. G.; Noyes, W. D. Clinical and Laboratory Studies of Novobiocin, a New Antibiotic. *A.M.A. Archives of Internal Medicine* **1956**, 98 (1), 1–7. <https://doi.org/10.1001/ARCHINTE.1956.00250250007001>.
- (55) Drugs@FDA: FDA-Approved Drugs. <https://www.accessdata.fda.gov/scripts/cder/daf/index.cfm?event=overview.process&ApplNo=050339> (accessed 2021-07-08).
- (56) Wesseling, C. M. J.; Wood, T. M.; Slingerland, C. J.; Bertheussen, K.; Lok, S.; Martin, N. I. Thrombin-Derived Peptides Potentiate the Activity of Gram-Positive-Specific Antibiotics against Gram-Negative Bacteria. *Molecules* **2021**, 26 (7), 1954. <https://doi.org/10.3390/molecules26071954>.
- (57) Thornsberry, C.; Hill, B. C.; Swenson, J. M.; McDougal, L. K. Rifampin: Spectrum of Antibacterial Activity. *Reviews of Infectious Diseases* **1983**, 5 (Supplement_3), S412–S417. https://doi.org/10.1093/CLINIDS/5.SUPPLEMENT_3.S412.
- (58) Ebbensgaard, A.; Mordhorst, H.; Aarestrup, F. M.; Hansen, E. B. The Role of Outer Membrane Proteins and Lipopolysaccharides for the Sensitivity of Escherichia Coli to Antimicrobial Peptides. *Frontiers in Microbiology* **2018**, 9 (SEP), 2153. <https://doi.org/10.3389/fmicb.2018.02153>.

- (59) Uchida, K.; Mizushima, S. A Simple Method for Isolation of Lipopolysaccharides from *Pseudomonas Aeruginosa* and Some Other Bacterial Strains. *Agricultural and Biological Chemistry* **1987**, 51 (11), 3107–3114. <https://doi.org/10.1080/00021369.1987.10868532>.
- (60) Furevi, A.; Stähle, J.; Muheim, C.; Gkotzis, S.; Udekwu, K. I.; Daley, D. O.; Widmalm, G. Structural Analysis of the O-Antigen Polysaccharide from *Escherichia Coli* O188. *Carbohydrate Research* **2020**, 498 (2020), 108051. <https://doi.org/10.1016/j.carres.2020.108051>.
- (61) Wang, Z.; Wang, J.; Ren, G.; Li, Y.; Wang, X. Influence of Core Oligosaccharide of Lipopolysaccharide to Outer Membrane Behavior of *Escherichia Coli*. *Marine Drugs* **2015**, 13 (6), 3325–3339. <https://doi.org/10.3390/md13063325>.
- (62) Doorduyn, D. J.; Heesterbeek, D. A. C.; Ruyken, M.; Haas, C. J. C. de; Stapels, D. A. C.; Aerts, P. C.; Rooijackers, S. H. M.; Bardoel, B. W. Polymerization of C9 Enhances Bacterial Cell Envelope Damage and Killing by Membrane Attack Complex Pores. *bioRxiv* **2021**, Epub, May 12, 2021. <https://doi.org/10.1101/2021.05.12.443779>.
- (63) Cox, G.; Sieron, A.; King, A. M.; De Pascale, G.; Pawlowski, A. C.; Koteva, K.; Wright, G. D. A Common Platform for Antibiotic Dereplication and Adjuvant Discovery. *Cell chemical biology* **2017**, 24 (1), 98–109. <https://doi.org/10.1016/J.CHEMBIOL.2016.11.011>.
- (64) Liu, Y. Y.; Wang, Y.; Walsh, T. R.; Yi, L. X.; Zhang, R.; Spencer, J.; Doi, Y.; Tian, G.; Dong, B.; Huang, X.; Yu, L. F.; Gu, D.; Ren, H.; Chen, X.; Lv, L.; He, D.; Zhou, H.; Liang, Z.; Liu, J. H.; Shen, J. Emergence of Plasmid-Mediated Colistin Resistance Mechanism MCR-1 in Animals and Human Beings in China: A Microbiological and Molecular Biological Study. *The Lancet Infectious Diseases* **2016**, 16 (2), 161–168. [https://doi.org/10.1016/S1473-3099\(15\)00424-7](https://doi.org/10.1016/S1473-3099(15)00424-7).
- (65) Nang, S. C.; Li, J.; Velkov, T. The Rise and Spread of Mcr Plasmid-Mediated Polymyxin Resistance. *Critical Reviews in Microbiology* **2019**, 45 (2), 131–161. <https://doi.org/10.1080/1040841X.2018.1492902>.
- (66) Vuorio, R.; Vaara, M. The Lipid A Biosynthesis Mutation LpxA2 of *Escherichia Coli* Results in Drastic Antibiotic Supersusceptibility. *Antimicrobial Agents and Chemotherapy* **1992**, 36 (4), 826–829. <https://doi.org/10.1128/AAC.36.4.826>.
- (67) Helander, I. M.; Mattila-Sandholm, T. Fluorometric Assessment of Gram-Negative Bacterial Permeabilization. *Journal of Applied Microbiology* **2000**, 88 (2), 213–219. <https://doi.org/10.1046/j.1365-2672.2000.00971.x>.
- (68) MacNair, C. R.; Stokes, J. M.; Carfrae, L. A.; Fiebig-Comyn, A. A.; Coombes, B. K.; Mulvey, M. R.; Brown, E. D. Overcoming Mcr-1 Mediated Colistin Resistance with Colistin in Combination with Other Antibiotics. *Nature Communications* **2018**, 9 (2018), 458. <https://doi.org/10.1038/s41467-018-02875-z>.
- (69) Li, X.; Sun, C. L. Piperidine and Piperazine Derivatives. World patent WO 2007/089462 A2, 2007.
- (70) Suzuki, N.; Kishimoto, K.; Yamazaki, K.; Kumamoto, T.; Ishikawa, T.; Margetić, D. Immobilized 1,2-Bis(Guanidinoalkyl)Benzenes: Potentially Useful for the Purification of Arsenic-Polluted Water. *Synlett* **2013**, 24 (19), 2510–2514. <https://doi.org/10.1055/S-0033-1338980>.
- (71) Berglund, A. J.; Bodner, M. J. Aryl Diamidines and Prodrugs Thereof for Treating Myotonic Dystrophy. U.S. patent US 2013/0281462 A1, 2013.
- (72) Lewis, J. E. M. Self-Templated Synthesis of Amide Catenanes and Formation of a Catenane Coordination Polymer. *Organic & Biomolecular Chemistry* **2019**, 17 (9), 2442–2447. <https://doi.org/10.1039/C9OB00107G>.
- (73) Akhtar, W. M.; Armstrong, R. J.; Frost, J. R.; Stevenson, N. G.; Donohoe, T. J. Stereoselective Synthesis of Cyclohexanes via an Iridium Catalyzed (5 + 1) Annulation Strategy. *Journal of the American Chemical Society* **2018**, 140 (38), 11916–11920. <https://doi.org/10.1021/jacs.8b07776>.

- (74) López-Cortina, S.; Medina-Arreguin, A.; Hernández-Fernández, E.; Berns, S.; Guerrero-Alvarez, J.; Ordoñez, M.; Fernández-Zertuche, M. Stereochemistry of Base-Induced Cleavage of Methoxide Ion on Cis- and Trans-1,4-Diphenylphosphorinanium Salts. A Different Behavior with a Phenyl Substituent. *Tetrahedron* **2010**, 66 (32), 6188–6194. <https://doi.org/10.1016/J.TET.2010.05.095>.
- (75) Wang, J.; Chou, S.; Xu, L.; Zhu, X.; Dong, N.; Shan, A.; Chen, Z. High Specific Selectivity and Membrane-Active Mechanism of the Synthetic Centrosymmetric α -Helical Peptides with Gly-Gly Pairs. *Scientific Reports* **2015**, 5 (April), 1–19. <https://doi.org/10.1038/srep15963>.
- (76) Amin, K., Dannenfelser, R.-M. In vitro hemolysis: Guidance for the pharmaceutical scientist. *J. Pharm. Sci.* **2006**, 5 (6), 1173–1176. DOI: 10.1002/JPS.20627.

